ANNALES
UNIVERSITATIS SCIENTIARUM BUDAPESTINENSIS DE ROLANDO EÖTVÖS NOMINATAE

SECTIO GEOLOGICA

TOMUS XV
1971.

REDIGUNT
B. GÉCZY
J. KISS
L. STEGENA

BUDAPEST
1972

ANNALES

UNIVERSITATIS SCIENTIARUM BUDAPESTINENSIS DE ROLANDO EÖTVÖS NOMINATAE

SECTIO BIOLOGICA
incepit anno MCMLVII

SECTIO CHIMICA
incepit anno MCMLIX

SECTIO GEOLOGICA
incepit anno MCMLVII

SECTIO GEOGRAPHICA
incepit anno MCMLXV

SECTIO HISTORICA
incepit anno MCMLVII

SECTIO IURIDICA
incepit anno MCMLIX

SECTIO LINGUISTICA
incepit anno MCMLXIX

SECTIO MATHEMATICA
incepit anno MCMLVIII

SECTIO PAEDAGOGICA ET PSYCHOLOGICA
incepit anno MCMLXIX

SECTIO PHILOLOGICA
incepit anno MCMLVII

SECTIO PHILOSOPHICA ET SOCIOLOGICA
incepit anno MCMLXII

PROFESSOR ELEMÉR VADÁSZ
(1885–1970)

Each organization of the Hungarian earth and mining sciences and everybody who has been related to these sciences was most shocked to receive the announcement of the death of Professor Elemér Vadász one of the greatest personalities of the Hungarian geology, the brave promoter of social development, who was always ready to work for any noble cause. It has been hard to accept that Professor Vadász's wide knowledge, wise words, humanism, active spirit, sparkling observations and remarks, delightful humour and self-irony should belong to the past for ever.

His life presents an imposing example of an unprecedentedly successful ouevre. Professor Vadász's textbooks became effective tools in the everyday work of Hungarian geologists and significantly helped the progress in geological prospecting for natural resources in this country.

Professor Vadász was a politically persecuted person for a long period but in spite of all the difficulties he could become a leading scientist of geology, whose name was equally well known all over Europe and whose outstanding work was awarded by the highest distinctions of the Hungarian state.

Professor Vadász showed a rare talent for finding the most important practical problems in his subject, already at the beginning of his career. His investigations were governed by the requirements of the accurate analysis of the geological phenomena in time and space. Several important and decisive sites of fossils were found by his long lasting, indefatigable survey at many places from the East Carpathian Mountains to Western Hungary. In determination of rock types and especially of zoofossils he reached such a level which was rare even among the leading scientists of this classical period of geology, when sophisticated instruments being used today were not available. How clearly proves his self-assurance and unprecedented experiences concerning zoofossils the following unintentional remark "It must be a plant fossil because I can't identify it."

Professor V a d á s z did pioneer work in the investigation of sedimentation, its conditions and in the problem of facies formation. He successfully delt with the exploration for black and brown coal, bauxite and manganese ore deposits in Hungary making use of his synthetical knowledge of stratigraphy and sediment geology. His experiences and skill has been asked for and utilized in other continents as well.

In the long series of papers, he has published, special attention sh uld be given to those reporting investigations on the geology of the Mecsek Mountains. This area has got one of the most complex geology in Hungary and if we take into consideration that he could use the very modest tools and methods of geological surveying and notice the fact that he worked practically alone we are impressed by the accuracy of his results.

After the liberation of the country in 1945 Professor V a d á s z could get back his chair at the Department of Geology and became active promoter of the education at our University. His organizational and educational work in the Department contributed significantly to the better understanding of the structure and geological history of this country. He was appointed to a Professorship as early as 1919, during the Hungarian Soviet Republic, but the reactionary government which took over, removed him from this office and he got back his position nearly three decades later. The high standard of his lectures his careful attention towards each student and coworker as well as his highly successful books, the "Analytical Geology", "History and Evolution of the Earth", and "Geology of Hungary" greatly contributed to the progress of the Hungarian geology as wellasso to the promotion of his collegues.

The "Geology of Hungary", which has been translated to some foreign languages (besides of the two Hungarian editions) made a new epoch by its strikingly new concept. Unlike the previous attempts for synthetization and interpretation of the geological structure of Hungary, where the sediments (predominantly the young ones) play a decisive role, it does not build on analogies with neighbouring areas but emphasizes the thorough examination of the particular situation and draws conclusions from the comparative analysis of Hungarian data.

Professor V a d á s z summarized the partial results of his investigations in some hundred papers, published his reflections to several results and aspects of geology, discussed in Hungarian and international periodicals, analyzed the history of geological prospecting at home and abroad. He placed special interest in writing the biography of J ó z s e f S z a b ó, a leading scientist of the classical period of geology in the last century.

Professor V a d á s z held many positions in various institutions and organizations. He played an active role in the work of the Society of the Hungarian Geologists and was on the editorial board of the official periodical of the Society. Professor V a d á s z's activity was honoured by the unprecedented title of the "Honorary Lifetime President" by the grateful members of the Society. His presidency in the Society of the Soviet-Hungarian Friendship shows how tirelessly he fought for the fiendship between peoples.

Professor V a d á s z's life is of historical importance. He worked in a period which was most critical both from a political as well as from a scientific point of view. He crowned and closed the classical period of geology in this country and made way for a new dynamic era.

Professor V a d á s z gave his creative work to the science, his affection, carefullness and wise advices to his family, to his many friends, co-workers and to the institutions he was connected with. His activity and attitude affected the whole country. He was a scientist and a noble-minded man "who always helped everybody, everywhere in any problem."

After the obituary

by Professor Elemér Szádeczky Kardoss

Member of the Hungarian Academy of Sciences

THERMOMAGNETIC ANALYSIS AND OPTICAL EXAMINATIONS OF POST-OROGENIC BASALTS FROM HUNGARY

by

M. M. ABDEL DAYEM – P. MÁRTON – E. SZALAY-MÁRTON

(Cairo University Faculty of Engineering, Geophysical Department, Cairo and Geophysical Institute of Loránd Eötvös University and State Institute of Geophysics, Budapest)

Received 13 April 1971

SUMMARY

Quite recently two of the present authors (P. M. and E. Sz-M.) have dealt with palaeomagnetism of postorogenic basalts from Hungary. The results of these studies have been published in details, in (Márton and Szalay, 1967) and (Márton and Szalay, 1968), whilst a concise summary of them can be found in (Márton and Szalay-Márton, 1970). As a part of the palaeomagnetic studies some thermomagnetic and microscopical examinations have also been pursued in order to understand the nature of the natural magnetization of the investigated basaltic rocks. In the present paper, the results of systematic thermomagnetic and ore microscopical studies made on these rocks will be reported.

Introduction

Basaltic lavas subject to the present thermomagnetic analysis and microscopic examinations may be found in Transdanubia near the Lake Balaton and at the northern foreground of the Mátra Mountains (North-Hungary), respectively Both normal and reversed polarities have been recorded by palaeomagnetic studies. The sampling localities and the related paleomagnetic polarities are summarized in Table 1.

From each locality one or more samples have been selected. From the samples small prisms of $1 \times 1 \times 2$ cm have been cut out for thermomagnetic analysis. One of the surfaces of these specimens have been polished and other pieces of the samples have similarly been prepared for microscopic examinations.

Thermomagnetic analysis

The small prism is magnetized at room temperature in a steady magnetic field of 8 kOe which is large enough to saturate all titanomagnetites. The magnetized specimen is set in a furnance beside an astatic magnetometer. Then the remanent magnetization of saturation I_{rs} of the specimen is measured with increase of temperature. When the specimen loses its magnetization at certain temperature it is cooled down to room temperature. Then it is remagnetized and reheated measuring its magnetization with increasing temperature.

Table 1

Sampling localities with their palaeomagnetic polarities

	Locality	Paleomagnetic polarity
1.	Uzsa Quarry	Normal
2.	Szebike Quarry	Normal
3.	Tátika Hill	Normal
4.	Sümeg Quarry	Normal
5.	Sümegprága Dyke	Normal
6.	Bazsi Quarry	Normal
7.	Zalaszántó Quarry	Normal
8.	Vindornya Quarry	Normal
9.	Gulács Quarry	Reversed
10.	Tótihegy Quarry	–
11.	Diszel Quarry	–
12.	Hegyestű Quarry	Normal
13.	Badacsony Quarry	Reversed
14.	Sztgyörgyhegy Quarry	Reversed
15.	Haláp Quarry	Reversed
16.	Kabhegy Quarry	Reversed
17.	Sághegy Quarry	Reversed
18.	Pécskő Quarry	Reversed
19.	Szilváskő Quarry	Reversed
20.	Nagykő Quarry	–
21.	Bagókő Quarry	Reversed
22.	Medvés Quarries	Reversed

Localities numbered as 1 to 17 are in Transdanubia and the remainders in North-Nógrád (North-Hungary).

Each thermomagnetic curve (magnetization against temperature) falls into one of the three classes as follows:

Class I. – (Fig. 1) Convex thermomagnetic curve indicating continuous change in the chemical composition of the magnetic minerals. In some cases the curve consists of a straight line or a concave part within the low temperature range indicating a homogeneous magnetic phase of low characteristic temperature. The maximum Curie-temperature, defined by $T_m = T$ at which $I_{rs}(T) = 0$, varies between 200°C and 560°C.

Class II. – (Fig. 2) The low temperature part of the thermomagnetic curve is similar to that of the samples belonging to Class I. The high temperature part of the curve, however, consists of a straight line indicating the presence of a homogeneous magnetic phase of high-temperature. The highest Curie-temperature recorded by the present experiments is 550°C. The proportion of this component is different in different samples.

Class III. – (Fig. 3) This class may be characterized by the predominance of a high temperature magnetic constituent. Contrasting

with the preceding two classes, here, the occurence of concave-shaped thermomagnetic curve is common. The curve possesses a small "tail" which may extend up to 600°C.

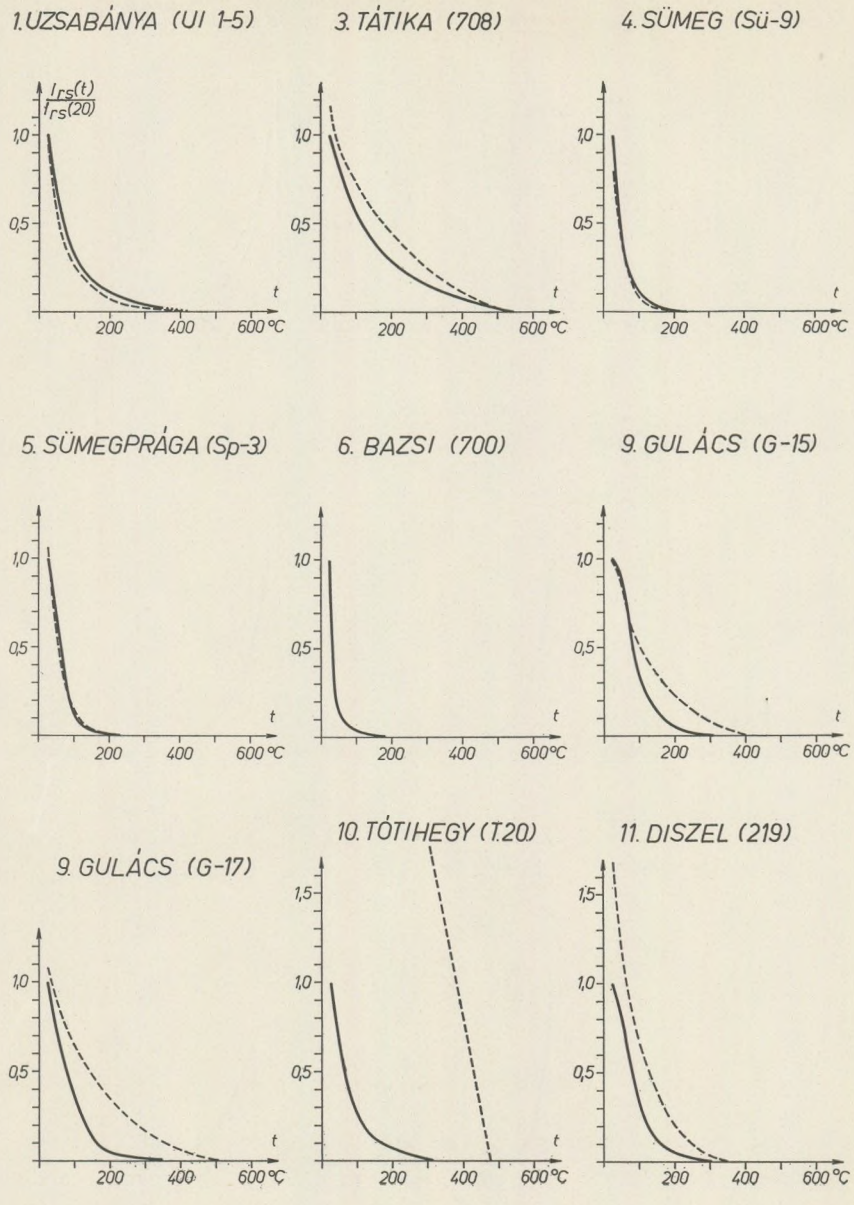

To explain the repeated heating curves obtained (Fig. 1 to 3) one must take into consideration that the first heating might take place to various temperatures depending on the minimum temperature T_m at

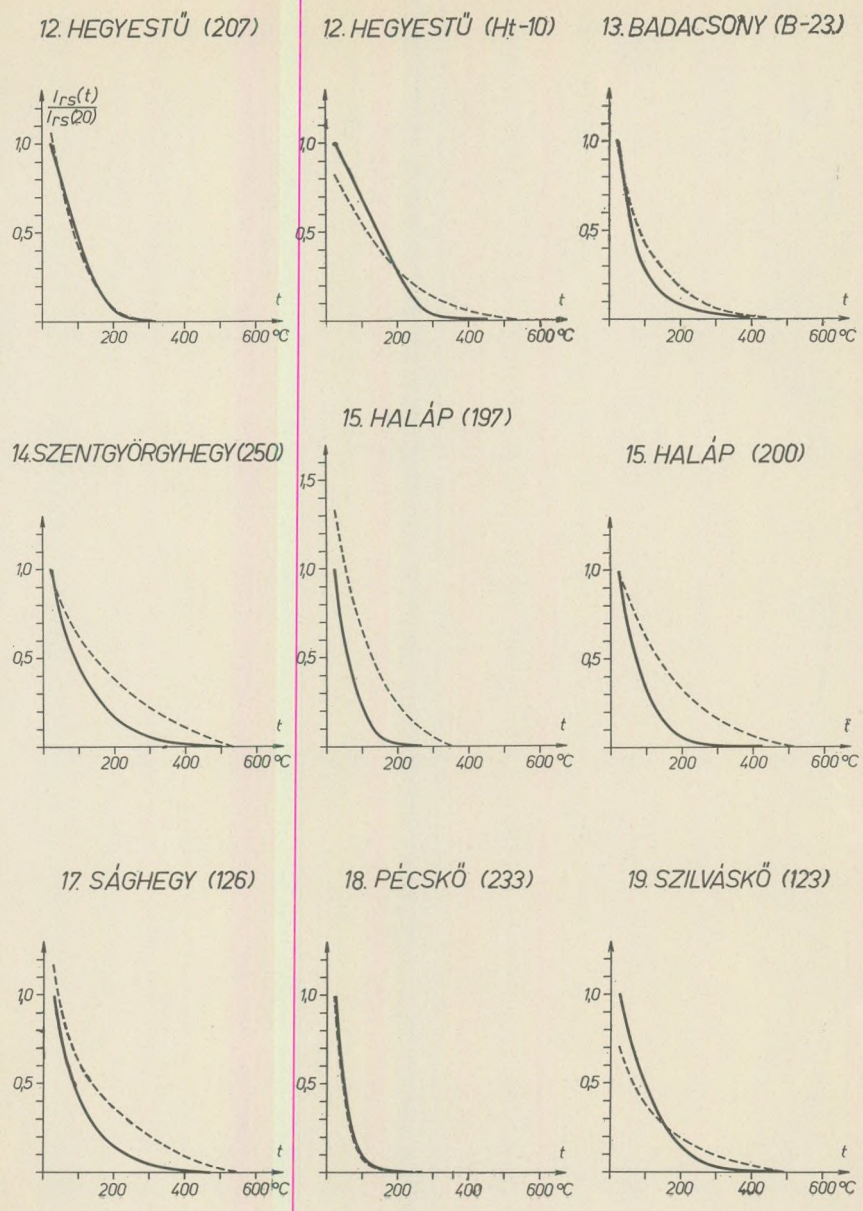

which $I_{rs}(T)$ turned to zero. In general, the low Curie-temperature samples give (almost) repeteable thermomagnetic curves, when heated up to or slightly above T_m. In all opposite cases, the repated heating curve refers to alterations which may be interpreted as an over-all oxidation of the magnetic constituents during the first heating of the specimen.

Optical examinations

The specimens' polished surfaces have been observed using a MIN-8 microscope both in air and under oil immersion at magnification up to 1400. These examinations have been carried out on the specimens in their untreated state as well as after heat treatment.

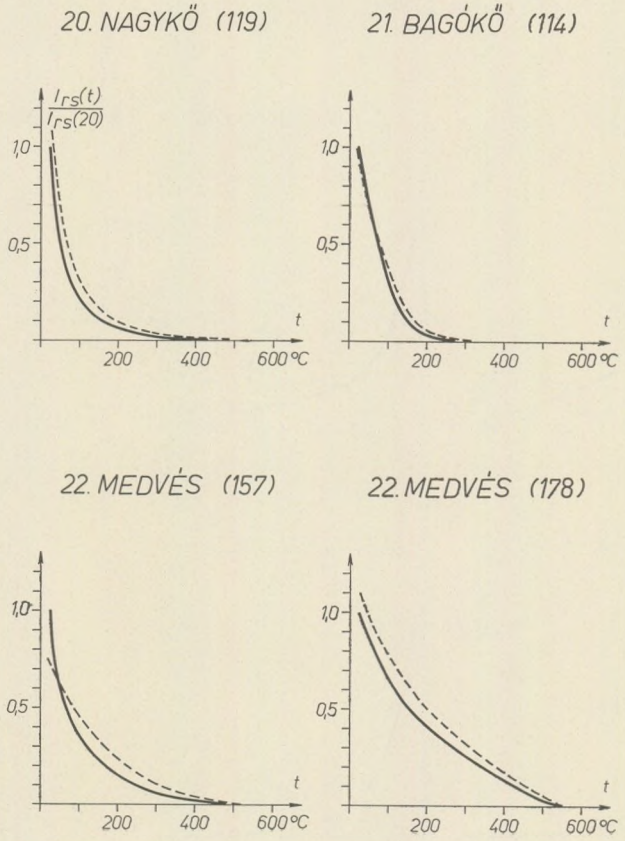

On the basis of the overall state of the polished sections the opaque minerals may also be classified into groups as follows:

G r o u p I. Homogeneous titanomagnetite grain . Color is brownish-grey with a slight lilac tint. Grains are of uniform size in the range of 5 to 50 μ. Ilmenite has been observed neither in independent grains nor as an exsolution product.

The samples belonging to this group are:

12. Hegyestű (Ht-10 and 207)
13. Badacsony (B-23)
18. Pécskő (233)
19. Szilváskő (123)
20. Nagykő (119)
21. Bagókő (114)
22. Medvés (157 and 178)

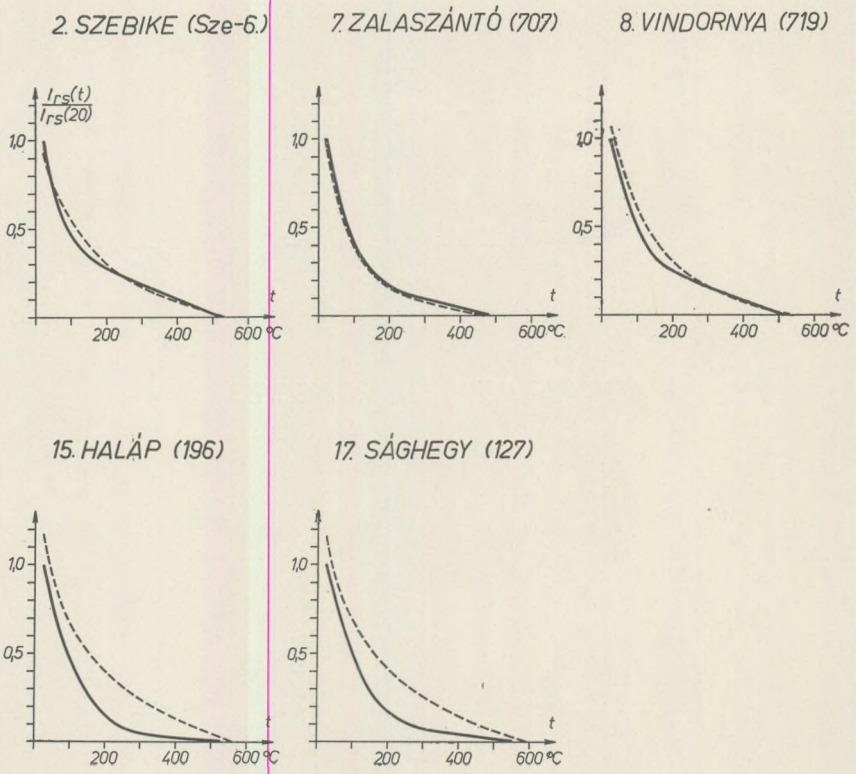

Group II. Homogeneous titanomagnetite grains crystallized in two generations with grain sizes of 100 to 500 μ, resp. of ~ 10 μ. Color is lilac. Grains of larger dimensions are resorbed. Separate ilmenite in various quantity.

These samples are:

1. Uzsa (UJ-1 – 5), (in larger grains oriented vitreous inclusions)
11. Diszel (219), (no ilmenite)
14. Sztgyörgyhegy (250),
15. Haláp (197) and 200),
17. Ság (126),

} (half of the opaques is ilmenite)

Group III. Homogeneous, lilac titanomagnetite. A number of the larger grains (50 to 200 μ) have sceletal structure. Fine opaque crystallites of sceletal habit are common.

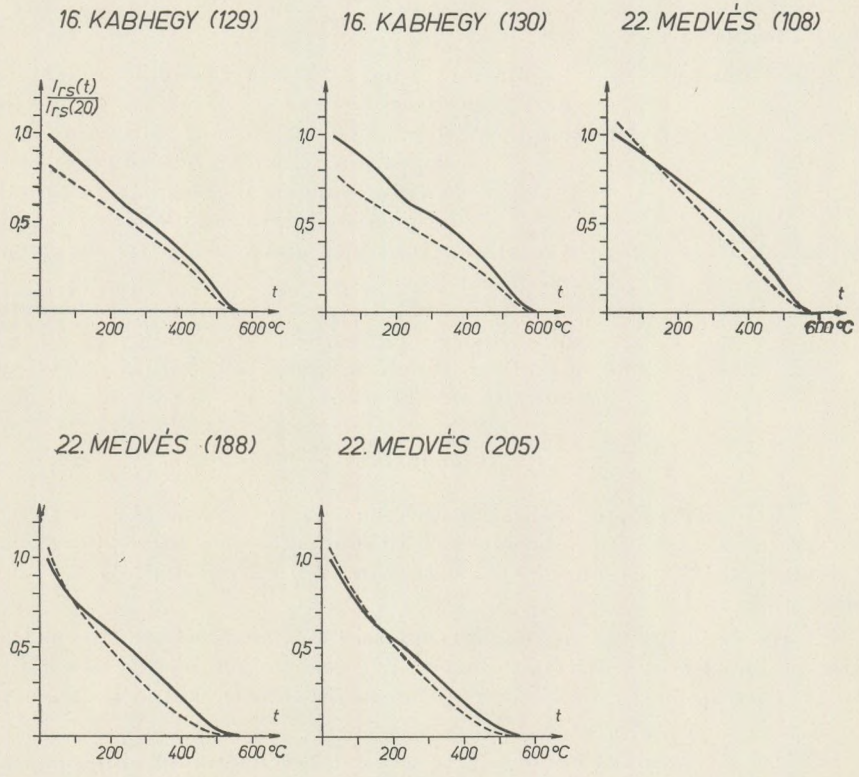

These samples are:

3. Tátika (708),
4. Sümeg (Sü-9),
5. Sümegprága (Sp-3),
6. Bazsi (700),
10. Tótihegy (T-20),

(fibres of 25 to 50 μ long on which neither anisotropy nor bireflexion have been observed)

G r o u p I V. Most titanomagnetite grains are homogeneous. Color is lilac. In some larger crystals of 150 to 250 μ ilmenite exsolution parallel to (111) may be observed. Separate ilmenite grains also occur.
The representative samples of the group are:

2. Szebike (Sze-6),
7. Zalaszántó (707),
8. Vindornya (719),
15. Haláp (196),
17. Sághegy (127),

G r o u p V. Oxidized titanomagnetite grains with low and high temperature alteration products.

These samples are:

9. Gulács (G-15), (oxidation from titanomagnetite to maghemite and hematite)
16. Kabhegy (129 and 130), (hematite exsolution is common, its appearence may be described either as waevy lamellar or box-like or spindle-like, subordinate maghemite)
22. Medvés (108), (oxidation from titanomagnetite to maghemite and hematite)
22. Medvés (188), (a few spindle-shaped exsolution of hematite, subordinate maghemite)
22. Medvés (205), (exsolved ilmenite, grid parallel to (111) subordinate maghemite)

Conclusions

1. The microscopic examinations have shown that the carriers of the magnetization of our basalts are titanomagnetites in various stages, of oxidation (L a r s o n et al, 1969) and (W i l s o n and W a t k i n s 1967).

2. Between the thermomagnetic classes and microscopic groups there exists a one to one correspondence. The thermomagnetic classes I, II and III correspond to the microscopic groups I to III, IV and V, respectively.

a) In the samples belonging to Class I the magnetic minerals have undergone neither low or high temperature oxidation after their solidification except the sample G-15 which contains many maghemite grains.

The authors have not succeeded in finding any closer correlation between thermomagnetic properties and opaque petrology within this Class. (The samples $T-20$ and 219 exhibit an anomalously great increase in I_{rs} after the first heating, a phenomenon which has remained to be explained.)

b) With the samples from Class II, the alteration of the titanomagnetites has confined to a slight high temperature oxidation leading for exsolution of ilmenite lemallae of moderate amount.

c) In the Class III, both low and high temperature alterations may be traced by microscopy. The high temperature oxidation is ubiquitous as it is shown by the abundant ilmenite and hematite exsolved in lamellae of several pattern. The low temperature oxidation, however, the presence of which is indicated by maghemite, is not significant.

REFERENCES

Márton, P.; Szalay, E. (1967): Paleomágneses vizsgálatok hazai bazaltkőzeteken. Magyar Geofizika, VIII. 2–3 pp. 67–76.

Márton, P.; Szalay, E. (1968): Paläomagnetische Untersuchungen an Basaltlaven von Ungarn. Acta Geol. Ac. Sci. Hung. Tom. 12 (1–4) pp. 291–305.

Márton, P.; Szalay-Márton, E. (1970): Secular changes, polarity epochs and tectonic movements as indicated by palaeomagnetic studies of Hungarian rock samples. Pure and Appl. Geophys. Vol. 81. pp. 151–162.

Larson, E.; Ozima, M.; Ozima, M.; Nagata, T.; and Strangway, D. (1969): Stability of remanent magnetization of igenous rocks Geophys. J. R. astr. Soc. 17. pp. 263–292.

Wilson, R. L.; Watkins, N. D. (1967): Correlation between petrology and natural magnetic polarity in Columbia plateau basalts. Geophys. J. R. astr. Soc. 12. pp. 405–424.

EXPANSIONS OF CERTAIN METEOROLOGICAL FIELDS IN CHEBYSHEV POLYNOMIALS

R. CZELNAI

(Meteorological Service of Hungary)

and

F. RÁKÓCZI

(Meteorological Institute of Loránd Eötvös University)

(Received: 1st Feb. 1971)

ZUSAMMENFASSUNG

Bei meteorologischer Datenerfassung ist es eine grundlegende Bestrebung deren zeitliche Aenderungen oder räumliche Verteilung mit einer, von der Praxis und der Theorie verlangten Genauigkeit zu beschreiben. Dieses Ziel kann durch die entsprechende Wahl der Zeitpunkte der Beobachtungen, und, im Falle von räumlicher Verteilung, durch die entsprechende Anordnung der Stationen erreicht werden. Räumliche Verteilungen sind im allgemeinen mit Isolinien dargestellt, wobei wir annehmen, dass die räumliche Verteilung des betreffenden Elements mit der Hilfe von kontinuierlichen Zweidimensionfunktionen beschrieben werden kann. Damit die Isolinien in der erwünschten Genauigkeit dargestellt werden können, brauchen wir meist eine grosse Menge von Information. Jedoch wächst die Menge der Information nicht proportionell mit der Anzahl der inanspruchgenommenen Probepunkte, da die individuellen Probepunkte auch Information bezüglich einander enthalten, das heisst, sie enthalten eine erhebliche Redundanz. Diese Redundanz hat einen gewissen Nutzen vom Standpunkt der Operationen des Fernmeldewesens und der Datenkontrolle, jedoch vor komplizierten Datenverarbeitungsoperationen ist es zweckdienlich diese aus dem Material der Beobachtungen zu entfernen. Die redundanzfreien, von einander unabhängigen Informationen ermöglichen die objektive Beschreibungen der wichtigsten Eigenarten des in Frage stehenden Feldes, und dies mit wenigen Parametern. Diese kompakte Beschreibung kann äusserst nutzvoll bei der Lösung gewisser Berechnungsaufgaben sein.

Im Interesse des angeführten Ziels werden meteorologische Felder im allgemeinen mit orthogonalen Polynomen dargestellt. Dies ermöglicht eine ausreichend pünktliche und ideal kompakte Charakterisierung der Felder, da, im allgemeinen, die in grosser Anzahl anwesenden Probepunkt-Daten auf eine ganz enge Gesamtheit der Koeffizienten der Polynome zurückgeführt werden kann.

In der vorliegenden Arbeit wird – nach R. G. Miller (1966) – eine kurze Beschreibung der Methode der Darstellung der meteorologischen Felder in Tschebishevschen Polynomen gegeben. Zur Ergänzung wird die Anwendung dieser Methode an einigen Beispielen demonstriert-

1. Description of the method

In order to expand planar fields in Chebyshev polynomials, the first step is to define a suitable grid, which may consist of equidistant points, or intersections of geographical longitudes and latitudes. The grid points have to be near enough to each other that their data should serve to indicate all characteristic features of the field which are important

from the point of view of the actual task. Let the grid points be x_i ($i = 1, 2, \ldots, m$) and y_j ($j = 1, 2, \ldots, m'$), where X and Y are the coordinates and the (x_i, y_j) positions can be calculated from an arbitrary initial point.

Let the field values, registered in the grid points, be z_{ij}, and let these values be expressed in the form of a power expansion:

$$z_{ij} = a_{00} + a_{10} x_i + a_{01} y_j + a_{20} x_i^2 + a_{11} x_i y_j + a_{02} y_j^2 + \ldots = \sum_{n=0}^{m-1} \sum_{k=0}^{m'-1} a_{nk} x_i^n y_j^k. \tag{1}$$

The highest powers of this expansion are $(m-1)$ and $(m'-1)$, respectively. The number of equations at our disposal equals the number of the a_{nk} unknown quantities.

Let us now introduce the following polynomials into formula (1):

$$f_{ni} = \sum_{r=0}^{n} A_{nr} x_i^r,$$

and (2)

$$g_{kj} = \sum_{s=0}^{k} B_{ks} y_j^s.$$

Thus for z_{ij} the following expression is obtained:

$$z_{ij} = b_{oo} f_{oi} g_{oj} + b_{1o} f_{1i} g_{oj} + b_{o1} f_{oi} g_{1j} + b_{2o} f_{2i} g_{oj} + b_{11} f_{1i} g_{1j} + b_{o2} f_{oi} g_{2j} + \ldots = \sum_{n=0}^{m-1} \sum_{k=0}^{m'-1} b_{nk} f_{ni} g_{kj}, \tag{3}$$

where the coefficients b_{nk} are functions of the values a_{nk}, and, if we choose: $A_{oo} = B_{oo} = 1$, then we obtain: $f_{oi} = g_{oj} = 1$, and formula (3) assumes the following form:

$$z_{ij} = b_{00} + \sum_{n=1}^{m-1} b_{n0} f_{ni} + \sum_{k=1}^{m'-1} b_{0k} g_{jk} + \sum_{n=1}^{m-1} \sum_{k=1}^{m'-1} b_{nk} f_{ni} g_{kj}. \tag{4}$$

The values z_{ij} have been given in mm' points, thus we have mm' equations. The number of unknown quantities is also mm', as the numbers of the coefficients b_{nk}, b_{no} and b_{oo} are: $(m-1)(m'-1)$, $(m'-1)$, $(m-1)$ and 1, respectively.

In order to simplify the task, four restrictions are made:

1. Both m and m' are odd numbers;
2. f_{ni} and g_{kj} are orthogonal polynomials, that is:

$$\sum_{i=1}^{m} f_{ri} f_{si} = 0,$$

and $$r \neq s \qquad (5)$$

$$\sum_{j=1}^{m'} g_{rj} g_{sj} = 0,$$

where:

$$r, s = 1, 2, \ldots, m-1$$

and respectively:

$$r, s = 1, 2, \ldots, m'-1.$$

In this way it is ensured that the coefficients A_{nr} and B_{ks} figuring in (2) are functions solely of the coordinates X and Y. The polynomials are independent from each other, thus they may be determined independently from each other. This is particularly important if we decide to increase the accuracy of the expansions by involving further coefficients, as now this can be done without recalculating the values of the already determined coefficients.

3. The grid points are equidistant, thus the coefficients A_{nr} and B_{ks} are the functions of m and m' only.

4. For the expansions the following orthogonal polynomials are used, which fulfil the above conditions and are generally referred to as C h e b y s h e v polynomials:

$$\sum_{i=1}^{m} f_{ni} = 0; \text{ and } \sum_{j=1}^{m'} g_{kj} = 0. \qquad (6)$$

The values of coefficients b_{nk} will be determined by the method of least squares from the z_{ij} grid point data. For these coefficients the following condition should be fulfilled:

$$\sum_{i=1}^{m} \sum_{j=1}^{m'} \left(z_{ij} - \sum_{n=0}^{m=1} \sum_{k=0}^{m'-1} b_{nk} f_{ni} g_{kj} \right)^2 = \text{minimum} \qquad (7)$$

Exploiting the restrictions imposed on the f_{ni} and g_{kj} values the system of equations assumes the following simple form:

$$\begin{aligned} b_{00} &= \sum_{i=1}^{m} \sum_{j=1}^{m'} z_{ij} : mm' = \bar{z}_{ij} \\ b_{no} &= \sum_{i=1}^{m} f_{ni} \sum_{j=1}^{m'} z_{ij} : m' \sum_{i=1}^{m} f_{ni}^2 \\ b_{ok} &= \sum_{j=1}^{m'} g_{kj} \sum_{i=1}^{m} z_{ij} : m \sum_{j=1}^{m'} g_{kj}^2 \\ b_{nk} &= \sum_{i=1}^{m} \sum_{j=1}^{m'} f_{ni} g_{kj} z_{ij} : \sum_{i=1}^{m} f_{ni}^2 \sum_{j=1}^{m'} g_{kj}^2 \end{aligned} \qquad (8)$$

The question may then be raised that how the individual terms of a polynomial expansion contribute to the description of the given meteorological field. This question may be answered by determining the reduction of the total variance achieved if the given term is subtracted from the field. In order to carry out this calculation the coefficients b_{no} b_{ok} and b_{nk} are multiplied above all by the following expressions respectively:

$$\sqrt{m' \sum_{i=1}^{m} f_{ni}^2}, \quad \sqrt{m \sum_{j=1}^{m'} g_{kj}^2}, \quad \sqrt{\sum_{i=1}^{m} f_{ni}^2 \sum_{j=1}^{m'} g_{kj}^2}$$

Then, according to (8), which defines the coefficients concerned, we obtain:

$$\begin{aligned} U_{no} &= \sum_{i=1}^{m} f_{ni} \sum_{j=1}^{m'} z_{ij} : \sqrt{m' \sum_{i=1}^{m} f_{ni}^2} \\ U_{ok} &= \sum_{j=1}^{m} g_{kj} \sum_{i=1}^{m} z_{ij} : \sqrt{m \sum_{i=1}^{m'} g_{kj}^2} \\ U_{nk} &= \sum_{i=1}^{m} \sum_{j=1}^{m'} f_{ni} g_{kj} z_{ij} : \sqrt{\sum_{i=1}^{m} f_{ni}^2 \sum_{j=1}^{m'} g_{kj}^2} \end{aligned} \tag{9}$$

By dividing the left side of (9) with the number mm' of grid points, we obtain the variances described by the f_n and g_k polynomials and by the "cross-polynomials" produced by the products $f_n g_k$. Finally, the variances $U_{nk}^2 : mm'$ can be standardised if they are divided by the total variance $S^2 : mm'$ of the field. The quantity S^2, expressed in the following form:

$$S^2 = \sum_{i=1}^{m} \sum_{j=l}^{m'} (z_{ij} - \bar{z})^2 = \sum_{i=1}^{m} \sum_{j=1}^{m'} z_{ij}^2 - mm' \bar{z}^2 \tag{10}$$

gives the sum total of the square deviations of the field values. The closseness of the approximation of the field with one given polynomial is obtained by:

$$r_{nk} = U_{nk}^2 : S^2 \tag{11}$$

where 100 r_{nk}^2 indicates the percentage of the total variance described by the given polynomial. This quantity figures in American literature as "per cent reduction" and is denoted by PR. The expression r_{nk} indicates the correlation coefficient between the given field and the orthogonal polynomial of the $nk-th$ order, and its value varies between $-1{,}0$ and $1{,}0$. In order to get rid of the negative values, it is usual to introduce the following characteristic quantity:

$$R_{nk} = (r_{nk} + 1)100. \tag{12}$$

Table I

Pressures and absolute geopotencials for the area bordered by the longitudes 5°E and 35°E, and by the latitudes 35°N and 55°N, 1st May, 1964

Surface pressure

j \ i	1	2	3	4	5	6	7
1	12	12	12	12	12	12	11
	14	13	14	10	13	12	13
2	22	21	20	19	16	14	15
	21	20	19	19	17	14	13
3	25	21	20	20	16	16	19
	23	21	19	21	17	16	16
4	23	20	19	19	17	18	19
	22	21	18	20	17	19	16
5	21	21	21	19	19	20	18
	24	21	21	18	21	21	18

Ia.

500 mb

j \ i	1	2	3	4	5	6	7
1	42	42	40	41	43	46	48
	41	44	41	41	44	46	49
2	54	53	52	52	52	56	56
	52	53	51	54	51	52	53
3	66	64	60	56	57	58	58
	62	63	58	56	56	57	57
4	73	71	69	66	66	65	60
	73	71	68	69	65	64	61
5	80	80	78	75	73	68	63
	83	79	80	75	75	67	66

Ib.

850 mb

j \ i	1	2	3	4	5	6	7
1	41	41	42	42	42	42	43
	43	41	43	42	42	41	41
2	50	51	50	48	45	45	48
	48	50	49	47	46	45	45
3	55	54	54	52	48	48	49
	54	53	54	51	50	50	49
4	56	55	53	53	52	51	50
	55	55	52	54	52	52	51
5	57	56	56	55	54	52	51
	55	54	54	54	54	53	52

Ic.

2. Examples for application

The described method has been applied for the expansions of the fields of the 850 mb and 500 mb contour patterns and of the ground level pressure in C h e b y s h e v polynomials.

The basic material was taken from the OO GMT charts for 1st May, 1964. The area under consideration was bordered by the eastern longitudes 5° and 35°, and by the northern latitudes 55° and 35°. Thus, Hungary was in the middle of this area. The grid was defined as consisting of the intersections of the geographic coordinates in 5 deg. intervals. The number of grid points was 35, as we had $m=7$ and $m'=5$. The grid point data calculated from the observed pressures and absolute geopotencials are presented in Tables Ia., Ib. and Ic.

For the sake of simplicity and compactness, in these tabulations only the last two figures are given. Taking into account the numbers m and m' at our disposal, it is easy to see that besides the mean values $b_{oo}=\bar{z}$ altogether $5\times 7-1=34$ polynomials can be used for the best possible expansions of these fields. From these 34 polynomials $(m-1)$ is the number of polynomials of f_n, $(m'-1)$ is the number of polynomials of g_k, while $(mm'-1)-(m+m'-2) = 24$ is the number of the so-called cross-polynomials. From among these terms: the polynomials f_n describe the east-west transitions within the field, while the polynomials g_k represent, quite similarly, the north-south transitions. The cross-polynomials give the two-dimensional features. Each of the f_n polynomials contain $m=7$ elements while the g_k polynomials contain $m'=5$ elements, and the cross-polynomials contain $mm'=35$ elements.

The values of the basic polynomials f_n and g_j which have been applied, are indicated in Tables IIa. and IIb.

The $f_i g_k$ cross-products which are also necessary for the calculations, are produced from the basic polynomials by multiplying the respective values of the polynomials f_{ni} and g_{kj} between each other. The tables of the cross-products $f_i g_k$ contain in our case $5\times 7 = 35$ elements and $(m-1)\cdot(m'-1) = 24$ such tables have to be produced. Each of the cross-product tables represents a distribution of the two-dimensional parameter field. These tables can be prepared in advance thus ,they are at our disposal for further calculations once and for all. With the aid of the 24 cross-polynomial product sets the possibility is given to express highly varied pictures. The physical sense of the cross-polynomials may be illustrated by the two examples given in Fig. 1/a and 1/b.

The cross-product polynomial $f_2 g_2$ represents a high field-value core in the central area and high field values in the NW, NE, SW, SE corners of the area. In this case low field values cover the areas north and south of the center and the areas east and west of the center. The cross-product polynomial $f_4 g_2$, on the other hand, produces a system of high and low field-value cells, in a way that the cells at the south and north boundary

Table IIa

The values of f_{ni} in case of $m = 7$, $m' = 5$

n \ i	1	2	3	4	5	6	7	$\sum_{i=1}^{7} f_{ni}^2$
1	−3	−2	−1	0	1	2	3	28
2	5	0	−3	−4	−3	0	5	84
3	−1	1	1	0	−1	−1	1	6
4	3	−7	1	6	1	−7	3	154
5	−1	4	−5	0	5	−4	1	84
6	1	−6	15	−20	15	−6	1	924

Table IIb.

The values of g_{kj}

j \ k	1	2	3	4
1	−2	2	−1	1
2	−1	−1	2	−4
3	0	−2	0	6
4	1	−1	−2	−4
5	2	2	1	1
$\sum_{j=1}^{5} g_k^{2j}$	10	14	10	70

of the area are symmetrical, and in the central zone of the area they are shifted and their diameters are latger.

Schematic field-value distribution represented by the cross-product polynomial $f_2 g_2$.

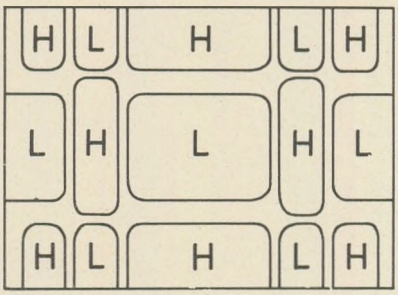

Schematic field-value distribution represented by the cross-product polynomial $f_2 g_2$

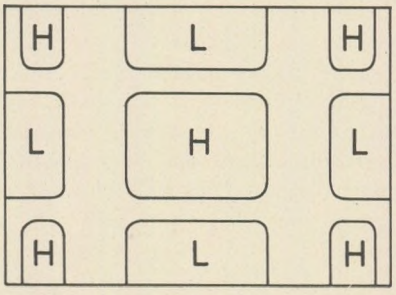

In order to make an effective reproduction of a given field, it is necessary to determine a minimum set of the basic polynomials and cross-polynomials which are sufficient to describe the field under study with the required accuracy. One also has to determine the coefficients of the selected individual polynomials.

The mathematical treatment of this task was outlined in the previous chapter. Now, starting from Table Ib, an example will be presented which shows the determination of the required coefficients.

The coefficient b_{oo} is obtained from the first equation of (8), as the mean value of the parameter field. Denoting the mean values by the symbols $\overline{p}$, $\overline{z}$, and $\overline{h}$ for the ground level pressure field, 850 mb contour patterns and 500 mb contour patterns respectively, these fields may be characterized by the following values:

$$\overline{p} = 17{,}74, \quad \overline{z} = 49{,}74, \quad \overline{h} = 59{,}74.$$

These are the b_{oo} coefficients of the respective fields, i.e. in case of reproducing the fields these values have to figure as first terms on the right side of (4).

We shall further need the values $mm'\overline{p}^2$, $mm'\overline{z}^2$, and $mm'\overline{h}^2$, as well as the values S_p^2, S_z^2 and S_h^2 defined by (10). Then the square roots of these values and the quantities $\sum_i \sum_j p_{ij}^2$, $\sum_i \sum_j z_{ij}^2$ and $\sum_i \sum_j h_{ij}^2$ have to be determined. All these values are compiled in Table III.

$mm'\overline{p}^3$ 11014,76	$mm'\overline{z}^2$ 86592,3	$mm'\overline{h}^2$ 124910,30
S_p^2 466,24	S_z^2 854,70	S_h^2 4532,70
S_p 21,56	S_z 29,25	S_h 67,32
p_{ji}^2 11481,00	z_{ji}^2 87447,00	h_{ij} 129443,00

Let us now determine the coefficients b_{no}. They are defined by the second equation of (8), from which it is seen that we have to calculate the values $m'\Sigma f^2{}_{ni}$. The quantities necessary for the calculation are to be found in the last columm of Table IIa. The details of this calculation are shown for the coefficient b_{1o}, of the 850 mb field:

$$b_{10} = \frac{\sum_{i=1}^{7} f_{1i} \sum_{j=1}^{5} z_{ij}}{m' \sum_{i=1}^{7} f_{1i}^2} = \frac{-3.259 - 2.257 - 1.255 + 1.241 + 2.238 + 3.241}{140} =$$

$$= -\frac{106}{140} = -0{,}757.$$

As it can be seen, the series of the sum total in the columns of Table Ib, and the values of basic polynomial f_{1i} were applied. The values of the other, b_{no}-type coefficients are obtained in an analogous way.

Coefficients of the type b_{ok} can be calculated on basis of the third equation of (8).

Accordingly:

$$b_{01} = \frac{\sum_{j=1}^{5} g_{1j} \sum_{i=1}^{7} z_{ij}}{70 \sum_{j=1}^{5} g_{1j}^2} = \frac{-2.293 - 1.337 + 1.371 + 2.381}{70} = \frac{210}{70} = 3{,}000.$$

For the calculations the horizontal line-totals from Table Ib and the values of the g_{ej} basic polynomials were applied. Further coefficients of this type are obtained as results of analogous calculations.

To determine the coefficients of the b_{nk} type one has to prepare the tables of the cross-product polynomials. These can be calculated by the indicated method from Tables IIa and IIb. Let us now see the calculation of b_{11} for the 850 mb field. According to (8):

$$b_{11} = \frac{\sum_{i=1}^{7} \sum_{j=1}^{5} f_{1i} g_{1j} z_{ij}}{\sum_{i=1}^{7} f_{1i}^2 \sum_{j=1}^{5} g_{1j}^2} =$$

$$= \frac{6.41 + 4.41 + 2.42 + 2.42 - 4.42 - 6.43 + 3.50 + 2.51 + 1.50}{280} -$$

$$- \frac{1.45 - 2.45 - 3.48 - 3.56 - 2.55 - 1.54 + 1.52 + 2.51 + 3.50}{280} -$$

$$- \frac{6.57 - 4.56 - 2.56 + 2.54 + 4.52 + 6.51}{280} = \frac{77}{280} = 0{,}275.$$

To determine the coefficients we have to use Table Ib, the table of the cross-product polynomials (which is not indicated here), and the Tables IIa and IIb.

The determination of the further quantities should not be difficult after having calculated the coefficients, as according to (9):

$$U_{10} = \sum_{i=1}^{7} f_{1i} \sum_{j=1}^{5} z_{1j} : \sqrt{5 \sum_{i=1}^{7} f_{1i}^2} = -\frac{106}{11{,}83} = -8{,}955$$

$$U_{01} = \sum_{j=1}^{5} g_{1j} \sum_{i=1}^{7} z_{ij} : \sqrt{7 \sum_{i=1}^{5} g_{1j}^2} = \frac{210}{8{,}37} = 25{,}110$$

$$U_{11} = \sum_{j=1}^{7} \sum_{j=1}^{5} f_{1i} g_{1j} z_{ij} : \sqrt{\sum_{i=1}^{7} f_{1j}^2 \sum_{j=1}^{5} g_{1j}^2} = \frac{77}{16{,}73} = 4{,}601.$$

On basis of (11) certain measures of the closeness of the approximations are to be obtained as:

$$r_{10} = \frac{U_{10}}{S} = -\frac{8{,}955}{29{,}25} = -0{,}30$$

$$r_{01} = \frac{U_{01}}{S} = \frac{25{,}11}{29{,}25} = 0{,}85$$

$$r_{11} = \frac{U_{11}}{S} = \frac{4{,}601}{29{,}25} = 0{,}16.$$

Percent Reductions, defined as 100 r^2_{nk}, take the values:

$$PR_{10} = 9, \quad PR_{01} = 72, \quad PR_{11} = 2;$$

and finally, the quantities R_{nk} (defined by (12)) assume:

$$R_{10} = 70, \quad R_{01} = 185, \quad \text{and} \quad R_{11} = 116.$$

In the course of this experiment all possible values have been determined for the investigated three fields. The results are summarized in Table IV.

Those b_{nk} values, which have substantial contributions to the analytical description of the field in question, have been underlined in Table IV. For reproducing the ground level pressure field to an accuracy of 90 per cent, ten b_{nk} values are sufficient, i.e. 28,6 per cent of all existing b_{nk} values. To describe the 850 mb field to an accuracy of 95 percent eight b_{nk} values suffice, thus 22,9 per cent of all possible values, and finally to reproduce the 500 mb field to an accuracy of 90 per cent four b_{nk} values i.e. 11,4 per cent of the possible values are enough. Surveying the underlined values of Table IV., one may observe that for all three levels, the values b_{10} and b_{01} are of crucial importance besides the coefficient b_{00} which represents the mean value. If only these were taken into account the field of ground level pressure would be reproduced with an accuracy of 61 per cent, the 850 mb field to an accuracy of 71 per cent and the 500 mb field with an accuracy of 85 per cent. In other words this would mean that an overwhelming part of the areal variance of the field values can be explained with a few polynomials.

It is obvious from the description of the method, that if once the b_{nk} coefficients are given (as in Table IV) then only the m and m' values are necessary to produce field values. Therefore, using the underlined values in Table IV the original fields can be easily reproduced to a high accuracy. In Tables Ia., Ib. and Ic. beneath the original values taken from the charts, the calculated values are also presented in brackets. As it could be rightfully expected these data pairs are in good agreement with each other.

Table IV

1st May 1964

		Surface pressure					850 mb					500 mb				
n	k	b_{nk}	U_{nk}	r_{nk}	PR	R_{nk}	b_{nk}	U_{nk}	r_{nk}	PR	R_{nk}	b_{nk}	U_{nk}	r_{nk}	PR	R_{nk}
1	0	−0,750	−8,87	−0,41	16,8	59	−0,757	−8,95	−0,30	9	70	−0,828	9,79	−0,14	2	86
2	0	−0,939	−9,29	−0,43	18,67	57	0,028	0,57	0,01	0	101	0,166	3,40	0,05	0	105
3	0	0,200	1,09	−0,05	0,3	95	0,500	2,73	0,09	1	109	0,433	2,37	0,03	0	103
4	0	0,047	1,30	0,06	0,4	106	0,040	1,11	0,04	0	104	−0,191	−5,30	−0,07	0	93
5	0	−0,050	−1,02	−0,05	0,3	95	−0,028	−0,57	−0,01	0	99	−0,081	−1,66	−0,02	0	98
6	0	0,014	0,95	0,04	0,2	104	−0,006	−0,41	−0,01	0	99	−0,003	−0,00	−0,00	0	100
0	1	1,714	14,32	0,66	43,7	166	3,000	25,11	0,85	72	185	7,357	61,57	0,91	88	193
0	2	−0,388	−3,84	0,18	3,2	118	−0,795	−7,87	−0,26	6	74	−0,622	−6,16	−0,09	1	91
0	3	0,571	4,77	0,22	4,8	122	0,285	2,38	0,08	0	108	0,357	2,98	0,04	0	104
0	4	−0,008	−0,17	−0,01	0,0	99	−0,008	0,17	0,00	0	100	0,002	0,04	0,00	0	100
1	1	0,004	0,06	0,03	0,0	100	0,275	4,60	0,16	2	116	−1,014	−16,96	−0,25	6	75
2	1	0,039	1,13	0,05	0,3	105	−0,039	−1,13	−0,04	0	96	0,031	0,89	0,01	0	101
3	1	0,150	1,16	0,05	0,3	105	0,533	4,13	0,14	1	114	0,116	0,89	0,01	0	101
4	1	−0,021	−0,82	−0,04	0,2	96	−0,002	0,08	0,00	0	100	−0,138	−5,41	−0,08	1	92
5	1	−0,027	−0,78	−0,04	0,2	96	−0,086	2,49	0,08	0	108	0,105	3,04	0,04	0	104
6	1	0,001	0,09	0,01	0,0	101	0,002	0,19	0,00	0	100	0,093	8,94	0,13	1	113
1	2	0,227	4,49	0,21	4,4	121	−0,254	−5,03	−0,17	2	83	0,005	0,09	0,00	0	100
2	2	0,108	3,70	0,17	2,9	117	0,088	3,02	0,10	1	110	0,134	4,59	0,07	0	107
3	2	−0,142	−1,30	−0,06	0,4	93	−0,071	−0,65	−0,02	0	98	0,202	1,85	0,02	0	102
4	2	−0,056	−2,60	−0,12	1,4	88	0,001	0,04	0,00	0	100	0,067	3,11	0,04	0	104
5	2	−0,003	−0,10	−0,04	0,0	100	0,079	2,71	0,09	1	109	0,083	2,84	0,04	0	104
6	2	0,011	1,22	0,06	0,32	106	0,128	1,93	0,06	0	106	−0,002	−0,33	−0,00	0	100
1	3	−0,192	−3,21	−0,15	2,3	85	0,092	1,54	0,05	0	105	0,082	1,37	0,02	0	102
2	3	−0,055	−1,59	−0,07	0,5	93	0,019	0,55	0,02	0	102	−0,056	−1,62	−0,02	0	98
3	3	0,150	1,16	0,05	0,3	105	0,283	2,19	0,07	0	107	−0,966	−7,48	−0,11	1	89
4	3	0,000	0,00	0,00	0,0	100	0,007	0,27	0,00	0	100	0,013	0,51	0,00	0	100
5	3	0,007	−0,20	−0,01	0,0	99	0,144	4,17	0,14	2	114	−0,013	−0,37	0,00	0	100
6	3	0,019	1,83	0,08	0,6	108	−0,002	−0,19	−0,00	0	100	−0,006	−0,57	−0,00	0	100
1	4	0,010	0,44	−0,02	0,0	98	0,106	4,69	0,16	2	116	−0,011	−0,48	−0,00	0	100
2	4	−0,013	−0,99	−0,05	0,3	95	0,055	4,21	0,14	1	114	0,028	2,14	0,03	0	103
3	4	0,002	0,04	0,00	0,0	100	−0,000	−0,00	−0,00	0	100	−0,055	−1,13	−0,01	0	99
4	4	−0,005	−0,05	−0,00	0,0	100	0,005	0,05	0,00	0	100	−0,035	−3,63	−0,05	0	95
5	4	−0,042	−3,21	−0,14	2,0	86	−0,006	−0,46	−0,01	0	99	−0,016	−1,22	−0,01	0	99
6	4	0,006	1,52	0,07	0,5	93	0,000	0,00	0,00	0	100	0,000	0,00	0,00	0	100

3. Conclusions

a) The Chebyshev polynomials, in accordance with former experiences reported in the literature [1, 2], are suitable means for the effective presentation of the fields of atmospheric pressure.

b) The fields expanded in Chebyshev polynomials can be stored in a highly compact form, practically in few figures, and from these figures they can be reproduced with an acceptable accuracy.

c) It can be expected that analogous fields expanded in Chebyshev polynomials should be characterized by nearly identical b_{nk} coefficients, and therefore these polynomial expansions could give an objective basis for the classification of analogous situations.

d) Expansions in orthogonal polynomials produce analytical expressions which are protential means of introducing initial field data into numerical prediction schemes.

It should be added that the expansions in Chebyshev polynomials are rather cumbersome but not very complicated tasks, which can be carried out effectively by computers.

Finally, let us mention that the expansions of meteorological fields in orthogonal polynomials seem to be particulary useful in investigating the interactions between various fields. This is due to the fact that the calculation of multiple regressions requires much work which rapidly increases with the number of parameters (predictors and predictandt) used for the description of the fields to be correlated.

Therefore, any possibility to reduce the number of these parameters (predictors), without any major loss of information content, should result in raising the efficiency of the whole procedure.

REFERENCES

Cehak, K. (1962): Die Verwendung von orthogonalen Polynomen in der Meteorologie-Application of Orthogonal Polynomes in Meteorologie. Arch. für Met., Geoph. und Bioklimatologie. S.A.B. 12. pp. 40 – 61.

Miller, R. G. (1966): Advanced Topics of Statistical Prediction in Meteorology. WMO Technical Note, No. 71. pp. 115 – 133. Geneva.

HYDROCARBON PROSPECTING AND GEOCHEMISTRY

by

V. DANK

(National Oil-and-Gas Trust, Budapest. Chair of Applied Geology, Loránd Eötvös University, Budapest)

(Received: 2 March, 1971)

РЕЗЮМЕ

Геологические условия Венгрии не позволяют покрытия потребностей в нефти и газе отечественными ресурсами. Однако, поскольку углеводороды отечественной продукции еще надолго останутся дешевыми и могут быть использованы наиболее экономично, должны быть предприняты всевозможные меры для того, чтобы потенциальные запасы страны в этих видах минерального сырья были бы подсчитаны с самой большой точностью. Данная работа по существу охватывает следующие области: исследования осадочных фаций, геохимия, диагенез, условия давления и температурный режим недр, а также сейсмические измерения. В этой статье излагается схема задач и мероприятий, предстоящих в области геохимии. Исследования миграции и скопления нефти и газа могут оказать значительную помощь в подсчете прогнозных запасов и постановки поисково-разведочных работ. Научная деятельность и оперативные работы, связанные с разведкой на нефть и газ, изображены в виде схемы. По этой схеме проводятся в Венгрии увязанные между собой научно-исследовательские и поисково-разведочные работы.

The world-wide increase of the importance of hydrocarbons (oil and natural gas) is a matter of common knowledge.

Their share in the Globe's energy balance was 3—4% at the turn of the century, exceeded 50% in 1970 and is expected to attain 75 to 80% by 2000.

In this country the global average of the share of hydrocarbons was reached by 1945, to reach then a round 44.5% in 1970. Long-term plans of the Nation have envisaged 54—55% for 1975 and 70% for 1985. Because of Hungary's geological conditions the country's needs for hydrocarbons cannot be covered from the national resources. And since home-produced hydrocarbons still are and will for long remain the cheapest and most economically utilizable of all kinds of energy-carriers of any origin (national, imported, etc.), efforts must be focussed to exploit all possibilities for the most rapid assessment of the country's potential hydrocarbon reserves.

What is meant in this paper by potential hydrocarbon reserves is the quantity of oil and hydrocarbon gas formed during the country's geological history in its territory and accumulated in commercially significant deposits.

The explored reserves and the quantities already stripped off are substracted from this amount.

The rest are the unexplored prognostic resources which should be explored as soon as possible.

Prospecting for mineral raw materials is most efficient in the case when the conditions and means of formation and accumulation are known, when the prospectors know where they have to look for what. This never attainable ideal model is what people have sought to approach for thousands of years with progressively more improved scientific and technological facilities.

The geological managers of hydrocarbon prospecting immediately include in their arsenal the available instruments, devices, methods and the freshest results of other disciplines.

The processes and laws of formation and accumulation of the mineral raw materials have to be thoroughly examined. If the geohistorical evolution of the territory is known, the phases of exploration and prospecting, the order of preference and perspectivity and the value of the individual area-units can be defined more precisely.

The problems solved during the stubborn activities of the past decades (laboratory investigations and prospecting operations) have shed light upon the intricate chain of processes connected with the origin, migration and accumulation of hydrocarbons.

Beside their theoretical importance, these processes provide criteria to *rely* upon in the practice of hydrocarbon prospecting.

Let us consider briefly the role geochemistry plays in hydrocarbon prospecting and see the geological problems to be solved by geochemistry for the recognition and discovery of new relationships and laws which may permit prospectors to become less and less dependent on "good luck" as a tool of succesful prospecting.

A handicap in prospecting is that hydrocarbons cannot be found at the site of their origin because of their migration and that they enter into chemical bonding with the minerals (mainly clay minerals) of the rocks. This makes it very difficult to trace the paths of migration of the substances.

In Fig. 1 the hydrocarbon research and prospecting operations are outlined. The figure shows the operations and phases of prospecting in which the contributions of geochemistry cannot be dispensed with.

Examining the composition of one kind of sediment of one area, one should be familiar first of all with the basement in the greatest possible number of points and over the largest possible area. The "bottom" of the subsiding sedimentary basin, the preformed surface of the basement, is crucial for the development and distribution of the facies and for the birth of the non-tectonic geological structures, and bottom movements do control the variations of the tectonic setting of the overlying sequences as well. In addition, the investigations of the basement, labelled as No 1 on the sketch of the programme, are important because the examination of the potential mother rocks here should be one of the starting points of investigations into migrations. Furthermore, a porous or fractured base-

ment horst block carrying a suitable, impervious overburden may readily trap masses of hydrocarbon migrating from the deeper-seated sedimentary sequences.

In square No 2 the complex stratigraphic subdivision of the Upper Tertiary formations, the subject of the investigations being conducted now, has been included. In the course of this work the thickness conditions have to be determined by indirect surficial geophysical methods, the results being supplemented continuously by deep drilling data. Deep drilling informations allow prospectors to determine the geological age of the formations, the geophysical logging of the deep holes being serviceable in regional correlations. The development of local stratigraphic scales on the basis of complex geological investigations is a starting point for assessing the spatial distribution of the identified facies (No 3).

The project termed in No 3 consists in determining the spatial distribution of the facies identified by direct observations of deep drill cores as well as by well-logging techniques. The approach to be used here is to seek to superimpose the results of indirect methods harmonically on the sound basis provided by empirical measurements, in order to span the distances between the drill holes and eventual outcrops: discontinuity which may engender difficulties.

As termed in No 4.1, prospectors should seek to detect syngenetical, mother-rock-type formations, in order to assess and summarize their recognizable characteristics. The geological identification of the sedimentary rocks intersected by deep drilling and the locating of the spatial distribution of the mother rocks (project 5.1) may be greatly enhanced by analysing deep drill cores for trace and minor elements; by determining their extractable and nonextractable organic components; by measuring the stable carbon isotope $^{13}C/^{12}C$ ratio in the carbonate of these samples and in their extractable and nonextractable organic components.

Project 4.2 has been aimed at determining the geochemical criteria for comparing reservoir rocks with special view to solve project 5.2, i.e. to outline the spatial distribution pattern of the facies. To achieve this goal, one needs $^{13}C/^{12}C$ isotope measurements both of the carbonates of reservoir rocks and their organic components, extractable and nonextractable, as well as analyses for trace elements, etc.

The function of geochemistry is extremely important for the execution of project No 4.3. Analysing the composition and spatial distribution of the fluids in the reservoir rocks belongs explicitely to the scope of geochemistry, like the analyses of mother rocks do. Here again, the isotope ratio $^{13}C/^{12}C$ has to be determined in the liquid hydrocarbon fractions of different boiling point as well as in the hydrocarbons and carbon dioxides of natural gases. The different boiling-point fractures of the liquid hydrocarbon systems have to be analysed for the same trace elements as it is the case with the mother rocks: Na, K, Ti, Co, Si, Pb, Al, Br, I, Mn, B, Ba, Sr, Zu, Fe, Cr, Cn, V, Ni, Mg, Zr.

Important tasks are to determine the isomeric ratios of light hydrocarbons up to C_7 in different hydrocarbon systems by means of capillary

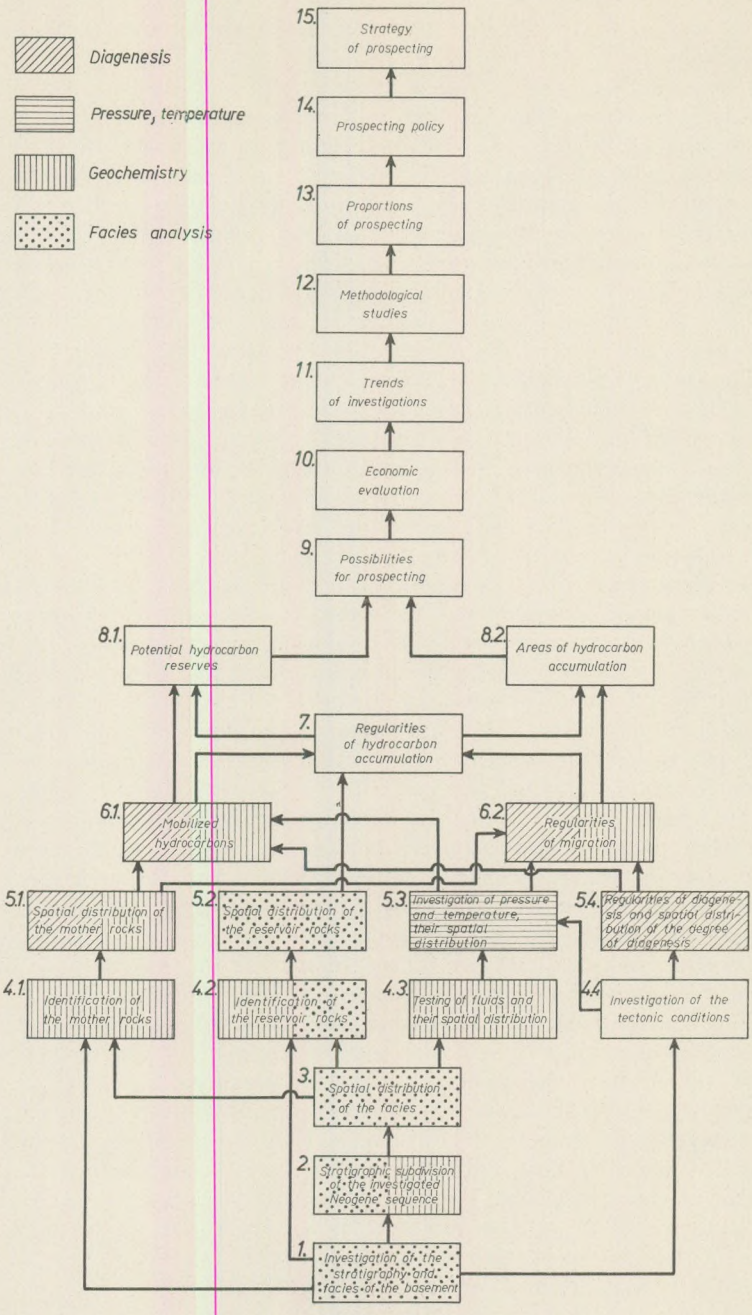
Diagenesis
Pressure, temperature
Geochemistry
Facies analysis
15. Strategy of prospecting
14. Prospecting policy
13. Proportions of prospecting
12. Methodological studies
11. Trends of investigations
10. Economic evaluation
9. Possibilities for prospecting
8.1. Potential hydrocarbon reserves
8.2. Areas of hydrocarbon accumulation
7. Regularities of hydrocarbon accumulation
6.1. Mobilized hydrocarbons
6.2. Regularities of migration
5.1. Spatial distribution of the mother rocks
5.2. Spatial distribution of the reservoir rocks
5.3. Investigation of pressure and temperature, their spatial distribution
5.4. Regularities of diagenesis and spatial distribution of the degree of diagenesis
4.1. Identification of the mother rocks
4.2. Identification of the reservoir rocks
4.3. Testing of fluids and their spatial distribution
4.4. Investigation of the tectonic conditions
3. Spatial distribution of the facies
2. Stratigraphic subdivision of the investigated Neogene sequence
1. Investigation of the stratigraphy and facies of the basement

Fig. 1

1. Basement stratigraphy and facies
2. Complex stratigraphic subdivisions of the investigated Neogene sequence
3. Spatial distribution of facies

4.1. Mother rock exploration
4.2. Reservoir rock exploration
4.3. Fluids and their spatial distribution
4.4. Tectonic conditions

5.1. Spatial distribution of mother rocks
5.2. Spatial distribution of reservoir rocks
5.3. Spatial distribution of pressure and temperature
5.4. Regularities of diagenesis and spatial distribution of the degree of diagenesis

6.1. Mobilized hydrocarbons
6.2. Regularities of migration

7. Regularities of the accumulation of hydrocarbon

8.1. Potential hydrocarbon reserves
8.2. Areas of hydrocarbon accumulations

9. Possibilities for prospecting
10. Economic evaluation
11. Trends of prospecting
12. Methodological studies
13. Proportions of prospecting
14. Prospecting policy
15. Strategy of prospecting

chromatography and to analyse petroleum in detail by using the *n-d-M* method permitting to assess the total amount of the paraffin-naphthene-base and aromatic hydrocarbons of petroleum. Serial analyses of the so-called aquifers in the petroliferous rocks, inclusive of the organic material content, are one of the prerequisites for the compilation of hydrogeological maps. Investigations should be run to get closer to the solution of the following problems:

The formation of the hydrocarbon system and of the different components stored in the reservoir is the result of the decomposition of organic compounds of higher C number or of the bonding of compounds comprising a lower number of C atoms.

How can the source of a hydrocarbon system contained in a reservoir and the path and mechanism of its migration from the mother rock to the place of accumulation be determined? To solve this problem one should envisage the use of infrared techniques (detecting porphyrine-skeletoned compounds, S- and O-containing compounds, asphalt-like components), because it were the porphyrine-skeletoned compounds that made possible the primary migration of hydrocarbons in the aqueous phase. The recognition of this fact is very important, as it may help find information to rely upon in developing a more generally valid definition of mother rock. Nota bene, if the possibility for the dissolution of

petroleum in water is granted, then the insoluble kerogens will be relatively enriched in the mother rock because of the ex-solution and off-migration of organic material therefrom. Regular examinations of the composition of thefluids may contribute to a better understanding of the size and mechanism of migrations, both vertical and lateral (investigations limited to one reservoir bed; regional investigations; nation-wide comparative studies, etc.).

The operations of project No 4.4 rely mainly on the results of well-logging and surficial geophysical (seismic) measurements. With analysing the various kinds of movements; determining their being compressive or disjunctive in character; studying the geological-structural setting of the area both vertically and horizontally, the afore-mentioned operations do not only help clarify the structural distribution pattern, but they are closely connected with, and very helpful, in exploring the diagenesis and alterations of the rocks (project No 5.4) as well as in determining the degree of diagenesis, the pressure and temperature conditions and the spatial distribution of these characteristics (project No 5.3). The question to be answered is the amount of hydrocarbon mobilized from the mother rock already defined spatially.

Under project No 6.1 partly the information on diagenesis, partly geochemical investigations including infrared spectrometry and isotopic geochemistry [measurements of insoluble kerogens, asphalts, their $^{13}C/^{12}C$ ratios, the isotopic ratios of carbonates, trace elements, $^{40}Ar/^{36}Ar$ ratios as determined in CO_2 and N gases, etc.] are utilized in an attempt at approximating the quantity of hydrogen that may have migrated off the mother rock. Combining all these methods as expounded in the previous paragraphs, project No 6.2 is to explore the laws and regularities of migration as they may apply to this phenomenon in general, to an entire basin, to its subbasins and to stratigraphic subdivisions, etc.

The results of projects 6.1 and 6.2 are to culminate in the performance envisaged under project No 7: determination of the laws of accumulation of hydrocarbons. What is reached with these investigations is the final summarization of fundamental and laboratory research which is properly the final aim of these working phases.

Project No 6.1 may lead directly to No 8.1 — the calculation of the potential hydrocarbon reserves. This gives the basis for the estimation of the rate and volume of prospecting even in the case when the requirements of No 7 or possibly of 8.2, a project very difficult to carry out, cannot be met because of the lack of information. Nota bene, before setting to the synthesis of No 9 the greatest difficulties are faced in meeting the requirements listed under No 8.1 and 8.2, i.e. in determining the hydrocarbon reserves which may have accumulated in the studied area (potential reserves) and in locating the zones of accumulation of the reserves thus estimated.

Further tasks of the management consist in assessing the perspectives and possibilities of prospecting (project No 9). Under project No 10 the potential hydrocarbon reserves are economically evaluated with consi-

deration of the current economic motivators and situation, and comparisons are made with the costs required and the labour force, equipment, etc. available. This is how the trends of prospecting are formulated under No 11. Under this project the working capacities and the character of the proposed perspectivic areas as well as the technologico-economic principles to be adopted are specified.

After these works the practical experiences, the scientific progress, the completed prospecting operations and the applied methods are reviewed and analysed. On the basis of the results of No 12 it is often necessary to switch back to several preceding projects in order to draw conclusions therefrom and to recommence prospecting after that. Cases when re-prospecting of areas which had been qualified by contemporary methods as having little perspective, if any, was succesful did not fail to occur in this country either.

Project No 13 is to formulate the proportions of prospecting in dependence on the potential reserves and the results of economic analyses. The volumes of preliminary geological investigations and exploratory drilling are to be specified both separately, with respect to one another, and combined. Special mention should be made of the growth of capacities and performance as a result of technological progress: a development which does cause changes in the proportions even if all the other circumstances remain unchanged.

Under No 14 the policy of prospecting is formulated. Prospecting policy has as its task to define the activities to be undertaken in the long run, 15 to 25 years, in dependence on the potential trends. This is where the Hungarian areas are ranked in terms of the order of preference.

Under No 15 a five-year plan of prospecting is prepared. This plan is then developed into annual operative plans, and the changes observed during the execution of each of these (discovery of large oilfields or results falling short of the average, etc.) are to be taken into consideration in the subsequent years' provisions of the five-year plan.

All these are to be based upon the most accurate possible determination of the potential Hungarian resources and upon the best possible definition of the trends and rates of hydrocarbon prospecting.

The estimation of the so-called prognostic reserves which are still to be explored is, as a rule, carried out every five years. The first work of this kind was undertaken in 1959–1960, the second in 1964, the third in 1969.

As evident from Fig. 1, geochemistry has to be very largely involved in the complex working process launched presently.

As for the evaluation of the perspectives of hydrocarbon prospecting, both the geological and economic conditions are determinant. To determine the amounts of the prognostic hydrocarbon reserves and of their potential spatial distribution is the task of the geologist, the analysis of the rentability of prospecting is to be performed by the economist.

The present paper has been aimed at defining the function (place) of the geochemical factors within the assemblage of geo-factors, at in-

dicating all what is to be done and at distributing the projects among the working places and at fitting them in the scheme outlined in Fig. 1.

The proposed scheme of activities is motivated by the following geological facts:

- Hungary's contemporary CH deposits developed after the Alpine orogeny. The Early Paleozoic accumulations of CH were mobilized, redeposited or dispersed under the influence of the Variscian orogeny, the Late Paleozoic-Mesozoic ones under that of the Alpine orogeny.
- Having been metamorphosed during the Variscian orogeny, the Lower Paleozoic mother rocks lost their CH content and their potential reserves could no longer supply materials for the accumulation of reservoirs in Late Paleozoic-Mesozoic times. Therefore, let us direct attention primarily to the post-Variscian events and formations.
- The Late Paleozoic-Mesozoic mother rocks discharged a part of their CH content already before the Alpine orogeny. The amount of CH they were still able to supply after the Alpine orogeny remains to be determined. It can be supposed, however, that the contemporary CH reservoirs of Hungary are the product of Neogene CH formation.
- In Late Paleozoic-Mesozoic time the territory of Hungary was part of the Tethyan geosyncline, in Neogene time it belonged to the Pannonian inland sea. The geological investigations of fluids should start from the consideration of the arrangement of the facial zones of these seas.
  One of the first problems to be solved should be to determine the facial zones of the Tethys and the Pannonian inland sea. As for the Tethys, its facial zones are essentially known.

Comparing the pre-Neogene core samples of our deep drill holes with the formations exposed in the Hungarian Central Mountains, the respective laboratory analyses should permit to determine the arrangement of the facial zones and to supplement the informations obtained in the mountainous regions of this country in order to develop the general stratigraphic scale for each particular facial zone.

The determination of the facial zones of the Pannonian inland sea should be carried out by uniform methods of investigations embracing the entire basin of the sea. On account of its subject this project should be performed by combined efforts of the nations sharing its territory. First of all, the sediments of the Pannonian inland sea, the Neogene sequence, should be subdivided stratigraphically in the fullest possible detail with the aid of the paleontological record and well-logging information (markers). The investigations of the extension, thicknesses and facial distribution of the individual horizons are to provide valuable data for the understanding of the paleogeographic pattern of the sea.

The investigations of the arrangement of the facies should be coupled with simultaneous efforts to find post-Variscian mother rocks and to explore their spatial distribution. For the identification of mother rocks, the geochemical methods applied succesfully in the region of the Algyő oilfield can be used.

In detecting Upper Paleozoic – Mesozoic – Paleogene mother rocks we should rely primarily on Central Mountains results. And all what we can afford now is to calculate averages by facial zones as deduceable from the general stratigraphic pattern. Therefore, efforts should be focussed to achieve this goal.

The possibilites for the detailed investigations of Neogene mother rocks are granted, and to obtain results seems to be just a matter of statistics. The distribution of mother rocks seems to be closely interrelated with the distribution pattern of the facies. Therefore, evaluations are to be carried out separately for each particular horizon and facies.

Parallel with investigating the facies distribution patterns and detecting the mother rocks, hydrocarbon prospectors should also tackle the regularities of the diagenesis of the Neogene sequence. The spatial distribution of the degree of diagenesis (degree of compaction and mineralogical-chemical alteration) should be explored. For, to determine the potential CH reserves it is a basic question to know the quantity of CH mobilized from the mother rocks in Neogene time. This, however, appears to be more simple in case of Neogene formations. Nota bene, the organic components of the mother rocks may be supposed to increase with increasing diagenesis. With a great number of analyses, this function – and hence the original and the present-day organic contents of the mother rocks – will be determinable. The difference between the original and present-day contents will equal the quantity of the mobilized organic material.

For the time being it looks very difficult to find out if the Upper Paleozoic-Mesozoic-Paleogene mother rocks may have supplied any hydrocarbon and if yes, how much. The relationship to be found between the quantity of organic components in the Neogene mother rocks and the degree of their diagenesis may be hoped to help answer this question, too.

Investigations of diagenesis may promote to determine both the amount of the mobilized organic matter and the time and regularities of migration. A gradually increasing amount of data indicate e.g. that diagenetical processes of dissolution and precipitation are subordinate in the hydrocarbon-filled reservoir. Therefore, the degree of the diagenesis of the reservoir indicates the time of the filling up of the reservoir.

The contemporary spatial distribution of the physico-chemical characteristics of fluids and of the pressure and temperature conditions may also contribute valuable information to the understanding of the regularities of migration.

If the regularities of migration and the quantity of the organic material mobilized in Neogene time are known, the potential CH reserves can be assessed. On the basis of the spatial distribution of the mother and

reservoir rocks, the regularities of migration and the structural conditions of the principal zones of accumulation can be located with very high probability.

The Geochemical Working Group of the National Oil-and-Gas Trust (National Gas Industry Laboratory) are measuring the parametres found to be useful and serviceable on the basis of earlier investigations, with special emphasis on the C^{13} ratio in carbonates, the isotopic ratio of C in the soluble and insoluble organic components, and the eventual anomalies of the trace element contents of the rocks. They analyse by infrared techniques the bitumen content of sedimentary rocks. Vertical migration above the hydrocarbon reservoirs is being examined by means of gas-chromatography and the determination of the C^{12}/C^{13} ratio. Soil gases are being analysed and the results geochemically evaluated. Hydrogeological-hydrochemical investigations are being conducted for the exploration of aquifers and the determination of their subsurface flow pattern and genetics.

The staff of the Department of Mineralogy and Geochemistry of József Attila University, Szeged, are carrying out complex analyses of the carbonates in sedimentary rocks [Ca/Mg ratio, process and degree of dolomitization, quantitative analyses of limestones, Mg-containing limestones and dolomites and/or clay minerals in carbonate rocks, petrographic investigations, studies on stilolitization]. They are investigating the insoluble organic components of sedimentary rocks (quantity and nature of the insoluble organic material; relationship between insoluble organic material – carbonates – clay minerals – trace elements). In addition, clay minerals are being analysed (adsorption properties; relations between salinity of solution – type of clay mineral – ionic adsorption; influence of dolomitization-inducing processes on clay minerals). Furthermore, they are studying the oxidation-reduction capacity of carbonaceous sedimentary rocks; evaluating the inorganic and organic factors responsible for oxidation-reduction capacity; characterizing, and classifying the rocks in such terms; comparing them with other parametres.

What still remains to be solved is to determine the quantity of organic components soluble in organic solvents; to determine the quantity of aminous acids in fossils, and also to get new research stations involved in the above projects and to coordinate their contributions.

TRILOBITICERAS (AMMONOIDEA, OTOITIDAE) FROM THE BAJOCIAN (MIDDLE JURASSIC) OF THE BAKONY MOUNTAINS

by

A. GALÁCZ

(Department of Paleontology, Eötvös Loránd University)

(Received: 27 February 1971)

РЕЗЮМЕ

Род Trilobiticeras B u c k m a n, относящийся к семейству Otoitidae, включает в себя аммониты, интересные с морфологической, систематической и стратиграфической точек зрения. У данного космополитного рода, имеющего, по-видимому, невыдержанный ареал распространения, до сих пор было известно всего 9 представителей, найденных на трех континентах. Рассматриваемый экземпляр, найденный в восточной части Средиземноморской зоогеографической области, относится к виду T. trilobitodes B u c k m.

Introduction

During the detailed processing of the Jurassic of the Bakony Mountains several exploratory trenches were dug on the Lókút hill (Fig. 1) in which the Jurassic formations have been uncovered. Out of these, in the detritus of the section uncovered near the well in the valley between the Lókút hill and the Kávàshegy, geologist P. J a k u s found a small otoitid ammonite while participating in a geological excursion to the area. In the course of the processing of the other fossils deriving from the Lókút hill this ammonite was found to represent an extraordinary find belonging to the genus *Trilobiticeras* of extremely rare occurrence. *Trilobiticeras* is also important from the stratigraphic point of view, as its presence has helped determine the age of the uncovered rock which had been impossible on the basis of the poor paleontological record available prior to this find.

Genus Trilobiticeras S. Buckman 1919

Type species. According to the original designation (B u c k m a n 1909 30, Pl. 115, fig. 1–4) – *Trilobiticeras trilobitoides* B u c k m a n, Inferior Oolite, Fossil Bed (upper part), Bradford Abbas, Dorset, England.

After re-examining the classical ammonite material collected from Cap San Vigilio by V a c e k (1886), W e s t e r m a n n (1964, p. 52 and 57) found "*Stephanoceras punctum* V a c e k" to be the phragmocone of a *Trilobiticeras*. On the strength of additional two English specimens

collected from Buckman's locality he stated that *T. trilobitoides* Buckm. was a synonym of *T. punctum* (Vacek) so that the type of *Trilobiticeras* would be this last-mentioned North Italian species.

However, not even on the basis of Westermann's own figures does it seem convincing to unite the two forms. His newer English finds (Westermann 1964, Pl. 6, fig. 5–6) are undoubtedly identical with the form of Cap San Vigilio, differring, however, from the type of *T. trilobitoides* Buckm.

The characters of the genus

Trilobiticeras includes involute, coronate, auriculate ammonites of small size. Resembling that of *Otoites*, the ornament is constituted by strong primary and high secondary ribs with a distinct row of tubercles on the flanks. The suture is Otoites-like, with three-branched lateral lobes and wide and high saddles.

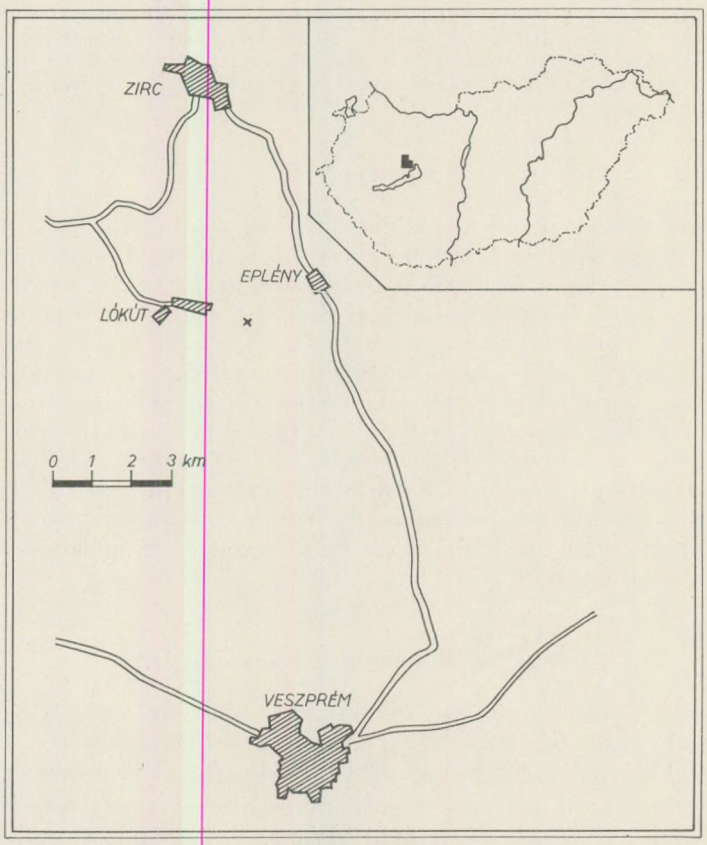

Fig. 1. Layout of the vicinity of Lókút
(x = location of exposure)

Forms referred to the genus

Beside the type species 4 additional species can be included in the genus Trilobiticeras.

Trilobiticeras punctum (V a c e k) 1886. It was W e s t e r m a n n who showed it to belong to the genus under consideration and who also included the type specimen of *T. platygaster* B u c k m a n (1909–30, Pl. 277.A) in this species. The two specimens found recently in England (W e s t e r m a n n 1964, Pl. 6, fig 5–6) also belong here.

Trilobiticeras depressum (W h i t e h o u s e) 1924. In his monograph on the otoitids, W e s t e r m a n n (1954) referred W h i t e h o u s e's *Otoites depressum* (1924, Pl. I, fig. 4–6) to the genus *Trilobiticeras*. During his revision of the Bajocian fauna of Western Australia, A r k e l l (1954, p. 170–71), partly with reference to W e s t e r m a n n, also classed this form to belong to this genus, though with a question mark. *Trilobiticeras* sp. nov. W e s t e r m a n n 1964. W e s t e r m a n n based this species on what had been published (B u c k m a n 1909–30 Pl. 277.B) as a paratype of *T. platygaster* B u c k m.

Trilobiticeras n. sp. indet. W e s t e r m a n n 1969. This new species deriving from the Bajocian of Alaska was described again by W e s t e r m a n n (1969).

Systematic position

B u c k m a n placed the genus *Trilobiticeras, inter alia,* with *Otoites* and *Docidoceras* (1909–30, T. A. III. p. 22), in the family Sphaeroceratidae.

S p a t h (1936, p. 13) referred B u c k m a n's genera belonging to the family Sphaeroceratidae, under the name Otoitinae, to the family Stephanoceratidae as a subfamily of this.

W e s t e r m a n n (1954) discussed *Trilobiticeras* as an independent genus of the subfamily Otoitinae. A r k e l l (1954) took *Trilobiticeras* to be a subgenus of *Otoites* and discussed it in the T r e a t i s e in the same systematic position (A r k e l l et al. 1957, p. L 287). In 1964 W e s t e r m a n n revised the systematics of the Otoitidae on the basis of sexual dimorphism. In this connection, *Trilobiticeras* was also taken to be a subgenus of *Docidoceras* and to represent a microconch (male) form of this genus. S c h i n d e w o l f (1965, p. 163) disagreed with this classification, for he discredited that *Trilobiticeras* might belong to the Otoitidae on the strength of the suture, and would not consider it a subgenus of *Docidoceras* either.

On the basis of its morphological characters *Trilobiticeras* should be referred to the family Otoitidae, but the stratigraphic hiatus, which separates this form occurring in the Discites Subzone from the *Otoites* appearing in the Sauzei Zone, makes the possibility of a subgeneric connection doubtful.

Placing *Trilobiticeras* in the genus *Docidoceras* on the basis of dimorphism may become justified only when the dimorphism of the ammonites is based on more general principles.

Geographic distribution and stratigraphic range

Trilobiticeras is a very rare ammonite: judging by the literature the number of specimens belonging here is as low as 9. These few specimens, however, were encountered on three continents: Europe (3 localities), North America (Western Alaska) and Western Australia. In Europe the English localities belong to the Northwest European faunal province, the localities of Northern Italy and Hungary belong to the Mediterranean realm, the Australian locality being in the Indo-Pacific region. Consequently, *Trilobiticeras* is a genuine cosmopolitan ammonite, possibly with a disjunct area.

Despite their having been found at great distances from one another, the representatives of *Trilobiticeras* have a very narrow stratigraphic range. From Alaska to Western Australia, all occurrences agree in age, all derive from the Lower Bajocian and, wherever an exact dating is possible, from the Discites Subzone of the Sonninia sowerbyi Zone. *Trilobiticeras* shows a close relationship with the genus *Docidoceras* as far as stratigraphic range and geographic distribution are concerned. And, beside morphological similarity, this has played an important role in the investigations of the dimorphism of the genus.

Dimorphism

It was W e s t e r m a n n (1964) who paired microconch *Trilobiticeras* — as a male subgenus — with *Docidoceras*. On the basis of his figures (loc. cit. Pl. 6, fig. 4—7) the two forms undoubtedly form a microconch-macroconch pair as far as their morphological characters are concerned. The similarity in whorl ornament between the two genera seems to have been observed already by B u c k m a n himself, for he first labelled his *T. trilobitoides* as a "Docidoceratan phaulomorph" (1909—30, Pl. 140, c.f. W e s t e r m a n n 1964, p. 57) .

Their stratigraphic range is indentical, too: both *Docidoceras* and *Trilobiticeras* are confined to the Discites Subzone. As a rule, the localities of forms surely belonging to *Trilobiticeras* have yielded *Docidoceras* specimens, too. Exception to the rule is only the Bajocian fauna of Western Australia. However, *Docidoceras* have recently been encountered in the Indo-Pacific region (Western New Guinea; W e s t e r m a n n — G e t t y, 1970, p. 244—47, Pl. 50), too.

On the basis of the above, the couple *Trilobiticeras-Docidoceras* is one of the most eloquent examples of the dimorphism of ammonites. It does not provide any contribution, however, to the paleobiological fundamentals of the theory. Therefore, C a l l o m o n's statement (1969, p. 116) that "... the sexual origin of the dimorphism in ammonites can never be proved ..." remains still valid. Accordingly, discussing *Tri-*

lobiticeras as an independent genus and adopting the conventional nomenclature does not contradict either morphological or paleobiological criteria.

Trilobiticeras trilobitoides Buckman 1919

Fig. 2, a–d

? 1885. *Sphaeroceras Sauzei*, d'Orb. Douvillé, H. 1885., p. 41. Pl. III. fig. 9.
* 1919. *Trilobiticeras trilobitoides*, nov. Buckman, S. S. 1909–1930., Pl. 115. fig. 1–4.
1954. *Trilobiticeras trilobitoides* Buckman, 1919. Westermann, G. 1954. p. 122.

Number of specimens: 1 internal mould of good preservation.
Dimensions: 29 mm 10,5 mm (36) 13 mm (45) 11 mm (38)
23 mm 9 mm (39) 14,5 mm (63) 7,5 mm (32,5)

Description: Small, slightly ellipticone microconch. Umbilicus deep, fairly broad, becoming a little wider in the last quarter of whorl. Whorl-section trapezoidal, with a wide venter. The greatest width can be measured at the level of the tubercles. Ornament well-developed, Otoites-like. Primary ribs short, strong, radial, ending in high tubercles from which pass slightly rursiradiate, sharp, high lateral ribs. On the last whorl there are 19 primaries and 41 secondaries. The body–chamber accounting for 3/4 of whorl and beginning at about 17 mm diametre contracts evenly towards the aperture, and its ribs become a little more widely spaced. The apertural region is poorly visible, as the specimen is just an internal mould and the lappets have not been preserved. The traces of the strong tubercles which used to be at the base of the lappets, however, are distinct on one flank (the other flank of the specimen has been lost to post-depositional subsolution). Suture line rather simple (Fig. 2 d), corresponding well in characters to the suture of *T. punctum* (Vacek) figured by Westermann (1964, Pl. 6, fig. 7 b).

Remarks: With its size ratios and ornament, the Lókút specimen agrees well with the type. There is, however, some difference in height:

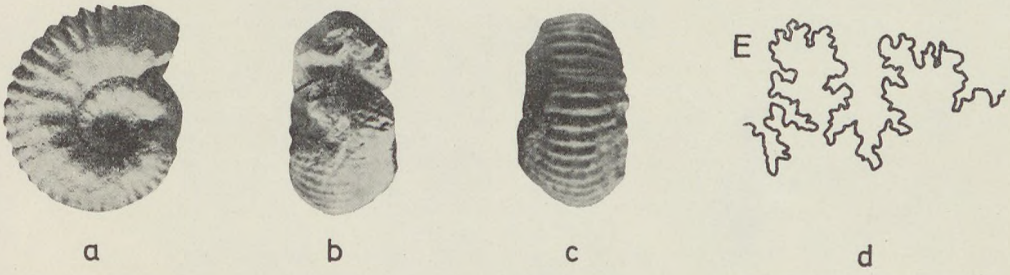

Fig. 2. Trilobiticeras trilobitoides Buckman
a) lateral view; *b)* ventral view; *c)* frontal view (natural size); *d)* suture line (magnification 5*x*)

the Lókút specimen is a little bigger than Buckman's type (a maximum of 29 mm in diametre). As for the "*Sphaeroceras Sauzei*" deriving from the Lower Bajocian of the vicinity of Toulon, it seems to belong to *Trilobiticeras*. As indicated in Douvillé's description (1885, p. 41), that specimen differs from *Otoites sauzéi* (d'Orb.) primarily by its smaller size. Although Douvillé did not give any absolute dimension, on the strength of his figure and the lowermost Bajocian age of the associated fauna his specimen may be supposed to belong to *T. trilobitoides* Buckm.

As for *T. trilobitoides*, it differs from *T. punctum* by the greater width of its whorl, by its coarser ribs and stronger tubercles, from *T. depressum* by its smaller size. The species, which Westermann based in 1964 on the paratype of *T. platygaster* (Buckman 1909–30, Pl. 277 B), is characterized by a more depressed cross-section, a somewhat wider umbilicus and more irregular ribs. As for the Alaskan form described by Westermann (1969), it can be distinguished from the other *Trilobiticeras* on the basis of its prorsiradiate ribs.

Occurence: The *Trilobiticeras* known so far were all found in the Discites Subzone of the Lower Bajocian. The exact stratigraphic position of the Lókút specimen is unknown. In the exposure which is now in a bad condition, just a few, stratigraphically undiagnostic *Phylloceras* and *Lytoceras*, as well as two specifically unidentifiable fragments of *Bradfordia* sp. were encountered. A few hundred metres away from the exposure there is a complete Bajocian profile, evidenced by fauna, of the same formation. In other parts of the Bakony Mountains (Csernye) the Sonninia sowerbyi Zone is well-known to occur with representatives of *Sonninia*, *Bradfordia* and *Docidoceras* (Géczy 1967).

The near-by Middle Jurassic section, whose rich paleontological material is being collected at present, is expected to yield additional information on the lowermost Bajocian ammonites, inclusive of *Trilobiticeras*.

REFERENCES

Arkell, W. J. – Playford, P. E. (1954): The Bajocian ammonites of Western Australia. Phil. Trans. Roy. Soc. London. Ser. B, No. 651, Vol. 237.

Arkell, W. J. – Kummel, B. – Wright, C. W. (1957): Mesozoic Ammonites. Treatise Inv. Pal., Part. L, Mollusca 4. Geol. Soc. America, Univ. Kansas Press.

Buckman, S. S. (1909–30): (Yorkshire) Type Ammonites. London.

Callomon, J. H. (1969): Dimorphism in Jurassic ammonites. Some reflections. In: G.E.G. Westermann ed.: Sexual dimorphism in fossil Metazoa and taxonomic implications. An IPUCE Symposium. IUGS Ser. A, No. 1. Stuttgart.

Douvillé, H. (1885): Sur quelques fossiles de la zone à Ammonites Sowerbyi des environs de Toulon. Bull. Soc. géol. France. (3) 13.

Géczy, B. (1967): Ammonoïdes jurassiques de Csernye, Montagne Bakony, Hongrie. Part II. Geol. Hung. Ser. Pal., fasc. 35.

Schindewolf, O. H. (1965): Studien zur Stammesgeschichte der Ammoniten. Lieferung IV. Abh. math.-nat. wiss. Kl. Akad. Wissensch. Mainz. Jahrg. 1965. No. 3.

Spath, L. F. (1936): On Bajocian ammonites and belemnites from Eastern Persia (Iran). Palaeont. Indica., N.S. VIII, Mem. 3.

Vacek, M. (1886): Über die Fauna der Oolithe von Cap S. Vigilio, verbunden mit einer Studie über die obere-Liasgrenze. Abh. k.-k. geol. Reichsanst. XII, 3.

Westermann, G. (1954): Monographie der Otoitidae (Ammonoidea). Beih. Geol. Jb. 15.

Westermann, G. E. G. (1964): Sexual-Dimorphismus bei Ammonoideen und seine Bedeutung für die Taxonomie der Otoitidae (einschliesslich Sphaeroceratinae; Ammonitina, M. Jura). Palaeontographica 124. A.

Westermann, G. E. G. (1969): The ammonite fauna of the Kialagvik Formation at Wide Bay, Alaska Peninsula. Part II. Sonninia Sowerbyi Zone (Bajocian). Bull. Amer. Paleont. Vol. 57. No. 255.

Westermann, G. E. G. – Getty, T. A. (1970): New Middle Jurassic Ammonitina from New Guinea. Bull. Amer. Paleont. Vol. 57. No. 256.

Whitehouse, F. W. (1924): Some Jurassic fossils from Western Australia. J. Roy. Soc. W. Austr. 11. 1.

AMMONITE FAUNAE FROM THE LOWER JURASSIC STANDARD PROFILE AT LÓKÚT, BAKONY MOUNTAINS, HUNGARY

by

B. GÉCZY

(Department of Paleontology, Eötvös Loránd University)

(Received: 23. Febr. 1971)

Известняки, вскрытые на легко доступном склоне Локутского холма, представляют собой все ярусы нижнеюрского отдела. Три зоны синемюрского яруса и шесть зон плинсбаха обоснованы фауной. Удивительно, как маломощная толща пород может служить основанием для восстановления продолжительного геоисторического развития района. Хотя в маломощной толще юры и приходится искать содержащие фауну слои, все же корреляционная диаграмма почти полностью заполнена.

Корреляция основывалась, в первую очередь, на присутствии северо-западно – европейских руководящих форм зон или подзон. Можно предположить, что ареалы этих видов расширились в период их расцвета. Следовательно, спорадические находки их в нижнеюрских отложениях Средиземноморской области являются синхронными с их акме. В принципе можно было бы также предположить, что вертикальное распространение этих видов было различным в Северо-Европейской и Средиземноморской зоогеографических провинциях соответственно и что некоторые группы мигрировали в новые районы, покинув свои оригинальные места обитания. Такой гипотезе противоречит факт, что последовательность руководящих видов является одинаковой в обеих зоогеографических провинциях.

Если хронологическое расчленение Локутского разреза правильно, то следует считаться с тем, что ряд представителей родов Protogrammoceras и Fuciniceras появились раньше, чем об этом можно прочесть в известных автору публикациях, по крайней мере, в восточных частях Средиземноморской области.

В количественном отношении обращает на себя внимание обогащение аммонитов на границе между зонами с davoei и stokesi. Зона с obtusum и верх зоны с jamesoni также характеризуются богатой фауной. Однако, зоны с semicostatum, ibex и stokesi отличаются бедной фауной. Зона с oxynotum до сих пор не обоснована фауной. Процентные содержания представителей семейств Phylloceratidae и Lytoceratidae как правило, являются бóльшими, чем в районах, расположенных вблизи подводных поднятий, но меньшими, чем во внутрибассейновых отложениях, более отдаленных от этих поднятий.

В горах Баконь уже Телеги-Рот (1934) установил, что „сколько разрезов лейаса, столько и схем стратиграфической последовательности пластов". Конда (1970) отнес различные разрезы к двум главным группам в зависимости от беспрерывности или невыдержанности осадконакопления. По данным Конды Локутский разрез принадлежит к типу беспрерывных разрезов нижней юры. Исследования фауны могли только подтвердить его мнение. В раннеюрскую эпоху район с. Локут представлял собою, по-видимому, такой участок бассейна, где органический детритовый материал, поступавший из районов подводных поднятий, время от времени изменял характер известняков ammonitico rosso.

Introduction

In the Bakony Mountains – a territory covered for the most part by Pleistocene sediments which have escaped post-depositional denudation – the localities offering comparatively continuous Jurassic sequences are relatively rare. In the northern Bakony Mountains, Lower Jurassic sequences of rather great thickness and good exposure are known to occur in the vicinity of Csernye and Lókút only. The Upper Sinemurian and Pliensbachian are dated in both areas by a rich Ammonite fauna. Whereas at Csernye the Toarcian includes fauna-rich beds too, in the manganiferous Toarcian beds of Lókút no ammonite has been found as of yet. However, at Lókút the Lower Sinemurian too can be subdivided by ammonites, while at Csernye this substage is represented by a thick sequence of cherts devoid of fauna. The two standard profiles provide mutually complementing contributions to the Lower Jurassic of Hungary.

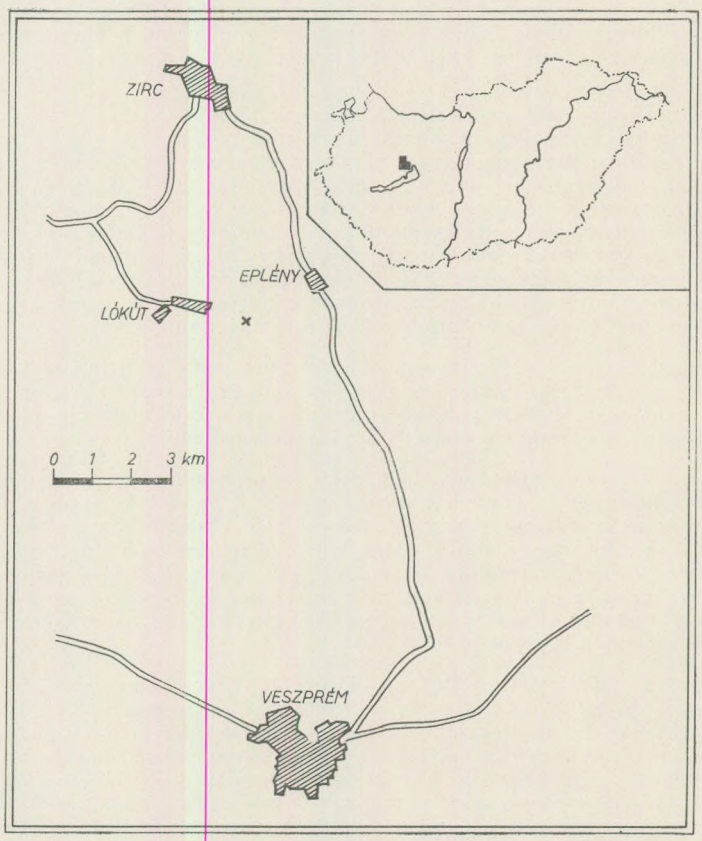

Fig. 1. Topographic sketch of the Lókút standard profile

The Lókút standard profile lies some 2 km to the ESE of Lókút in the vicinity of Zirc, at the SE extremity of the Lókút hill, to the S of Olaszfalu village.

The geological significance of the locality was recognized by Telegdi Roth (1934). The first detailed geological description was published by Kovács (1963). This author distinguished at Lókút two Ammonite faunae by the zones of

Amaltheus margaritatus and
Arietites bucklandi.

According to Noszky (1961), it is solely the Arnioceras semicostatum Zone that can be identified at Lókút by the presence of the zonal index species. Between 1961 and 1970 Konda re-investigated the Lókút profile in detail. New diggings have enabled him to collect an abundant fauna from – this time already continuous – exposure. The surfaces sampled had an average size of 2 m^2. It was Konda who entrusted the present writer with elaborating the fauna. The author whishes to use this opportunity to extend his thanks for it. In 1970 Konda gave a detailed, large-scale, geological map, section und up-to-date description of the locality. In the present paper the biostratigraphical results have been summarized.

Lithologically, in the Lower Jurassic of Lókút three main types of facies can be distinguished:

(3) manganiferous clays and marls;

(2) Ammonitico Rosso limestone and its variant containing crinoids, sponge spicules and *Bositra;*

(1) yellowish-white oölitic limestone.

(1) is exposed at the foot of the hill, in an abandoned quarry. Since the lower part of the overlying pink crinoidal limestone contains Hettangian brachiopods, the oölitic limestone seems to belong to the Lower Hettangian.

(2) The pink to red crinoidal limestone and the subsequent cherty and *Bositra*-bearing limestones, overlying the crinoidal one, represent the thickest formation of the Lókút hill. Ammonites have so far been found in this formation only. The fauna shows a very irregular distribution in the sediments. In the Ammonitico Rosso limestone sequence consisting of a total of 400 beds, as few as 25 beds were found to contain macrofauna. The fossiliferous horizons are typical representatives of the Ammonitico Rosso limestone, the thick unfossiliferous interlayers are characterized by accumulations of biogenic materials. (2) spans the stratigraphic range of the Sinemurian and Pliensbachian Stages. In spite of the temporary lack of the prerequisites for fossilization during the deposition of the afore-mentioned interlayers, the fossiliferous beds provide information about almost all of the zones of the two stages. A comparison of the 25 fossiliferous beds with one another gives insight into Mediterranean faunal evolution.

(3) With a view to the synchronous manganese ore deposition in the adjacent territories and to the fossiliferous Aalenian formations exposed at the top of the Lókút hill, the fauna-free manganiferous clays and marls belong to the Toarcian Stage.

SINEMURIAN

1. Arietites bucklandi Zone

The lowermost Sinemurian was discovered by K o n d a during the preparations for the excursion of the Colloquium on Mediterranean Jurassic Stratigraphy held in 1969 in Budapest. Forming a lens within the pink crinoidal limestone, this ammonitic clayey limestone, hardly attaining some 10 cm in thickness (Bed 100), pinches out still within the quarry in the direction of the Kávashegy. It contains large ammonites: poorly preserved internal moulds which are slightly compressed in many cases. The ammonites belong tho the following species:

Geyeroceras cf. *cylindricum* (S o w e r b y, 1831)
Tragolytoceras cf. *altecinctum* (H a u e r, 1866)
Tragolytoceras sp.
Tragolytoceras ? n. sp. aff. *ferstli* (H a u e r, 1854)
Tragolytoceras ? sp.
Canavarites n. sp. aff. *ligusticus* (C o c c h i in C a n a v a r i, 1882)
Coroniceras (Metophioceras) cf. *conybeari* (S o w e r b y, 1816)
Coroniceras (Metophioceras) cf. *longidomus* (Q u e n s t e d t, 1885)
Coroniceras (Metophioceras) n. sp.
Coroniceras (Metophioceras) sp.
Vermiceras sp.

In the fauna the representatives of Phylloceratidae are rather scarce (4%), Juraphyllitidae are absent, the share of Lytoceratidae is 24%, while Ammonitinae account for 72% of the fauna.

Predominant in the fauna are the representatives of *Coroniceras (Metophioceras)*. In addition, the *Tragolytoceras* are significant. The metophioceratids date the fauna convincingly as corresponding to the basal part of the Bucklandi Zone. According to D e a n, D o n o v a n and H o w a r t h (1961, p. 449), the appearance of the subgenus *Metophioceras* marks the base of the Sinemurian (= Conybeari Subzone). In the southern Bakony Mountains, B ö c k h (1873) recorded the presence of "*Ammonites*" *conybeari* – and, in this connection, that of the Bucklandi Zone – as early as a century ago. The northern Bakony occurrence will support the opinion concerning the distribution of *Metophioceras* and justify the present writer in drawing the following two biostratigraphic conclusions:

1. it is only the part below the ammonitic bed of the pink crinoidal limestone that may belong to the Upper Hettangian,
2. the first traces of the Ammonitico Rosso facies appear in the lowermost Sinemurian already.

Although a thin, pinching-out ammonitic intercalation does not represent a well-mappable change in facies, the break in sedimentation, the concentration of the fauna, the manifestations of subsolution here indicate a difference from the earlier Hettangian sediments showing many features which are still reminiscent of Upper Triassic sedimentation. Even though the Hettangian-Sinemurian boundary is not sharp, yet it does represent a significant change as compared to earlier sedimentation.

2. Arnioceras semicostatum Zone

Up in the profile the crinoidal beds are followed by a new ammonitic bed (Bed 120). This purple-pink to greenish-grey limestone contains scant and poorly preserved ammonite fragments:

Phylloceras ? sp.
Peltolytoceras altiformis (B o n a r e l l i, 1900)
Ectocentries cf. *altus* (H a u e r, 1856)
Ectocentrites n. sp. aff. *canavarii* (B o n a r e l l i, 1900)
Ectocentrites ? sp. aff. *contraria* (F u c i n i, 1901)
Arnioceras sp.
Arnioceras ? sp.
Paracoroniceras ? sp.

On the strength of the presence of *Arnioceras* and the absence of *Asteroceras*, Bed 120 is referred to the Semicostatum Zone interpreted in the broader sense so as to include the Caenisites turneri Zone. In the Semicostatum Zone the number of Phylloceratidae is a little higher (7%). Juraphyllitidae are absent. Lytoceratidae account for 36% of the fauna, especially Ectocentrites is frequent among them. Ammonitinae are predominant (57%) in the fauna.

3. Asteroceras obtusum Zone

Towards the middle stretch of the profile an enrichment of silicosponge spicules and chert nodules can be observed in the crinoidal limestone. A new ammonitic limestone intercalation appears in the cherty crinoidal sediments (Beds 206 – 209). This intercalation of some 50 cm thickness was recorded by K o n d a in the Lókút profile as well (Profile A, Bed 3). The ammonites enclosed in the red, compact limestone are internal moulds of medium preservation, showing, in many cases, traces of subsolution on both sides. These limestones of typical Ammonitico Rosso facies contain the following fauna:

Phylloceras oenotrium (F u c i n i, 1901)
Phylloceras sp.
Geyeroceras cylindricum (S o w e r b y, 1831)
Partschiceras sp.
Juraphyllites cf. *lunensis* (D e S t e f a n i, 1886)
Juraphyllites sp.
Paradasyceras ? n. sp.
Lytoceras sp.

Angulaticeras dumortieri (Fucini, 1903)
Anglaticeras sp.
Arnioceras mendax (Fucini, 1902)
Arnioceras mendax plicatella (Fucini, 1902)
Arnioceras rejectum (Fucini, 1902)
Arnioceras cf. *insigne* (Fucini, 1902)
Arnioceras cf. *speciosum* (Fucini, 1902)
Arnioceras simile (Fucini, 1902)
Arnioceras arnouldi (Dumortier, 1867) ?
Arnioceras sp.
Asteroceras cf. *stellare* (Sowerby, 1815)
Asteroceras saltriense (Parona, 1896)
Asteroceras suevicum (Quenstedt, 1884)
Asteroceras cf. *reynesi* (Fucini, 1903)
Asteroceras sp.
Asteroceras ? sp.
Aegasteroceras cf. *sagittarium* (Blake, 1876)
Aegasteroceras sp.
Eparieties cf. *undaries* (Quenstedt, 1885)
Eparietites sp.
Epophioceras cf. *landrioti* (d'Orbigny, 1850)
Oxynoticeras cf. *soemanni* (Dumortier, 1867)
Oxynoticeras sp.
Xipheroceras sp.

The author takes this opportunity to express his gratitude to professors Dr. Donovan and Dr. Mouterde for the help they were so kind to give to him by identifying the representatives of *Aegasteroceras* and *Epophioceras*. The presence of *Asteroceras*, *Aegasteroceras* and *Eparieties* confirms convincingly that the fauna belongs to the Obtusum Zone.

The fauna is likely to span the whole range of the middle (Stellare Subzone) and upper (Denotatus Subzone) parts of the zone.

20% of the investigated fauna are constituted by Phylloceratidae, 13% by Juraphyllitidae, 9% by Lytoceratidae, and 58% by Ammonitinae. Within the last-mentioned taxon the *Arnioceras* (55%) are predominant. The subfamily Asteroceratinae shares 30% of the fauna.

4. Echioceras raricostatum Zone

The upper part of the cherty crinoidal limestone is characterized by the abundance of *Bositra*. In this member, ammonites were collected from Bed 291. The scarce fauna of very poor preservation comprises the following forms:

Phylloceras sp.
Partschiceras sp.
Juraphyllites sp.
Lytoceras ? sp.
Audaxlytoceras ? sp.
Tropidoceras sp. aff. *actaeon* (d'Orbigny, 1844)

The single *Tropidoceras* specimen is closely related to Hauer's "*Ammonites actaeon*" (1856, Pl. 9, fig. 6, 7), a species which occurs, accord-

ing to Donovan (1958), together with forms belonging to the Raricostatum Zone in the territory of Langeneckgrat, Germany. Parona (1896, Pl. II, fig. 4) recorded the same form from the Sinemurian. Although *Tropidoceras*, as a rule, are characteristic of the lower part of the Ibex Zone, in the Mediterranean areas a larger vertical range of the representatives of *actaeon* should be reckoned with. With a view to the succesive relations of its occurrence, Bed 291 is still referred to the upper part of the Sinemurian.

PLIENSBACHIAN

1. Uptonia jamesoni Zone

The red, crinoidal, cherty, *Bositra*-bearing limestone member grades upwards into a typical Ammonitico Rosso limestone. The lowermost fossiliferous limestone bed (Bed 436) was found to contain a single *Metaderoceras* ? sp. Bed 439, in its turn, is very rich in fauna, with partly shelled ammonite moulds in a good state of preservation:

Phylloceras cf. *hantkeni* (Schloenbach in Prinz, 1904)
Phylloceras sp.
Partschiceras sp.
Calliphylloceras cf. *emeryi* (Bettoni, 1900)
Calliphylloceras cf. *calais* (Meneghini, 1867–1881)
Calliphylloceras sp.
Lytoceras altum Vadász, 1910
Aegolytoceras cf. *czjzekii* (Hauer, 1853)
Juraphyllites libertus (Gemmellaro, 1884)
Juraphyllites sp.
Metoxynoticeras cf. *involutum* (Pompeckj, 1907)
Metaderoceras gemmellaroi (Levi, 1896) ?
Metaderoceras n. sp. aff. *submuticum* (Oppel, 1856)
Metaderoceras n. sp.
Metaderoceras sp.
Metaderoceras beirense Mouterde, 1970
Uptonia cf. *angusta* (Quenstedt, 1849)
Uptonia regnardi (D'Orbigny, 1844) n. subsp.
Uptonia sp.
Tropidoceras sp.
Liparoceras (Becheiceras) sp.
Protogrammoceras n. sp.
Protogrammoceras sp.
Protogrammoceras ? sp.

This fauna is referred to the uppermost Jamesoni Zone. The Jamesoni Zone is indicated by the presence of *Metoxynoticeras involutum* (cf. Futterer, 1893, p. 294; Pompeckj, 1907, p. 284 and Pia 1913, p. 57) and *Uptonia angusta* (cf. Donovan, 1954, p. 42). The single *Tropidoceras* specimen cannot be considered, in se, an evidence of the Ibex Zone, considering all what was written earlier about the *Tropidoceras acteon* group. In Mediterranean areas the representatives of *Metaderoceras* are characteristic of the Ibex Zone (cf. Dubar et al., 1967, p. 831). Their abundance at Lókút indicates the proximity of the Ibex

Zone. As for Arkell (1957, p. 247), he considered, erroneously, the genus *Metaderoceras* (Type: *Ammonites muticus* d'Orbigny, 1844) Spath (1925, p. 363) to be an objective synonym of the genus *Crucilobiceras* (Type: *C. crucilobatum* Buckman, 1920) Buckman, 1920. The inner whorls of the primitive *Metaderoceras* of Lókút are ornamented by strong, widely spaced outer tubercles resembling the ornamentation of the adult whorls of some *Apoderoceras* species (cf. *Apoderoceras ferox* Buckman, 1925, Pl. 451) characterizing the lower part of the Jamesoni Zone. Therefore, *Metaderoceras* are likely to have been produced by the evolution of the *Eoderoceras-Apoderoceras* lineage rather than being derivatives of the bituberculate *Crucilobiceras* confined to the lower part of the Raricostatum Zone. Consequently, the separation of the two genera is justified (Mouterde, 1970).

11.1% of the fauna of Bed 439 are shared by Phylloceratidae, 14,6% by Juraphyllitidae, 1,5% by Lytoceratidae, and 72,8% by Ammonitinae. Most abundant are the representatives of the genus *Juraphyllites* which is succeeded in frequency by *Metaderoceras*, *Calliphylloceras*, *Protogrammoceras* and *Uptonia*, respectively. The genera *Metoxynoticeras*, *Tropidoceras* and *Liparoceras* are represented by one specimen each.

As known presently, the *Protogrammoceras* did not occur anywhere in so old formations as they did in the Lókút profile. Since the first appearance of *Protogrammoceras* places the birth date of the superfamily Hildocerataceae in a new light, it has been found reasonable to figure the most typical ammonites of Bed 439 already before the publication of the monograph on the Lower Jurassic ammonites of the Bakony Mountain (Plates I–VII).

2. Tragophylloceras ibex Zone

The two unfossiliferous limestone beds following above the Jamesoni Zone are overlain again by ammonitic red limestones (Beds 441–460) which, however, contain just sporadical internal moulds of ammonites:

Phylloceras cf. *meneghinii* (Gemmellaro, 1874)
Phylloceras cf. *zetes* (d'Orbigny, 1849)
Phylloceras bonarelli (Bettoni, 1900)
Phylloceras sp.
Partschiceras sp.
Calliphylloceras geyeri (Bonarelli, 1895)
Calliphylloceras cf. *emeryi* (Bettoni, 1900)
Juraphyllites libertus (Gemmellaro, 1884)
Juraphyllites sp.
Harpophylloceras eximium (Hauer, 1854)
Meneghiniceras sp.
Lytoceras cf. *postfimbriatum* (Prinz, 1904)
Tropidoceras sp. (= *Cycloceras actaeon* in Futterer, 1893, Pl. XII fig. 2. non d'Orbigny, 1843)
Coeloceras ? n. sp. aff. *avanzatii* (Fucini, 1905)
Liparoceras sp.
Fuciniceras dubari (Cantaluppi – Montanari, 1968)
Fuciniceras sp. aff. *boscense* (Reynes, 1868)

Protogrammoceras costicillatum (Fucini, 1900) n. subp. (= *F.* cf. *costicillatum* in du Dresnay, 1963)
Protogrammoceras exiguum (Fucini, 1904)
Protogrammoceras sp.

Unfortunately enough, no index species has been found in Bed 441. Beds 442 to 455 are unfossiliferous. It is probable that these beds belong to the lower part of the Ibex Zone (Tropidoceras masseanum Subzone). Beds 456 to 460 seem to correspond to the upper part of the Ibex Zone. One specimen of *Tropidoceras* can still be found and a small number of *Protogrammoceras* and *Fuciniceras* also occur here, but *Prodactylioceras* is still absent.

Fuciniceras dubari was placed by Cantaluppi – Montanari (1968, p. 75) in the Upper Carixian. These authors regard as its synonym the species described from the High Atlas (*"Fuciniceras* sp. B" Dubar, 1961, p. 255, Text-fig. 7) which Dubar considers to belong to the Davoei or Ibex Zone.

In the Ibex Zone, Phylloceratidae are predominant (52.8%). The share of Juraphyllitidae is 24.7% of the fauna, that of Lytoceratidae 5.6% and that of Ammonitinae 16.9%.

In the Ibex Zone all species are represented by a small number of specimens. Comparatively most frequent are the forms related to *Calliphylloceras emeryi*.

3. Prodactylioceras davoei Zone

a) *Lower and middle part*

Having a total thickness as low as 23 cm, Beds 461 and 462 contain a relatively more abundant ammonite fauna. The enclosing rock is a red limestone, locally crinoidal. Let us quote the ammonites found here·

Phylloceras hantkeni (Schloenbach in Prinz, 1904)
Phylloceras zetes (d'Orbigny, 1849)
Phylloceras bonarellii (Bettoni, 1900)
Phylloceras sp.
Partschiceras sp.
Calliphylloceras geyeri (Bonarelli, 1895)
Calliphylloceras emeryi (Bettoni, 1900)
Calliphylloceras microgonium (Gemmellaro, 1884)
Juraphyllites libertus (Gemmellaro, 1874)
Juraphyllites cf. *diopsis* (Gemmellaro, 1884)
Juraphyllites cf. *frechi* (Meister, 1913)
Juraphyllites sp.
Harpophylloceras eximium (Hauer, 1854)
Meneghiniceras sp.
Lytoceras cf. *postfimbriatum* (Prinz, 1904)
Radstockiceras sp.
Tropidoceras cf. *actaeon orientale* (Rremer, 1965)
Coeloceras sp. aff. *pettos* (Quenstedt, 1843) ?
Coeloceras ? *indunense* (Meneghini, 1881)
Coeloceras ? *indunense tardevoluta* (Bettoni, 1900)
Coeloceras ? *incertum* (Fucini, 1905)
Coeloceras ? sp.

Prodactylioceras psiloceroides (Fucini, 1905)
Androgynoceras cf. *maculatum* (Young et Bird, 1822)
Androgynoceras capricornus (Schlotheim, 1820)
Fuciniceras dubari (Cantaluppi, 1968)
Fuciniceras detractum (Fucini, 1900)
Fuciniceras n. sp. (= *F.* cf. *boscense* in Cantaluppi – Montanari, 1968, Pl. 13, fig. 3.)
Fuciniceras sp.

Androgynoceras cf. *maculatum* was collected from Bed 461, *A. capricornus* from Bed 462. For the identification of *A. capricornus*, the author has to extend his sincerest thanks to Professor M. K. Howarth. *A. maculatum* is the index fossil of the lower, *A. capricornus* of the middle subzone of the Davoei Zone (cf. Dean et al. 1961, p. 466, 467). Hence it is probable that the fauna of the two Lókút beds may represent the lower and middle parts of the Davoei Zone.

37.2% of the fauna is constituted by Phylloceratidae, 17.3% by Juraphyllitidae, 1.7% by Lytoceratidae and 43.8% by Ammonitinae. *Calliphylloceras emeryi* and *Juraphyllites libertus* are the most frequent forms.

b) *Upper part*

The richest fauna of the Lókút hill has been yielded by Beds 464 and 465. Either of the two beds is 20 cm thick. Both show an irregular distribution and accumulation of the ammonites. A few ammonites of Bed 465 have preserved their shells; some of the large *Phylloceras* and *Lytoceras* are represented by internal moulds affected by subsolution and thus exhibiting even their septa. These specimens were enclosed parallel to the bedding plane, but fell prey to heavy subsolution together with the upper part of the bed. With a view to the abundance of species, the faunae of the two beds are considered separately.

Bed 464:

Phylloceras hantkeni (Schloenbach in Prinz, 1904)
Phylloceras meneghinii (Gemmellaro, 1874)
Phylloceras cf. *zetes* (d'Orbigny, 1849)
Phylloceras sp.
Calliphylloceras emeryi (Bettoni, 1900)
Calliphylloceras sp.
Partschiceras sp.
Juraphyllites libertus (Gemmellaro, 1884)
Juraphyllites telegdirothi (Kovács, 1934)
Juraphyllites cf. *diopsis* (Gemmellaro, 1884)
Juraphyllites planispira (Reynes, 1868)
Juraphyllites sp.
Harpophylloceras eximium (Hauer, 1854)
Meneghiniceras sp.
Lytoceras cf. *fimbriatoides* (Gemmellaro, 1884)
Lytoceras n. sp. aff. *baconicum* (Vadász, 1910) ?
Aegolytoceras cf. *fuggeri* (Geyer, 1893)
Coeloceras sp. aff. *pettos* (Quenstedt, 1843)
Coeloceras sp.
Prodactylioceras cf. *davoei* (Sowerby, 1822)

Prodactylioceras italicum (Meneghini in Fucini, 1900)
Phricodoceras (Hemiparinodiceras?) urcuticum (Géczy 1959) ?
Protogrammoceras detractum (Fucini, 1900)
Protogrammoceras costicillatum (Fucini, 1900)
Protogrammoceras cf. *pantanellii* (Fucini, 1900)
Fuciniceras cf. *dilectum* (Fucini, 1900)
Fuciniceras sp. aff. *ambiguum* (Fucini, 1900)?
Fuciniceras lavinianum (Meneghini in Fucini, 1900)
Fuciniceras sp.

With the appearance of the typical representatives of *Prodactylioceras* and the higher abundance of the representatives of *Protogrammoceras–Fuciniceras*, Bed 464 belongs to the upper part of the Davoei Zone. *Protogrammoceras detractum* is particularly abundant in the bed, being characteristic of the transitional Carixian-Domerian beds as shown by Cantaluppi and Montanari (1968, p. 74).

The present writer earlier considered *Hemiparinodiceras* to be a subgenus of *Liparoceras*. On the strength of recent samplings, however, its affinity with *Phricodoceras* is more probable and it seems to be very closely related to the forms referred to *Phricodoceras lamellosum* (d'Orbigny, 1844) by Buckman (1920, Pl. 149).

In terms of specimens the fauna is constituted for 21.1% by Phylloceratidae, 31.0% by Juraphyllitidae, 2.9% by Lytoceratidae and 45.0% by Ammonitinae. Of the Phylloceratidae the species *Calliphylloceras emeryi* is most abundant (63 specimens of a total of 602), to be followed by *P. hantkeni* (10 specimens). Of the Juraphyllitidae the species *Juraphyllites planispira* (46 specimens) and *J. libertus* (33 specimens) and *J. telegdirothi* (30 specimens) are most frequent. Of the Ammonitinae, *Protogrammoceras detractum* was found to predominate with 141 specimens accounting for 23% of the entire fauna! The other *Protogrammoceras* and *Fuciniceras* species are represented in very low numbers of specimens only.

Bed 465:

Phylloceras hantkeni (Schloenbach in Prinz, 1904)
Phylloceras meneghinii (Gemmellaro, 1874)
Phylloceras disciforme (Reynes, 1868)
Phylloceras zetes (d'Orbigny, 1849)
Phylloceras bonarellii (Bettoni, 1900)
Partschiceras sp.
Calliphylloceras emeryi (Bettoni, 1900)
Calliphylloceras microgonium (Gemmellaro, 1884)
Juraphyllites libertus (Gemmellaro, 1884)
Juraphyllites cf. *libertus* (Gemmellaro, 1884)
Juraphyllites telegdirothi (Kovács, 1934)
Juraphyllites planispira (Reynès, 1868)
Juraphyllites cf. *diopsis* (Gemmellaro, 1884)
Juraphyllites sp.

Harpophylloceras cf. *eximium* (Hauer, 1854)
Meneghiniceras bicicolae (Bonarelli, 1895) n. subsp.?
Lytoceras cf. *fimbriatoides* (Gemmellaro, 1884)
Lytoceras sp. aff. *secernendum* (De Stefani, 1887)
Audaxlytoceras sp.
Radstockiceras n. sp.
Coeloceras sp.
Coeloceras ? *fallax* (Fucini, 1905)
Coeloceras ? *fallax irregularis* (Fucini, 1905)
Coeloceras ? cf. *asperum* (Fucini, 1905)
Coeloceras ? cf. *indunense* (Meneghini, 1881)
Prodactylioceras cf. *italicum* (Meneghini in Fucini, 1900)
Phricodoceras sp. aff. *imbricatum* (Bettoni, 1900)
Liparoceras (Becheiceras) gallicum (Spath, 1936) n. subsp.
Androgynoceras sp.
Oistoceras sp.
Protogrammoceras n. sp. (= *normanianum* in Fucini, 1905) non d'Orbigny, 1844
Protogrammoceras costicillatum (Fucini, 1900)
Protogrammoceras detractum (Fucini, 1900)
Protogrammoceras n. sp.
Fuciniceras cf. *coniungens* (Fucini, 1900)
Fuciniceras sp. aff. *ruthenense* (in Fucini, 1900 non Reynès, 1868)
Fuciniceras n. sp. (= *F.* cf. *boscense* in Cataluppi – Montanari, 1968)
Fuciniceras cf. *capellinii* (Fucini, 1899) ?
Fuciniceras sp.

The appearance of *Oistoceras* in NW Europe is characteristic of the upper part of the Davoei Zone (Oistoceras figulinum Subzone), though subordinate representatives of Oistoceras can also be found together with the first representatives of *Amaltheus* (cf. Dean et al., 1961, p. 468). Similar is the case with *Liparoceras (Becheiceras)*. Since no *Amaltheus* has so far been found in Bed 465, this bed is placed too in the Davoei Zone on the basis of *Oistoceras*. However, it is quite plausible that the condensed fauna may also include forms occurring in the Amaltheus stokesi Zone.

The new *Radstockiceras* species is characterized by extreme compression, a very narrow umbilicus and a richly differenciated suture line. The new *Liparoceras (Becheiceras)* subspecies is also more compressed than the nominate subspecies of *gallicum*. The closely spaced ribs of the new *Protogrammoceras* are slightly sigmoidal, the venter being heavily tricarinate.

In the fauna the share of Phylloceratidae is 29.1%, that of Juraphyllitidae 35.7%, that of Lytoceratidae 5.6%, and that of Ammonitinae 29.6%. Most frequent species is *Juraphyllites planispira* (114 of the total number of 586 specimens). *Juraphyllites telegdirothi* (39 specimens) is also very frequent. The genera *Radstockiceras*, *Phricodoceras* and *Bechei-*

ceras are represented by one specimen each, *Androgynoceras* and *Oistoceras* by a total of five specimens. The population of *Coeloceras* is also very subordinate. The representatives of *Protogrammoceras* and *Fuciniceras* show a little more varied specific composition as compared to that observable in Bed 464, being characterized by the predominance of *P. costicillatum* and *P. detractum* here too.

4. Pleuroceras spinatum Zone

The Amaltheus margaritatus Zone in the strict sense is absent at Lókút. Bed 465 is overlain by crinoidal limestones of greyish to purple-pink colour (Beds 466 – 473) containing just sporadical and single representatives of ammonites:

Phylloceras hantkeni (Schloenbach in Prinz, 1904) n. subsp.
Phylloceras sp. aff. *frondosum* (Reynes, 1868)
Calliphylloceras emeryi cf. *diversisulcatum* (Kovács, 1939)
Lytoceras sp.
Emaciaticeras cf. *lottii* (Gemmellaro, 1885)
Emaciaticeras cf. *dolosum* (Fucini, 1899)
Emaciaticeras sp. (Bonarelli)
Paltarpites meneghinii (Bonarelli, 1899)

The only specimen of *Paltarpites meneghinii* was found in Bed 466. The systematic position of the species is a point of controversy. Bonarelli placed the species conditionally in the genus *Harpoceras*, admitting, however, its possible affiliation with the genus *Polyplectus* (1899, p. 203). Cantaluppi (1967, p. 46) conditionally referred *meneghinii* to the genus *Protogrammoceras*, indicating, however, its possible affiliation with the genera *Paltarpites* and *Polyplectus*, too. According to Pinna (1969, p. 13), *meneghinii* would belong to the *Protogrammoceras* genus, too. On the basis of the narrow umbilicus, the sharp ventral area, the well-developed external saddle, *meneghinii* stands closer to the type of *Platyharpites platypleurus* Buckman, 1927, than to the types of the genera *Protogrammoceras*, *Polyplectus* or *Lioceratoides*. Arkell (1957, p. 256) included the genus *Platyharpites* in the genus *Paltarpites*. According to Buckman, *platypleurus* would belong to the Argutus Hemera, i.e. to the lower part of the Spinatum Zone. Pinna suggests *P. mediterraneum* to occur also in the Spinatum Zone.

The only specimen of *Emaciaticeras* cf. *lottii* was found in Bed 467, several specimens of *E.* cf. *dolosum* and *E.* sp. were collected from Bed 473. Therefore it is probable that the uppermost fossiliferous bed belongs to the upper part of the Spinatum Zone (cf. Dubar et al. 1967, p. 832).

Because of the marked scarcity of the fauna, it would be rather difficult to give any quantitative evaluation of the fauna of the Spinatum Zone. Nevertheless, the representatives of *Phylloceras* and *Lytoceras* seem to show a slight increase in percentage (Phylloceratidae 28.6%, Juraphyllitidae 0.0%, Lytoceratidae 16.7%, Ammonitinae 64.7%).

The Spinatum Zone is overlain with a break in sedimentation by the Toarcian manganiferous sequence.

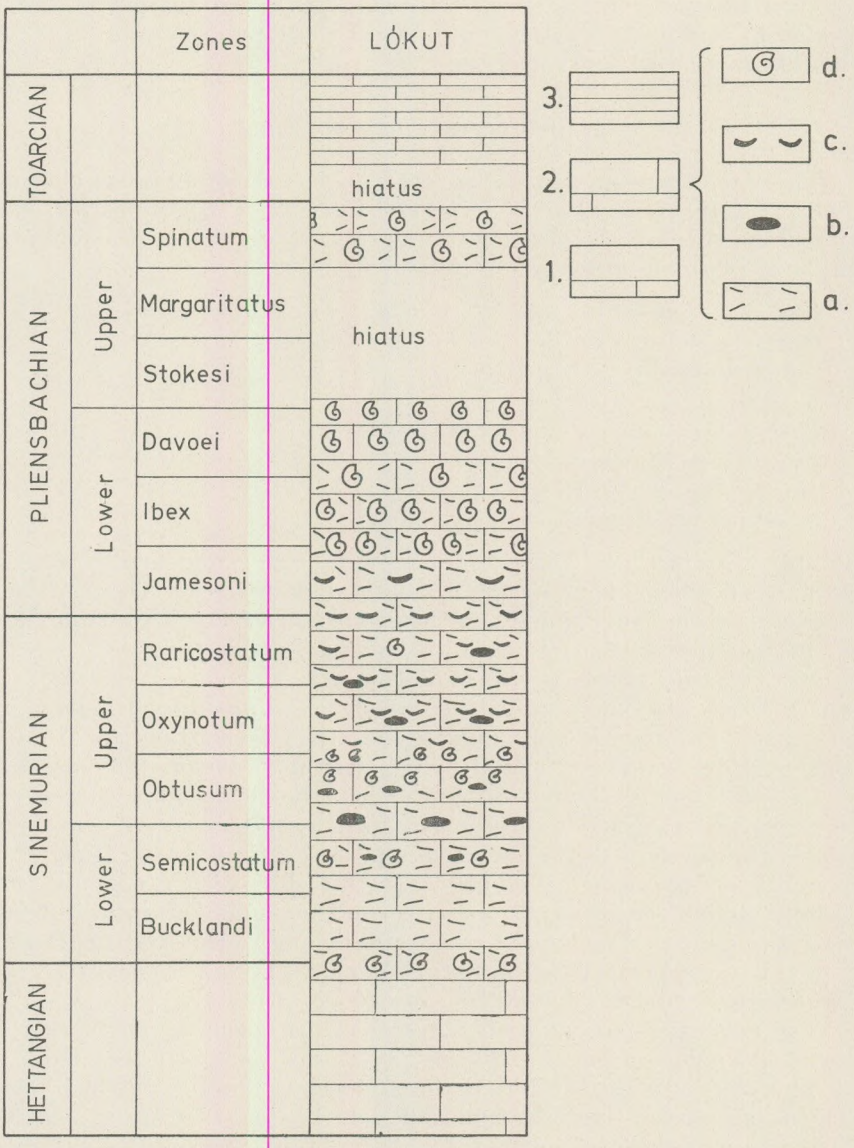

Fig. 2. Correlation diagram of the Lókút standard profile
1. oölitic limestone
2. Ammonitico Rosso limestone
(a) with crinoids; *b)* with chert nodules; *c)* with Bositra; *d)* with ammonites
3. manganiferous sequence

Conclusions

The limestones exposed on the easily walkable slope of the Lókút hill represent all stages of the Jurassic system. Three zones of the Sinemurian Stage and six zones of the Pliensbachian are evidenced by fauna. Surprisingly enough, very little "material" (rock) is sufficient to record a long range of geohistorical events. Although fossiliferous beds have had to be looked for in the Jurassic sequence of low thickness, the correlation diagramme is almost completely filled up.

Correlation has been based primarily on the occurrences of NW European zonal or subzonal indices. It may be supposed that the realm of these species was widened during their acme. Consequently, their sporadical Mediterranean occurrences are synchronous with their acme. In principle, it would also be possible that the time ranges of the species may be different in the Northwest European and the Mediterranean provinces and that some groups would have migrated to new areas after abandoning their original habitat. This hypothesis, however, is contradicted by the identity of the susccessions of the index species in both faunal provinces.

If the chronological subdivision of the Lókút profile is correct, several *Protogrammoceras* and *Fuciniceras* species must have appeared earlier than shown by the references known to the author, at least as far as the eastern Mediterranean areas are concerned.

Quantitatively, the increase of the ammonite populations on the boundary of the Davoei-Stokesi Zones is remarkable. The Obtusum Zone and the top of the Jamesoni Zone are also characterized by a rich fauna. The Semicostatum, Ibex and Stokesi Zones, in turn, are poor in species. The Oxynotum Zone is not evidenced by any faunal record as of yet. The percentage ratio of the Phylloceratidae and Lytoceratidae, as a rule, is higher than in the near-seamount zones, being, however, lower than in the basinal sediments occurring far away from the seamounts.

In the Bakony Mountains it was recognized already by Telegdi Róth (1934) that "the stratigraphic successions of the Liassic vary from profile to profile". K o n d a (1970) referred the various profiles to two main types in dependence on the continuity or discontinuity of sedimentation. According to K o n d a, Lókút belongs to the type of continuous sedimentation. The investigations of the fauna have confirmed his statement. In the Early Jurassic the area of Lókút may have been a basin portion, where the organic detritus supplied from the seamounts caused temporary changes in the character of the Ammonitico Rosso limestone.

REFERENCES

Arkell, J. W. (1957): Mesozoic Ammonoidea (in: Moore, C.: Treatise on Invertebrate Paleontology, Part. L. 4. Kansas).

Bonarelli, G. (1899): Le Ammoniti del „Rosso Ammonitico" descrite e figurate da Giuseppe Meneghini. Bull. Soc. Malac. Ital, 20, Pisa.

Böckh, J. (1873): Die geologischen Verhältnisse des südlichen Theiles des Bakony. Mitt. Jahrb. k. u. Geol. Anstalt. 2, Budapest.

Bremer, H. (1965): Zur Ammonitenfauna und Stratigraphie des unteren Lias (Sinemurium bis Carixium) in der Umgebung von Ankara (Türkei). Neues Jahrb. Geol. Paläont. Abhandl. 122, Stuttgart.

Buckmann, S. S. (1909–1930): Type ammonites. London.

Cantaluppi, G. (1967): Le ammoniti Domeriane della Val Ceppelline (Suello-Prealpi Lombarde). Atti Ist. Geol. Univ. Pavia. 18, Pavia, 1967.

Cantaluppi, G., Montanari, L. (1968): Carixiano superiore e suo passagio al Domeriano a NW di Arzo (Canton Ticino). Boll. Soc. Paleont. Ital. 7. Modena.

Dean, W. T., Donovan, D. R., Howarth, M. K. (1961): The Liassic ammonite zones and subzones of the Nort-West European province. Bull. British. Mus. Nat. Hist. Geol. 4/10, London, 435–506. P. 63–74.

Donovan, D. T. (1954): Synoptic supplement to T. Wright's "Monograph on the Lias Ammonites of the British Islands". Palaeont. Soc. London.

Donovan, D. T. (1958): The Lower Liassic Ammonite Fauna from the Fossil Bed at Langeneckgrat near Thun (Median Prealps).
Schweizer. Palaeont. Abh. 74, Basel. 1–58. P. 1–7.

Dresnay, R. du (1963): Quelques Ammonites de la partie inférieure du Pliensbachien (Carixien et Domérien pro parte) du jbel Bou-Rharraf.
Not. Serv. Géol. Maroc. 23, Rabat.

Dubar, G. (1961): Description de quelques Protogrammoceras et Fuciniceras du Pliensbachien inférieur.
in: Colloque sur le Lias. Bull. Rech. Géol. Min. Mém. 4. Paris.

Dubar, G., Foucault, A., Mouterde, R.: Le Lias moyen des environs de Huescar.
Bull. Soc. Géol. France. 7. ser. 9, Paris, 1967.

Dubar, G., Gabilly, J. (1964): Le Lias moyen de Saint-Vincent-Sterlange et de Saint-Cry-en-Talmondais. Compt. Rend. Acad. Sci, Paris, 259, Paris, 1964.

Futterer, K. (1893): Die Ammoniten des mittleren Lias von Östringen.
Mitt. grosserzog. Badisch. geol. Landesanst. 2, Heidelberg.

Hauer, F. (1856): Über die Cephalopoden aus dem Lias der nordöstlichen Alpen. Denkschr. Math. Naturwiss. Class. Akad. Wiss. Wien. 11, Wien.

Konda, J. (1970): Lithologische und Fazies-Untersuchung der Jura-Ablagerungen des Bakony-Gebirges.
Ann. Inst. Geol. Hung. 50/2, Budapest.

Kovács, L. (1936): Die stratigraphischen Verhältnisse der Liasbildungen am Lókúter Hügel im Bakonygebirge.
Abhandl. Miner. Geol. Inst. Tisza Univ, Debrecen. 7, Debrecen, 1936.

Mouterde, R.: Le Lias moyen de Sao Pedro de Muel. I. Céphalopodes.
Comun. Serv. Geol. Portugal, 54, Lisboa, 1970.

Noszky, J. (1961): Les formations jurassiques de la Hongrie.
Annal. Inst. Geol. Hung. 49, 2. Budapest.

Parona, C. F. (1896): Ammoniti del Lias inferiore del Saltrio.
Mém. Soc. Paléont. Suisse 23, Geneve.

Pia, J. (1914): Untersuchungen über die Gattung Oxynoticeras.
Abhandl. k. k. Geol. Reichsanst. 23, Wien.

Pinna, G. (1969): Revisione delle Ammoniti figurate da Giuseppe Meneghini nelle Tav. 1–22 della "Monographie des fossiles du calcaire rouge ammonitique". Mem. Soc. Ital. Sci Nat. 18, Milano, 1969.

Pompeckj, J. F. (1907): Notes sur les Oxynoticeras du Sinémurien du Portugal et remarques sur le genre Oxynoticeras. Commun. Commiss. serv. geol. Portugal 6. Lisboa.

Telegdi Roth K. (1934): Daten aus dem Nördlichen Bakony-Gebirge zur jungmesozoischen Entwicklungsgeschichte der „Ungarischen Zwischenmasse". Math. Naturwiss. Anzeig. Ung. Akad. Wiss. 52, Budapest.

PLATE I

1. *Calliphylloceras* cf. *emeryi* (Bettoni, 1900). Bed: N° 439.
2. *Partschiceras* sp. „
3. *Juraphyllites libertus* (Gemmellaro, 1884) „
4. *Juraphyllites libertus* (Gemmellaro, 1884) „

Foto: Quaiser

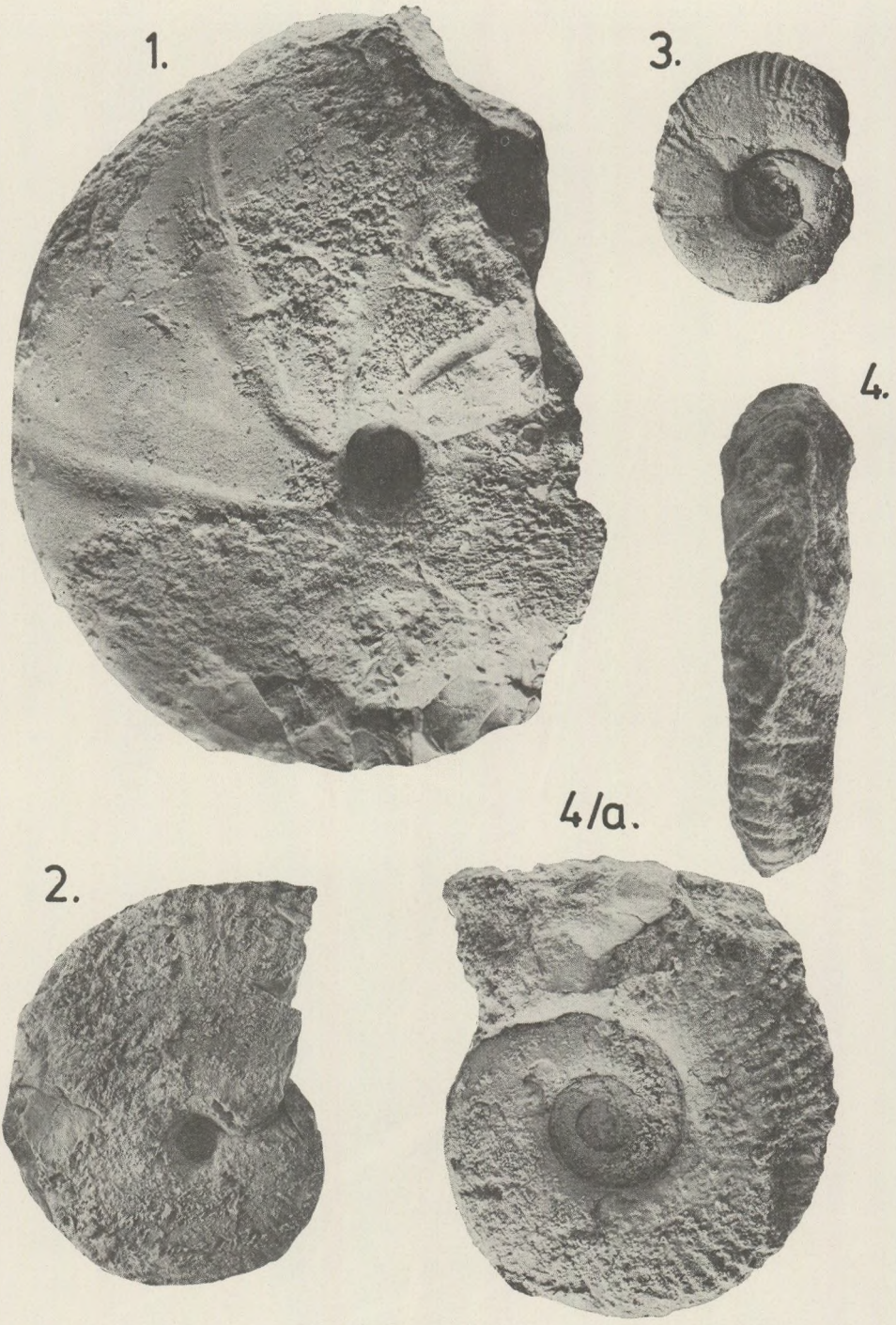
1.
3.
4.
4/a.
2.

PLATE II

Lytoceras altum V a d á s z, 1910. Bed: 439.

Foto: Q u a i s e r

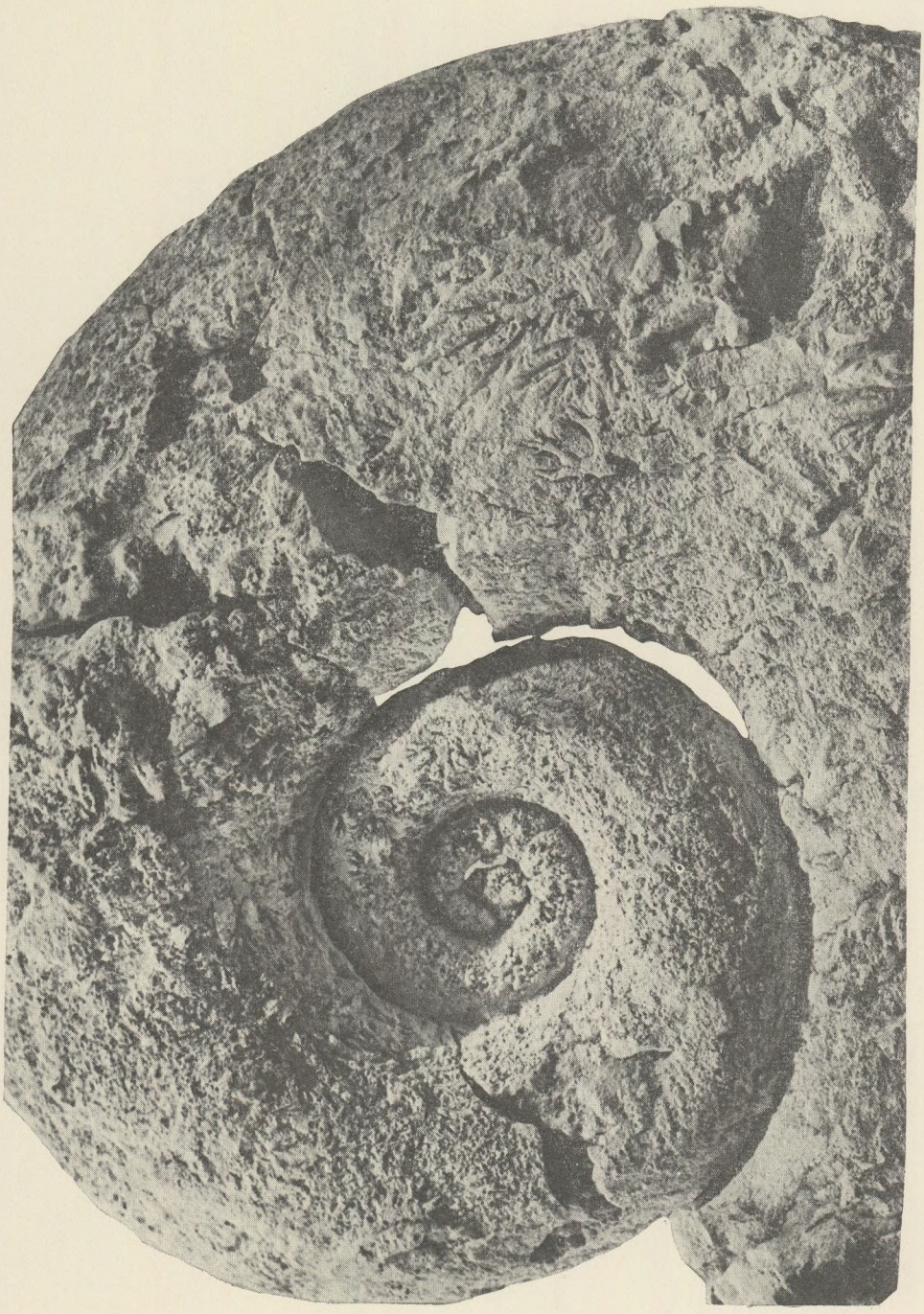

PLATE III

1. *Metoxynoticeras* cf. *involutum* (P o m p e c k j, 1907). Bed: N° 439.
2. *Metaderoceras beirense* M o u t e r d e, 1970.

Foto: Q u a i s e r

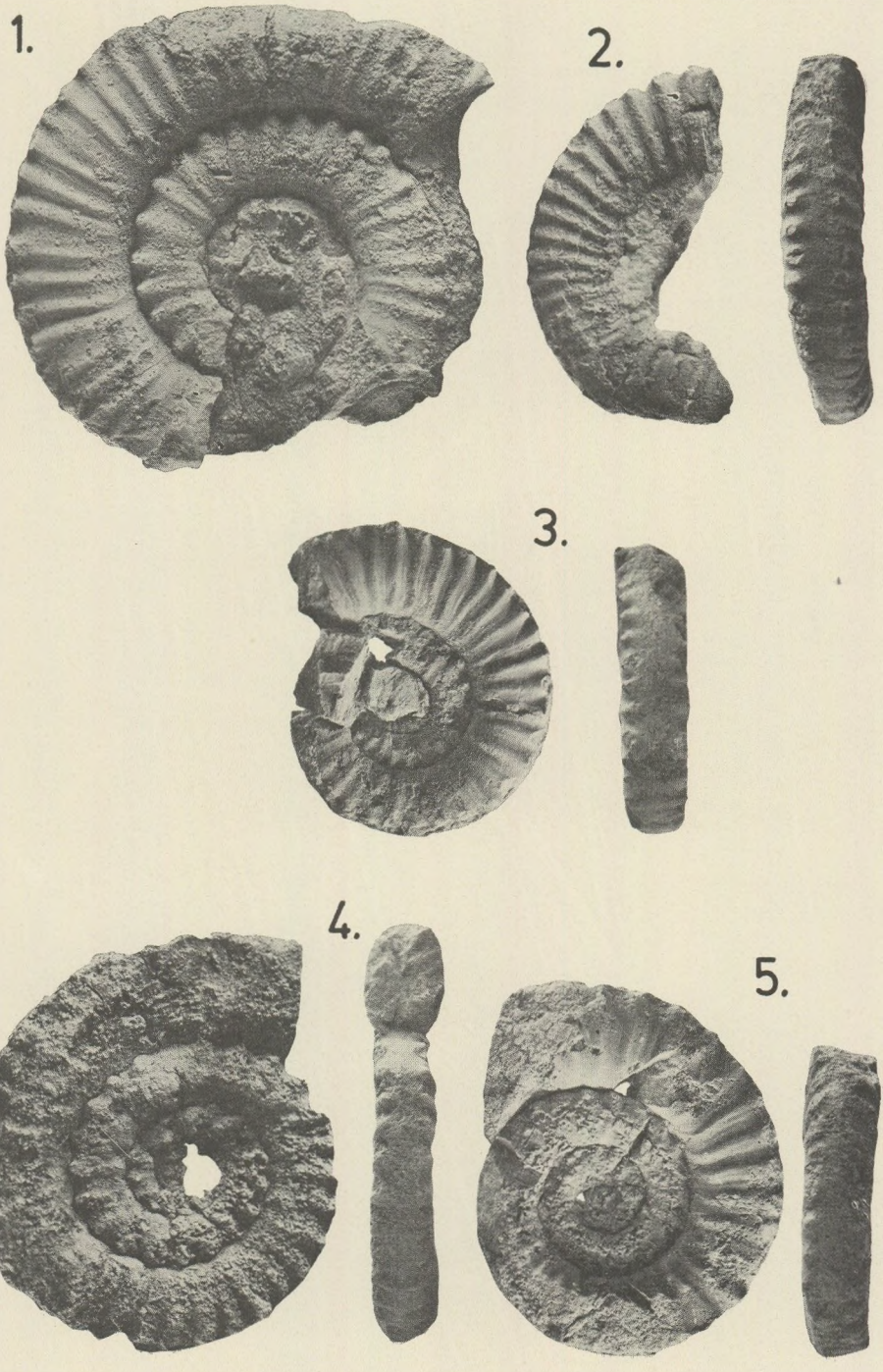
1.
2.
3.
4.
5.

PLATE IV

1. *Metaderoceras densinodum* (Quenstedt, 1849) ? Bed: N° 439.
2. *Metaderoceras* n. sp. aff. *submuticum* (Oppel, 1856)
3. *Metaderoceras* n. sp. aff. *submuticum* (Oppel, 1856)
4. *Metaderoceras* cf. *beirense* Mouterde, 1970
5. *Metaderoceras* n. sp. aff. *submuticum* (Oppel, 1856)

Foto: Quaiser

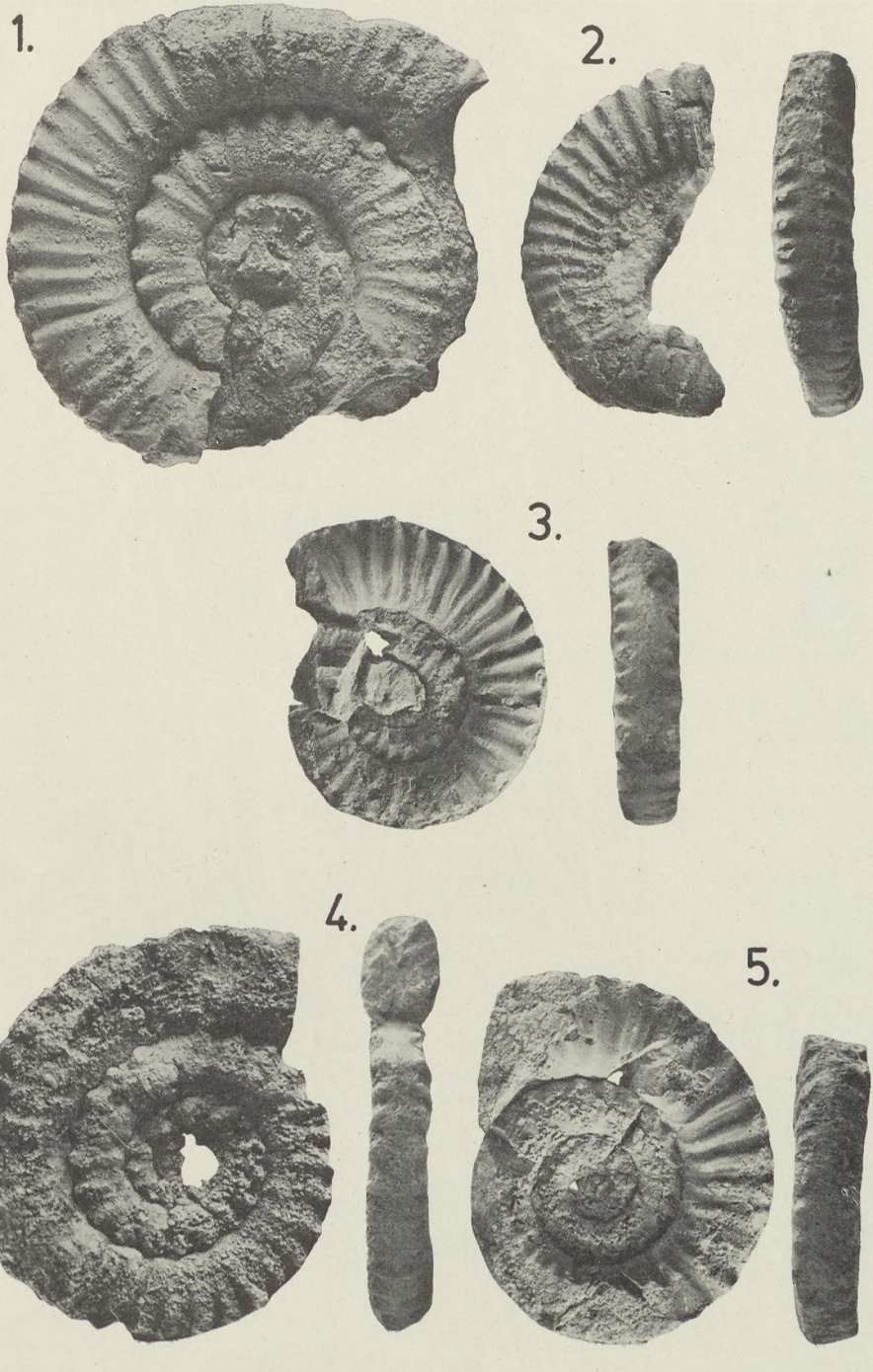
1.
2.
3.
4.
5.

PLATE V

1. *Uptonia* n. sp. Bed: N° 439
2. *Uptonia* cf. *angusta* (Quenstedt, 1849) ? „
3. *Metaderoceras beirense* Mouterde, 1970 „

Foto: Quaiser

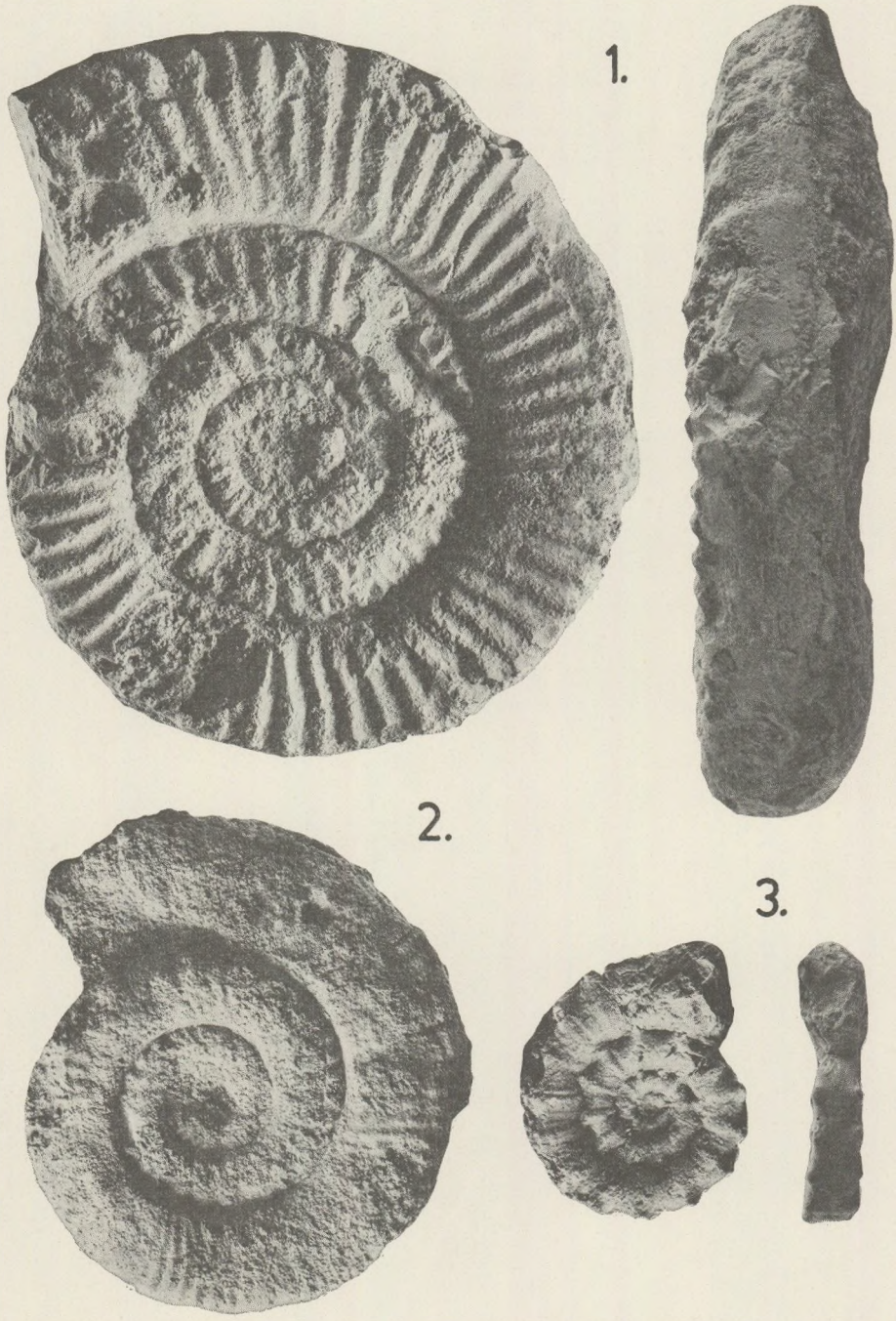
1.
2.
3.

PLATE VI

1. *Uptonia* n. sp. Bed: N° 439
2. *Uptonia regnardi* (d'O r b i g n y, 1844) n. subsp. „
Foto: Q u a i s e r

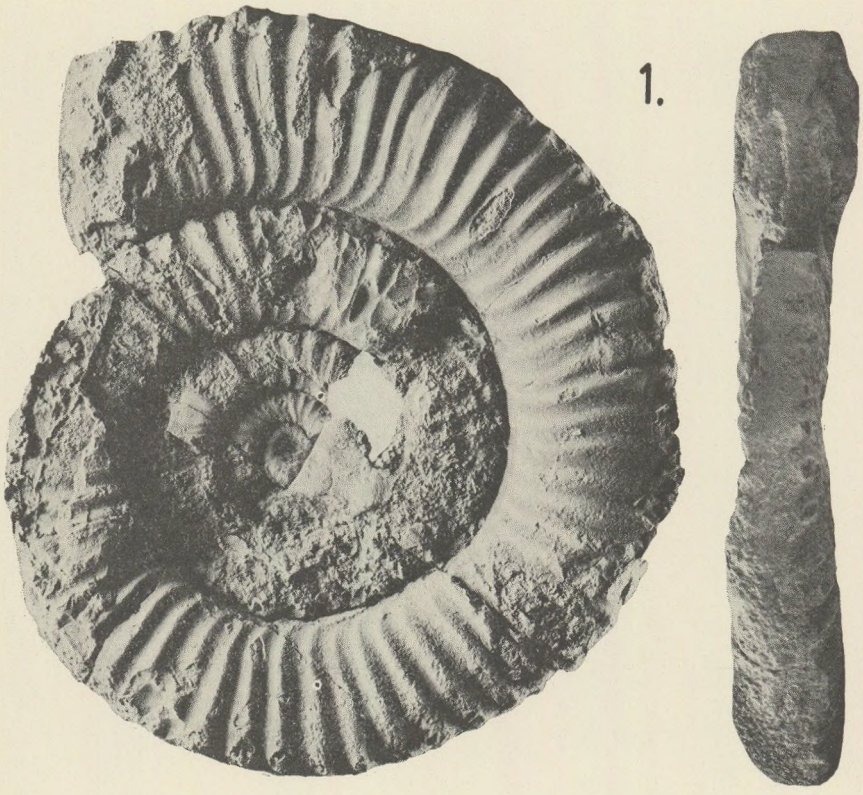
1.

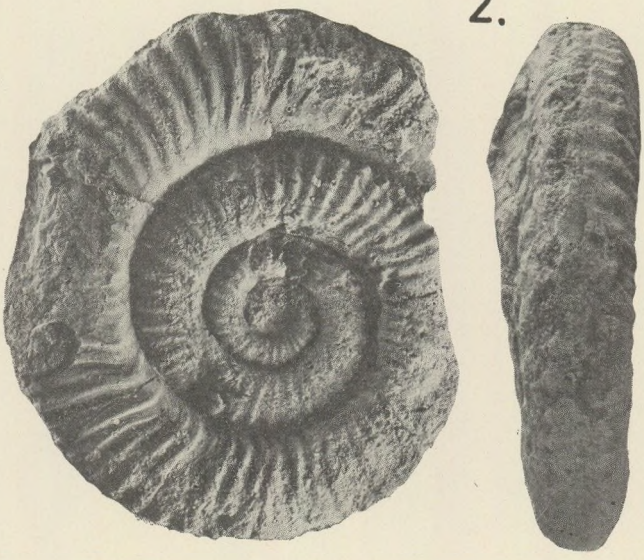
2.

PLATE VII

1 – 3. *Protogrammoceras* n. sp. Bed: N° 439
4. *Tropidoceras* sp. „
5. *Liparoceras (Becheiceras)* sp. „

Foto: Quaiser

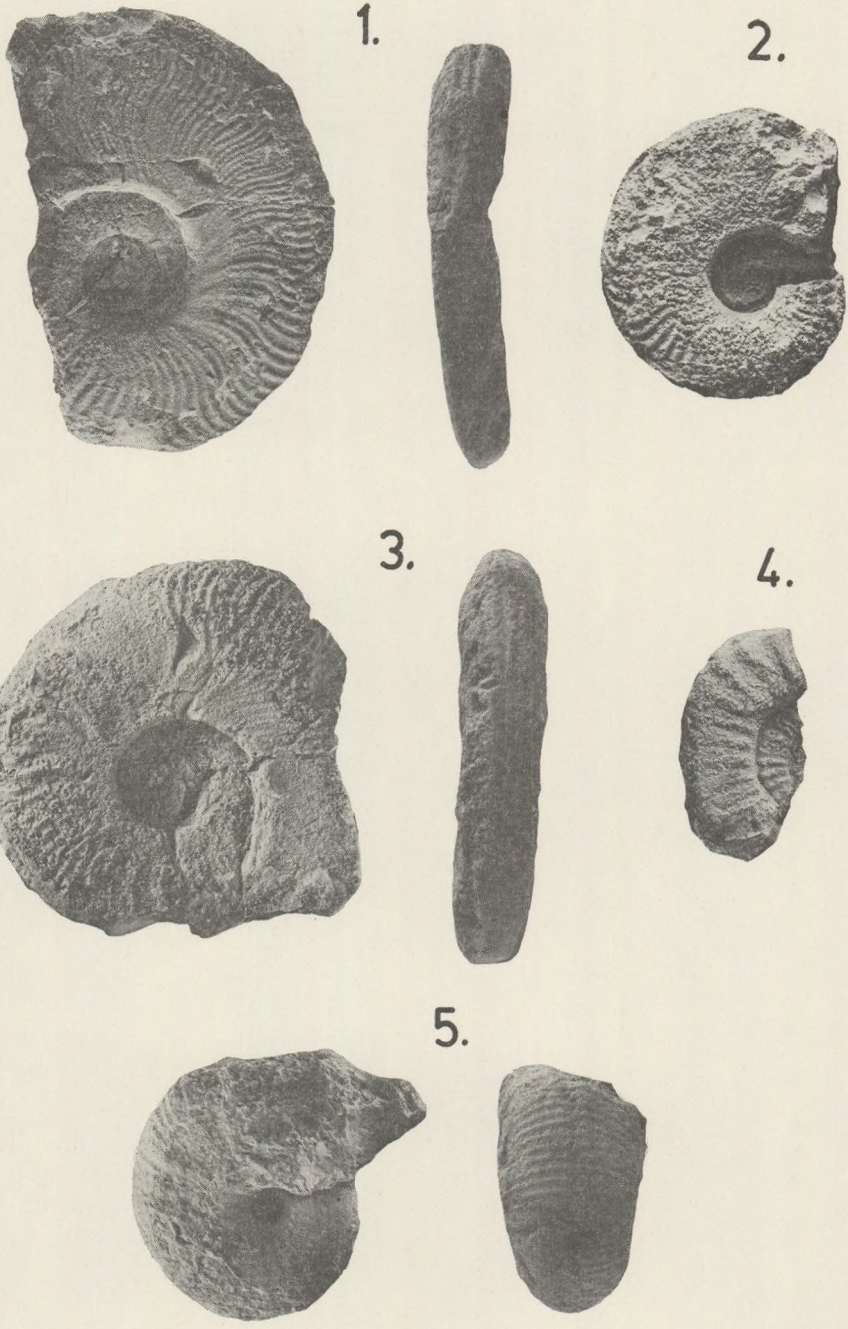
1.
2.
3.
4.
5.

A COMPARISON BETWEEN THE NORMAL AND REGIONAL MAGNETIC FIELDS OF HUNGARY

by

K. KIS

(Geophysical Institute of Loránd Eötvös University)

(Received: 3. March 1971)

РЕЗЮМЕ

В настоящей статье приводится один метод, служаший для определения карт нормального магнитного поля. Метод основан на теории фильтрации. Дается краткое описание нормального поля, определенного с уравниванием при помощи полиномов и сравниваются результаты двух методов.

Introduction

In constructing the magnetic anomaly map we need a reference horizon from which we can calculate the magnitude of the magnetic anomalies. This reference horizon is represented by the normal field. Usually the normal field of a given country is obtained by a polynomial adjustment of the data measured on the basic network of the country. This network is composed of nearly equally spaced station (B a r t a, 1957). The magnetic components which were measured on the stations of the basic network are approximated with a second degree polynomial of the geographical coordinates, using a least squares procedure:

$$E = E_0 + a\Delta\varphi + b\Delta\lambda + c\Delta\varphi^2 + d\Delta\varphi\Delta\lambda + e\Delta\lambda^2, \qquad (1)$$

$$\Delta\varphi = \varphi - \varphi_0 \quad \text{and} \quad \Delta\lambda = \lambda - \lambda_0,$$

where E is a component of the normal field, E_0 is the value of this component belonging to the point (φ_0, λ_0), a, b, c, d, e are the coefficients of the polynomial which are to be determined from the measurements, $\Delta\varphi$ and $\Delta\lambda$ are the latitude and longitude differences, measured from the point (φ_0, λ_0).

In Hungary, during this century two surveys of these kind were completed. The surveys and the evaluation of the measurements carried out by the Hungarian Geophysical Institute, "Roland Eötvös" in the years 1949 – 50 and 1964 – 65. The average distance between the stations of the basic network was 20 – 25 km, their number was 300 (Fig . 1). The declination and the vertical and horizontal components of the field were measured at every station. The results of the second survey were reduced to 1965.0, and the local anomalies were eliminated by three consecutive

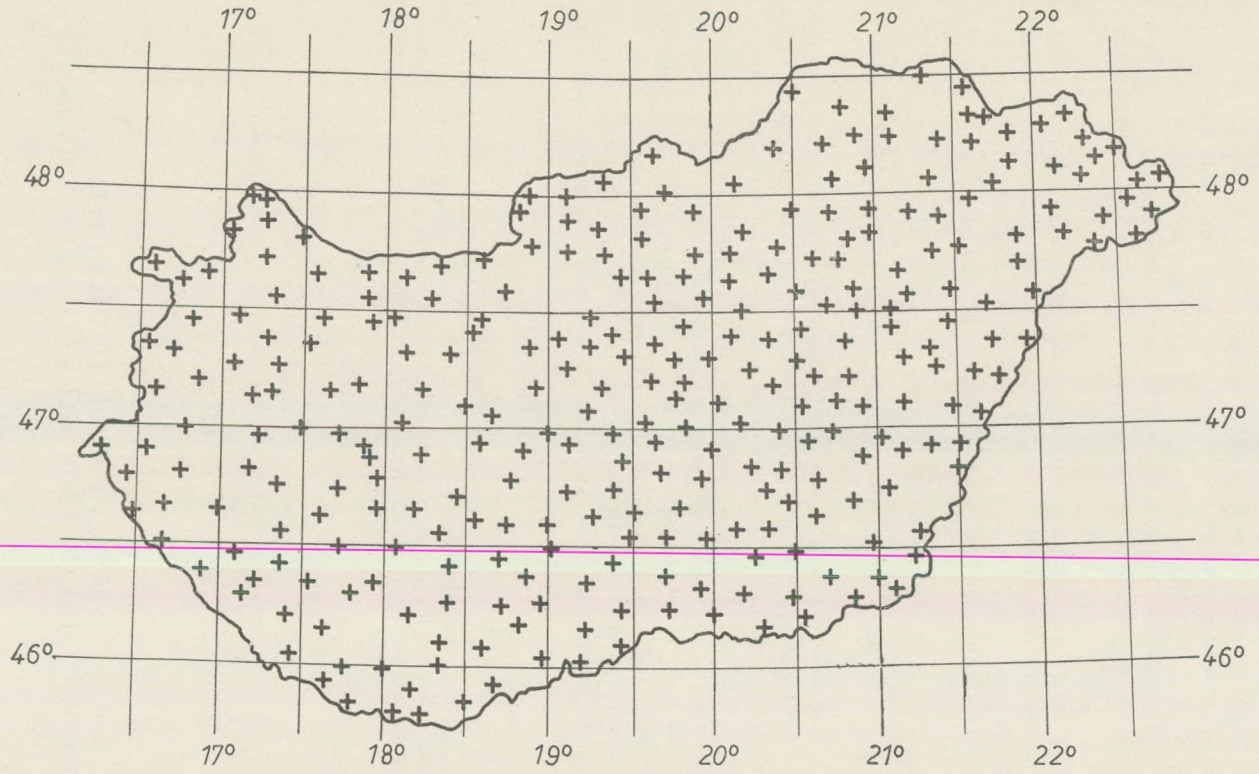

Fig. 1. The stations of the magnetic basis network in the years 1964 – 65

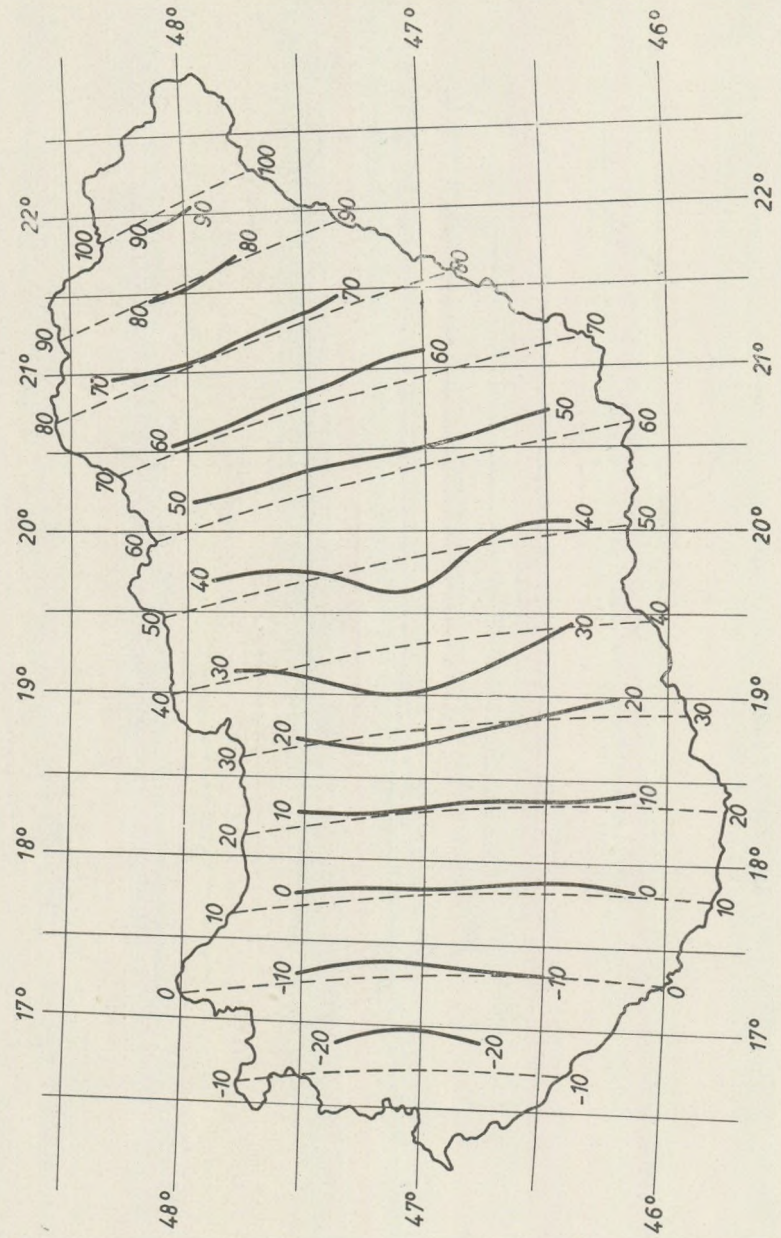

Fig. 2. The isogon-lines of the normal value of declination (dashed lines) and the isogon-lines of the regional field (full-lines) in 1965.0.

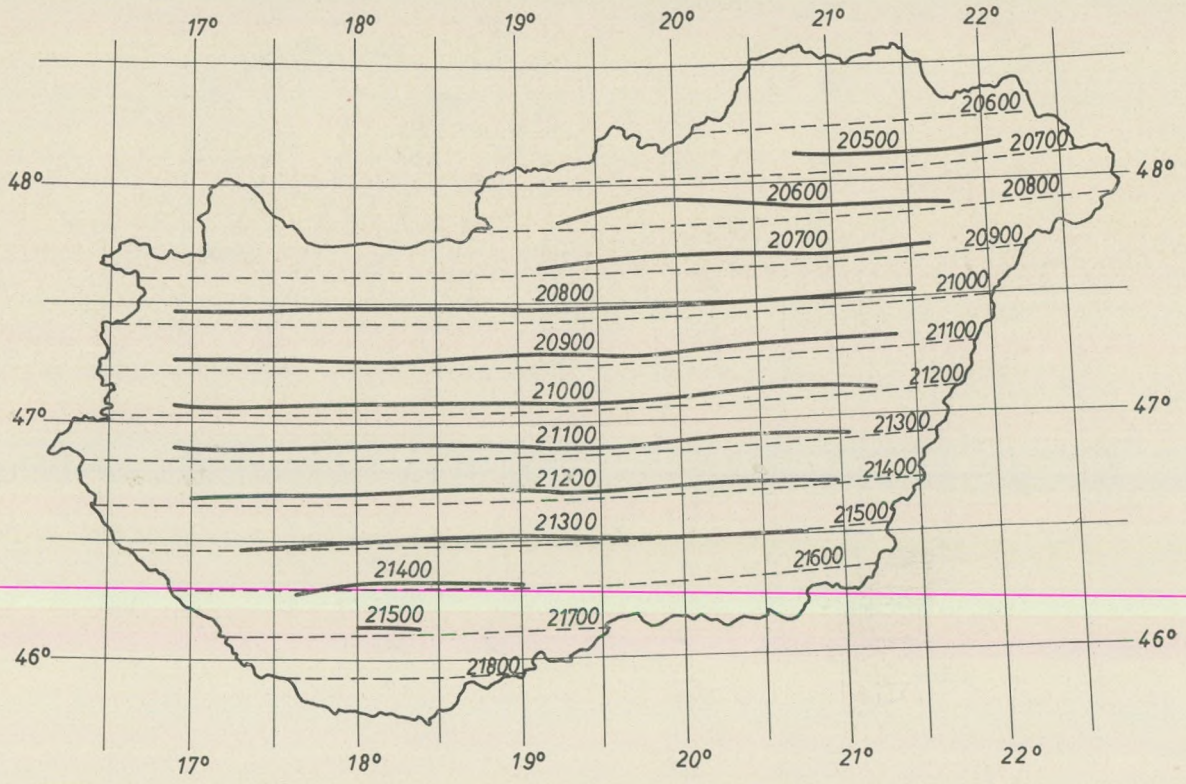

Fig. 3. The isodinam-lines of the normal value of the horizontal intensity (dashed-lines) and the isodinam-lines of the horizontal intensity of the regional field (full-lines) in 1965.0.

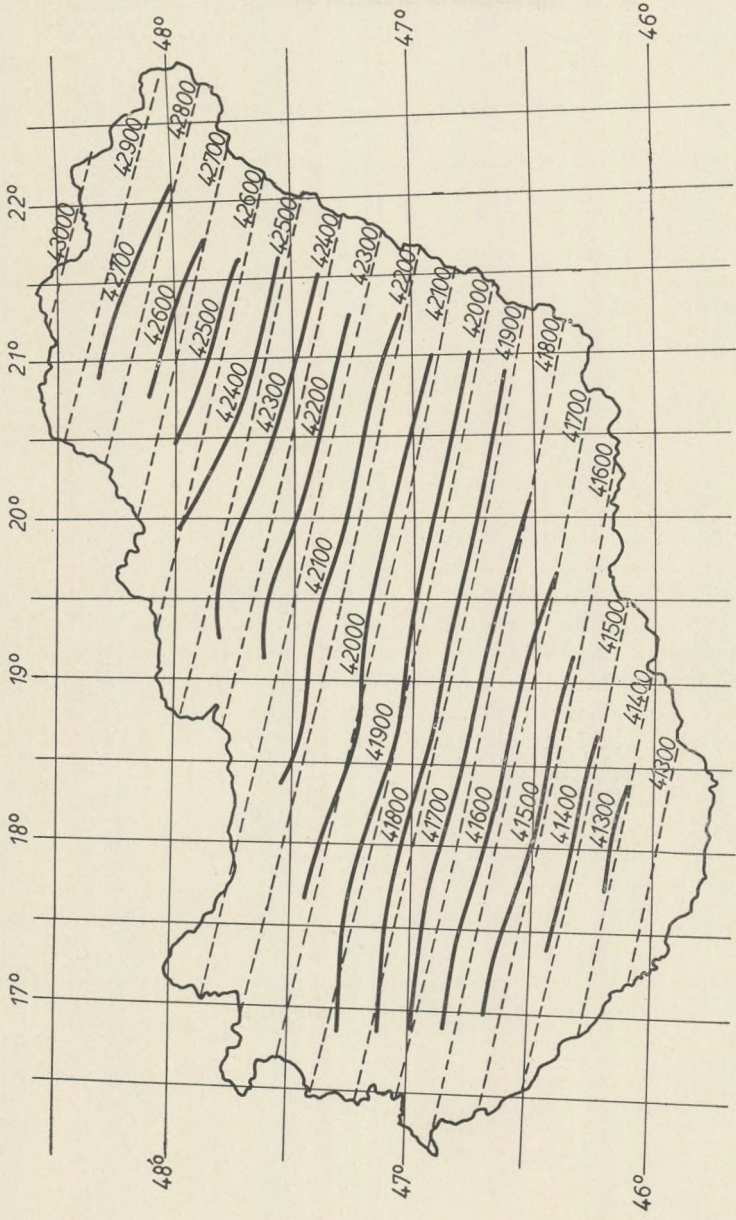

Fig. 4. The isodinam-lines of the normal value of the vertical intensity (dashed-lines) and the isodinam-lines of the vertical intensity of the regional field (full-lines) in 1965.0.

adjustments. The stations characterized by anomalies greater than a prescribed value were omitted during the three adjustments. The normal formules and the isodinamlines of the normal values were obtained by the third polynomial adjustment (Figs. 2, 3 and 4, respectively, dashed-line) (A c z é l and S t o m f a i, 1968):

$$D_{1965.0} = -21.87' - 0.10859\Delta\varphi + 0.31918\Delta\lambda + \tag{2}$$
$$+ 0.0005524\Delta\varphi^2 + 0.0004023\Delta\varphi\Delta\lambda - 0.00009791\Delta\lambda^2$$

$$H_{1965.0} = 22026.42\gamma - 9.22855\Delta\varphi - 0.01752\Delta\lambda + \tag{3}$$
$$+ 0.0027472\Delta\varphi^2 - 0.0006282\Delta\varphi\Delta\lambda + 0.00057366\Delta\lambda^2$$

$$Z_{1965.0} = 40832.71\gamma + 10.69786\Delta\varphi + 1.30976\Delta\lambda - \tag{4}$$
$$- 0.0070827\Delta\varphi^2 + 0.0003716\Delta\varphi\Delta\lambda + 0.00020691\Delta\lambda^2$$

where

$$\Delta\varphi = \varphi - 45°30' \quad \text{and} \quad \Delta\lambda = \lambda - 16°00'.$$

Interpolation and filtering

For the construction of the regional field based on interpolation we used the data of the 1964–65 survey of the Hungarian Geophysical Institute "Roland Eötvös" (Fig. 1). The random data as the function of φ latitude and λ longitude respectively are distributed nearly evenly on the territory of the country. The random data were interpolated into the points of a square grid using weighted averages.

We performed the weighted averaging on the surface of the Gauss-sphere which fitted well to the latitude of Hungary. We used the following expression for the weighting function (M e s k ó, 1967):

$$s(r', \varkappa') = \pi \left(\frac{\varkappa'}{36}\right)^2 e^{-\left(\frac{r'\varkappa'\pi}{36}\right)^2}, \tag{5}$$

where r′ means the distance measured in average sampling units, $\varkappa'$ is a parameter. Only those data were taken into account which were situated within a distance less than three sampling units from the given grid point. We used the cosine formula of spherical trigonometry:

$$\cos q = \cos \vartheta_2 \cos \vartheta_1 + \sin \vartheta_2 \sin \vartheta_1 \cos (\lambda_2 - \lambda_1), \tag{6}$$

where the pole distances ϑ_1 and ϑ_2 are given as

$$\vartheta_1 = 90° - \varphi_1 \quad \text{and} \quad \vartheta_2 = 90° - \varphi_2. \tag{7}$$

Furthermore, introducing

$$L = R \arccos q, \tag{8}$$

we get

$$r' = l/d \tag{9}$$

In expression (8) R is the radius of the Gauss-sphere $R = 6378.512966$ km, in (9) d is the average sampling unit.

During the interpolation of the random data we had to digitize the weighting function also randomly. The transfer properties of the random weighting function depart from those of the continuous one. In the calculation the parameter $\varkappa' = 6$ of the weighting function seemed to be the most favourable. The transfer function of the randomly digitized, normalized weighting function is given by

$$S(\varrho', \varkappa') = \sum_{k=1}^{N} \frac{s(r'_k \varkappa')}{\sum_{i=1}^{N} s(r'_i, \varkappa')} e^{-j\varrho' r'_k}, \tag{10}$$

where

$$\varrho' = \varrho \cdot d, \tag{11}$$

ϱ' is the relative angular frequency, and

$$\varrho' = \sqrt{\omega'^2 + \psi'^2} \tag{12}$$

(V é g e s, 1970). In Figs. 5 and 6 several amplitude-spectra of the randomly digitized weighting functions are presented as the function of ω' and ψ' respectively according to the expression

$$|S(\varrho', \varkappa')| = \sqrt{\left(\sum_{k=1}^{N} \frac{s_k}{\sum_{i=1}^{N} s_i} \cos(\varrho' r'_k)\right)^2 + \left(\sum_{k=1}^{N} \frac{s_k}{\sum_{i=1}^{N} s_i} \sin(\varrho' r'_k)\right)^2}, \tag{13}$$

where N means the number of the points taken into account in the interpolation at a given grid point. From the investigations concerning the

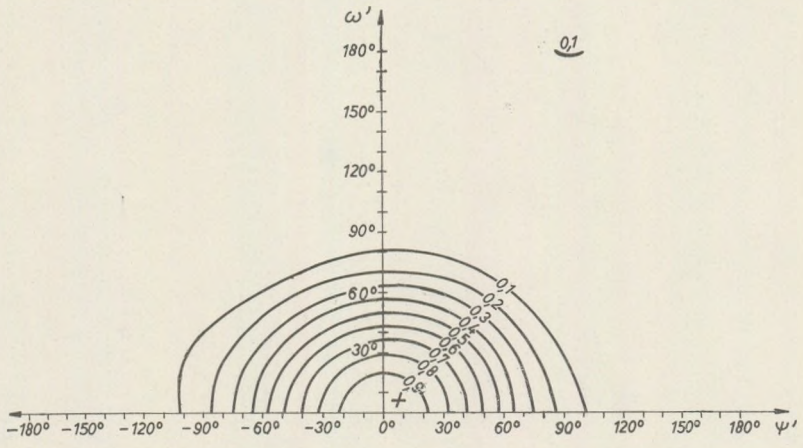

Fig. 5. The amplitude spectrum of the interpolation

amplitude-spectra of the randomly digitized weighting functions it is evident that they have no circular symmetry as in the continuous case. The reason of this distortion is the random digitizing and the use of a sampling unit greater than that prescribed by the sampling theorem. For removing the distortions we applied a low-pass filter. For this the weighting function (5) was applied again with the parameter $\varkappa' = 9$. Although the weighting function was digitized in the points of the square grid, the real transfer properties had slightly departed from those of the continuous one. For the determination of the transfer function of a symmetrical coefficient set the

$$S(i\omega_0, j\psi_0) = c_{00} + 2\sum_{k=1}^{M} c_{k0} \cos ik\omega_0 + 2\sum_{l=1}^{M} c_{0l} \cos jl\psi_0 + \tag{14}$$

$$+ 4\sum_{k=1}^{M}\sum_{l=1}^{M} c_{kl} \cos ki\omega_0 \cos lj\,\psi_0$$

connection was suitable (M e s k ó, 1970), where

$$\omega_0 = \psi_0 = \frac{\pi}{18}, \quad i = 0, \ldots, 18, \quad j = 0, \ldots, 18 \tag{15}$$

and c_k means a matrix element of the digitized weighting functions. c_{oo} is the central element of the matrix, k and l are indices corresponding to the direction of two axes. The transfer function is shown in Fig. 7.

At last for carrying out smoothing we had to construct the convolution of the two variables of the weighting function matrix and the interpolated data. The results of the convolution are swhon in Figs. 2, 3 and 4 (full-line).

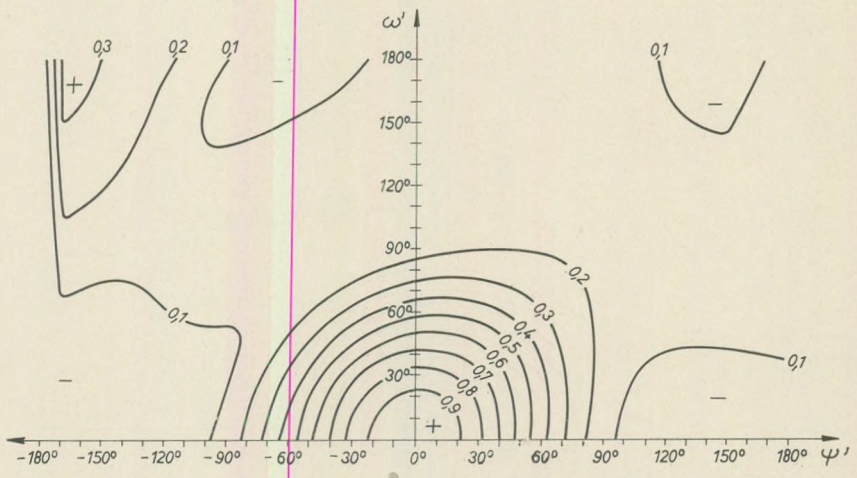

Fig. 6. The amplitude spectrum of the interpolation

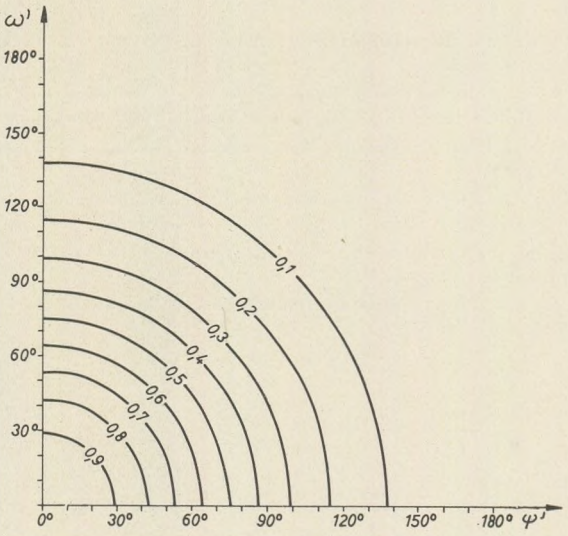

Fig. 7. The amplitude spectrum of the filtering

Discussion

If we compare the magnetic normal field and the magnetic regional field we find a systematic difference, the magnitude of which in the vertical component is 100—150 gammas, in the horizontal component is 150—200 gammas and in the declination is 10′. The directions of the isodinam-lines of the magnetic normal field and the magnetic regional field—apart from minor fluctuations — are roughly identical. The systematic differences in the level can be attached to the difference of two methods. The influences of the anomalistic areas appear in all coefficients determined by the polynomial adjustment, in spite of the omission of the anomalistic stations. On the maps computed with the interpolation and filtering this influence can appear only locally. The small anomalies are eliminated by the low-pass filter. The regional magnetic field, constructed using the second method fits well to the real field. The different directions of the isodinam-lines can be explained with the different resolution of the two methods. The character of the field defined by the polynomial adjustment is determined by the degree of the polynomial while the resolution of the regional field in the latter case is influenced by the filtering and sampling distance collectively.

If we regard the regional magnetic field as a reference horizon and construct this also for the neighbouring countries by the same method, it will be possible to fit this maps to one another. Using the normal fields this fitting is impossible. A more exact comparison can be given with the aid of a statistical investigation of the two fields.

REFERENCES

Aczél E. – Stomfai R. (1968): Az 1964–65. évi magyarországi földmágneses alaphálózat mérés. Geofizikai Közlemények XVII. 3.

Barta Gy. (1957): Földmágnesség. Akadémiai Kiadó Budapest.

Geofizikai Kutatási Módszerek III. Felszíni geofizika (1970). Szerkesztő Stegena L.

Meskó A. (1966): Gravity interpretation an information theory, I. Annales Univ. Sci. Bp. IX. 15–29.

Meskó A. (1969): Gravity interpretation and filter theory. Design and application of low-pass filters. Annales Univ. Sci. Bp. XIII. 67–80.

Véges I. (1970): Map plotting with weighted average on the surface of a circular disc. Pure and Applied Geophysics Vol. 78.

Zurflueh, E. G. (1967): Application of two dimensional linear wavelength filtering. Geophysics Vol. XXXII. No. 6.

RELATIONSHIP BETWEEN SUBSIDENCE INVERSIONS AND LOW LEVEL JETS

by

M. M. CSÁSZÁR

(Department of Meteorology, Eötvös University, Budapest)

(Received: 28. Aug. 1971)

РЕЗЮМЕ

В настоящей работе исследуется опускающееся течение воздуха, что характерно для антициклонов. Распределение градиентов температуры приводится в аналитическом виде и показано аэрологической диаграммной бумаге. Во второй части делается попытка для обяснения связи между эволюцией переходов, сопровождающих опускающиеся течения воздуха и изменением энергетических соотношений при этом, с целью доказать наше предположение: с уменьшением инверсионних слоев, по сушеству в антициклоне выражается тенденция перейти к состоянию статической стабильности и переход польной потенциальной энергии в кинетическую сопровождается появлением струй на низком уровне.

It is a scientifico-historical fact, that the development of cyclones and anticyclones, as great dimension atmospheric formations, cannot be explained on the basis of thermic reasons, only. To follow their genesis and development with an approximative accuracy is possible by thermodynamic methods. On the basis of the compensation principle realized by Dienes at the beginning of the century, consequences may be drawn regarding the dynamic processes evolving in the systems. However, the then still imperfect upper-air measurements gave no possibility to prove the consistence of theory with practice. At the beginning of the twenties Bjerknes and others published the theory concerning the genesis of frontal cyclones. Later on, Palmen, Rossby, Sutcliffe and others enriched by their results the information referring to the genesis and development of cyclones. At the same time we know relatively little, even today, about anticyclones. The discovery of some phenomena characteristic of anticyclones – as for instance radiation and subsidence inversions, free foehn, low level jets – proved that anticyclones cannot be regarded by far as being passive symmetrical formations.

In studies treating the development of cyclones and anticyclones we often encounter the description and application of the well-known "compensation principle". F a u s t (1953) applied also the compensation model in his "Zero level" investigations when going into details of the horizontal and vertical mass-flow processes. The "Zero level" can be found in each and every case beneath the tropopause, where the mean value of vertical motions is 0, whereas the ageostrophic mass current

attains a maximum value. In Faust's model (see Figure 1) the strengthening of the anticyclones to compensate the near the ground divergence is explained by the air transport between the upper level of the friction layer and the tropopause. According to his calculations, the highest mass convergence is caused by the so-called" counter gradient" winds, which concentrate in the "Zero level". Below this level a descending, while above it an ascending air current evolves. The descending air current, which turns dry adiabatically and extends over nearly the entire

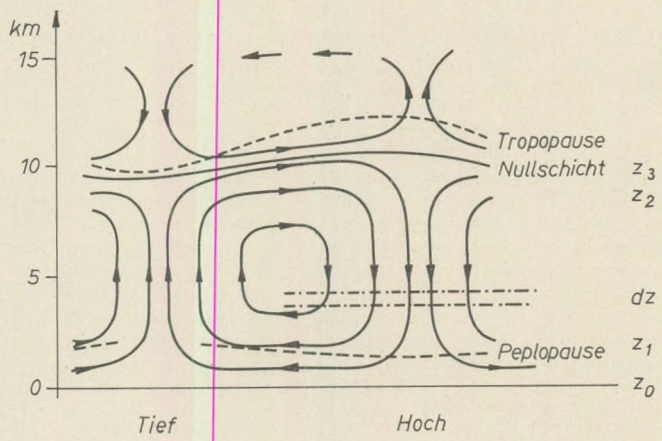

Fig. 1. Faust's model concerning the compensation principle

troposphere, brings about temperature inversions. This fact was already noticed by Margules (1903), and later on Cadez (1960) proved that such inversions cannot be regarded as stationary, as with the increase of their intesity their thickness decreases, and later on they disappear completely. Cadez's train of thoughts can be followed in Faust's model. The air outflow of the anticyclone can be observed at the bottom level only, between levels z_0 and z_1 while inflow occurs in greater heights at z_2-z_3. If at level z_2 the temperature does not change and there is no air inflow between levels z_1 and z_2, the mutual arrangement of the particles is constant in time. At the beginning of the process the lapse rate of temperature was constant in layers z_1-z_2, which was less than the dry adiabatic lapse rate. In case of dry, adiabatically descending air motion the pressure difference between the bottom and top levels of a dz thickness cut out from the descending zone will be constant. However, the barometric altitude scale decreases downwards, which is unanimous with the assertion that the metric thickness of the layer is decreasing.

The mutual position of the actual lapse rate of temperature and the dry adiabatic lapse rate in case of descending air motion can be followed on the thermodynamic diagram (see Figure 2).

1. Let us assume that the layer bordered by the isobars 550 and 650 mb, has a lapse rate smaller than the adiabatic one: $\gamma < \gamma_a$. The angle between the curve of state and the adiabatic is α_0. In the course of subsidence the layer sinks to 850 – 750 mb; its temperature changes according to the dry adiabatic (the potential temperature is constant), stage AB gets into position $A'B'$. The angle between the curve of state and the adiabatic increases, the stability becomes stronger: $\alpha < \alpha_0$.

2. Let the stratification be dry adiabatic $\gamma = \gamma_a$. After the subsidence stage CD is in position $C'D'$. The curve of state coincided originally with the dry adiabatic: the angle between the two is: $\varepsilon_0 = 0$, it was 0 also after the subsidence: $\varepsilon_0 = 0 = \varepsilon$.

3. In case of an unstable stratification, when $\gamma > \gamma_a$, the angle between the dry adiabatic and the curve of state is β_0. Following the subsidence, stage EF is in a position of $E'F'$, the angle increased: $\beta_0 < \beta$, and thus the instability increased, too.

4. If after the subsidence the air layer spreads out horizontally and the air pressure difference decreases towards the edges, the increase in stability during the subsidence is even more marked (stages HG and $H'G'$).

Cases 1 (and 4), characteristic of anticyclones, indicate that the stability of the stratification increases in case of descending air motions. If the descending air layer was originally sufficiently stable, the descent leads first to an isothermy and then to the development of an inversion (marked by stage $H'G'$).

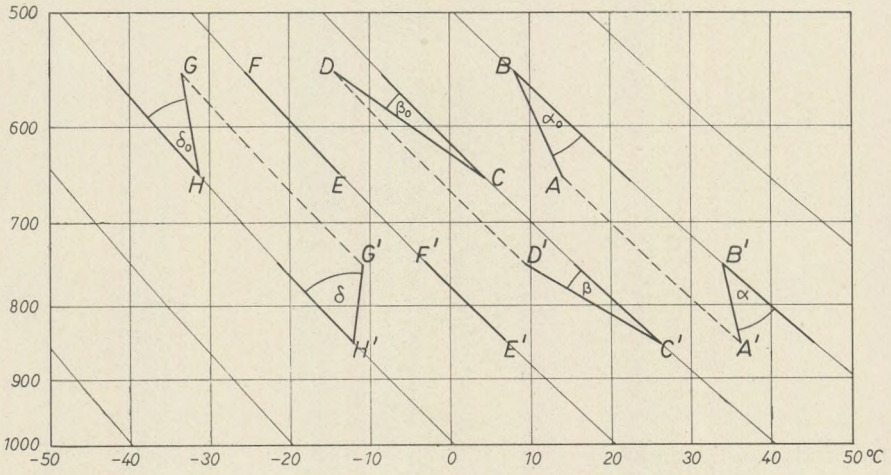

Fig. 2. Follow up of state changes on aerological diagrams in the case of atmospheric compression

The local variation of the lapse rate of temperature as a function of pressure and cross section, can also be indicated analitically. As a starting point the Poisson-equation is applied:

$$\frac{T}{T_0} = \left(\frac{p}{p_0}\right)^{\frac{AR}{c_p}} \tag{1a}$$

or else in a logarithmic form:

$$\ln T - \frac{AR}{c_p} \ln p = \ln T_0 - \frac{AR}{c_p} \ln p_0 \tag{1b}$$

T, p, T_0, p_0, are the temperature and pressure of the particle at levels z and z_0, respectively. $T = T(z)$, $p = p(z)$, $T_0 = T_0(z)$, $p_0 = p_0(z)$, $z = z(z_0)$.

Applying to equation (1b) and differentiating

$$\frac{1}{T_0}\frac{dT_0}{dz_0} - \frac{AR}{c_p}\frac{1}{p_0}\frac{dp_0}{dz_0} = \left(\frac{1}{T}\frac{dT}{dz} - \frac{AR}{c_p}\frac{1}{p}\frac{dp}{dz}\right)\frac{dz}{dz_0} \tag{2}$$

as $\varrho s\, dz = \varrho_0 s_0 dz_0$, the cross section of the fixed mass will change from s_0 *to* $s(z)$, and this is applied to equation (2).

$$\frac{1}{T_0}\frac{dT_0}{dz_0} - \frac{AR}{c_p}\frac{1}{p_0}\frac{dp_0}{dz_0} = \left(\frac{1}{T}\frac{dT}{dz} - \frac{AR}{c_p}\frac{1}{p}\frac{dp}{dz}\right)\frac{\varrho_0 s_0}{\varrho s} \tag{3}$$

$$\frac{1}{T_0 \varrho_0 s_0}\frac{dT_0}{dz_0} - \frac{AR}{c_p}\frac{1}{p_0 s_0 \varrho_0}\frac{dp_0}{dz_0} = \frac{1}{T}\frac{dT}{dz\varrho s} - \frac{AR\,1\,dp}{c_p\,\varrho s p dz} \tag{4}$$

after cancelling and as $Ag/c_p = \gamma_a$ we obtain

$$\frac{dT_0}{dz_0}\frac{1}{p_0 s_0} + \gamma_a \frac{1}{p_0 s_0} = \frac{dT}{dz}\frac{1}{ps} + \gamma_a \frac{1}{ps} \tag{5}$$

multiplied by sp

$$\frac{dT_0}{dz_0}\frac{sp}{s_0 p_0} = \frac{dT}{dz} + \gamma_a \tag{6}$$

or

$$\left(\frac{dT_0}{dz_0} + \gamma_a\right)\frac{sp}{s_0 p_0} = \frac{dT}{dz} + \gamma_a \tag{7}$$

$$\frac{dT_0}{dz_0}\frac{sp}{s_0 p_0} + \frac{dT_0}{dz_0} - \frac{dT_0}{dz_0}\frac{dT}{dz} = \gamma_a\left(1 - \frac{sp}{s_0 p_0}\right) \tag{8}$$

after reducing the equation into the standard form

$$\frac{dT_0}{dz_0} - \frac{dT}{dz} = \frac{dT_0}{dz_0}\left(1 - \frac{sp}{s_0 p_0}\right) + \gamma_a\left(1 - \frac{sp}{s_0 p_0}\right) \tag{9}$$

and finally

$$\frac{dT_0}{dz_0} - \frac{dT}{dz} = \left(\frac{dT_0}{dz_0} + \gamma_a\right)\left(1 - \frac{sp}{s_0 p_0}\right) \tag{10}$$

Thus for the change in lapse rate the following results are obtained:

At subsidence $1 - \frac{sp}{s_0 p_0} < 0$ because $\frac{sp}{s_0 p_0} > 1$

At subsidence the same particles are present, the change in cross section of the particles is approximately the same, the pressure change is a logaritmic one. The logarithmic pressure increase is higher than the linear cross section increase, $\frac{sp}{s_0 p_0} > 1$. When studying equation (10), we find that in case of atmospheric subsidence:

$$\text{if: } \left(\frac{dT_0}{dz_0} + \gamma_a\right) < 0 \qquad \text{(originally unstable)}$$

$$\frac{dT_0}{dz_0} - \frac{dT}{dz} \qquad \text{increases, while}$$

$$\text{if: } \left(\frac{dT_0}{dz_0} + \gamma_a\right) > 0 \qquad \text{(originally stable state)}$$

$\frac{dT_0}{dz_0} - \frac{dT}{dz}$ decreases, which means that at subsidence the stable state is even more stable, while the instable one is even more instable. Stabiliza-

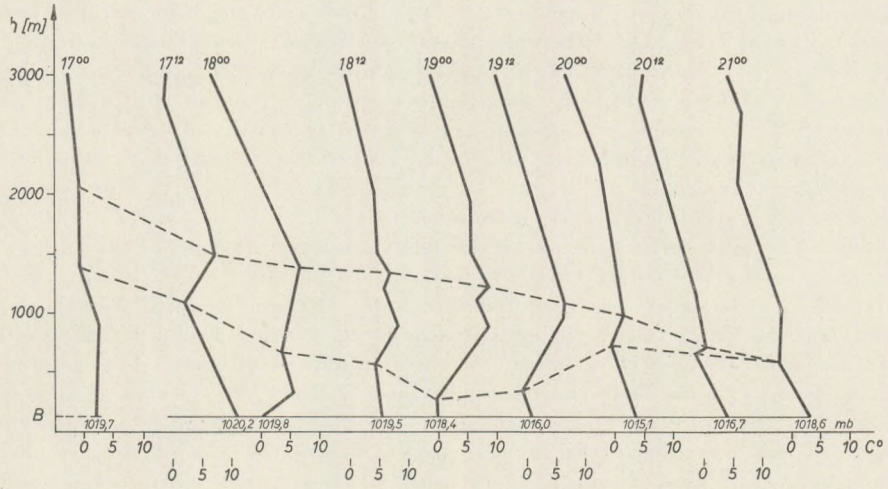

Fig. 3. Illustration of high aerological atmospheric ascents up to 3000 m, between February 17^{00} and February 20^{12}, 1961

tion and inversion formation can be observed mostly where a strong descent and a divergence coincide, that is at the upper boundary of the divergence zone.

To prove the above argumentation the inversion development was followed till the point of cessation between February 17^{00} and February 20^{12}, 1961 in a winter anticyclonic situation by means of radiosonde ascents made in Budapest. In Figure 3 the surface pressure is indicated by P_s, which showed very little fluctuation during the 4 days under study. The upper and lower boundary of subsidence inversion is indicated by dotted lines. On the 17th the first day of observation, at 00 o'clock only stability and isothermy could be observed. Following a gradual decrease in lapse rate an inversion was formed becoming thicker in the first half of the period then, with the increase in intensity the thickness decreased, and disappeared finally. In table 1 the thickness of the inversion layer and the lapse rate values are indicated on the relevant days at 00 and 12 GMT.

Table 1

	17^{00}	17^{12}	18^{00}	18^{12}	19^{00}	19^{12}	20^{00}	20^{12}
Lapse rate in C°/100 m	0,0	−0,75	−0,44	−0,35	−0,09	−0,87	−0,66	−1,25
Thickness *dz* of the inversion layer in *gpm*	616	600	770	1480	1643	820	260	80

We shall now follow the inversion development through energy considerations. The development stage of cyclones, anticyclones and other meteorological systems is often measured on the basis of the kinetic energy represented by them. The systems getting more or less intensified may be regarded as those gaming or losing kinetic energy. During the process of kinetic energy increase or decrease, the sources and sinks of kinetic energy become important, where anticyclones are to be regarded as sources, and cyclones as sinks.

T. Ando (1951) and, independently of him, Ozorai (1952) proved that as an effect of internal energy increase and potential energy decrease during the subsidence, the air masses accelerate. We shall prove that this process leads to an increase in wind at the bottom of the troposphere above the friction layer, to the appearance of low level jet-like wind maxima, and to the strengthening of the vertical wind shear. This phenomenon seems to be in harmony with the low level jet criteria. The low level jet is the zone of wind increase occurring from time to time in the lower troposphere above the friction layer, as well as that of the vertical wind shear. The most frequent occurrence of these phenomena is between 400 and 900 m, and they cannot be identified with the prefrontal increase in wind, when the concentration band of the velocity is to be observed

on the ground. E. Jakus (1971) while studying the relation of low level jets and the synoptic situation drew attention to the role of anticyclones. Studying the energetic conditions of anticyclones presents no difficulty when the dry, adiabatically descending air motion and air mass transport conditions of Faust are guaranteed.

Under these conditions and on the basis of the well-known energy equation, a change in kinetic energy is only followed by a change in potential energy and internal energy

$$\delta K = -\delta(P+I)$$

where $(P+I)$ is the sum of the potential and internal energy, called the total potential energy. The value of released energy was already studied by Margules, in his paper entitled "Energy of Storms". It was Lorenz who in 1955 gave an answer to the question as to the amount of potentially released ratio in a given state, and this amount is now called available potential energy, in his honour. Margules's theory has been further developed by Qort (1964), Smith (1969) and others. At present the field of primary importance of studies treating atmospheric energy is the concept of available potential energy. The available potential energy is the difference between the total potential energy and the minimum potential energy – reached following the adiabatic redistribution of the atmosphere –, that is to say, the minimum potential energy is the total potential energy of the stationary state. Determining it would be useful only in case if the resulting available potential energy would also indicate as to what state the atmosphere tends to reach.

Ando and Ozorai in their studies established that in the course of anticyclone dissolution with the decrease in $(P+I)$ the air masses accelerate. However, the low level jet phenomenon was then not yet been recognized. It was thus not possible to identify the possibility of acceleration with the existence of low level jets appearing in the inside of anticyclones above the friction layer, though the nocturnal breakdown of the ground inversion with steep wind gradients, a phenomenon first remarked by Durst in 1933, is here observed apparently to be associated with the sudden lowering of an upper inversion.

The process which converts available potential energy into kinetic energy, represented by $C = -\{\omega\alpha\}$, is often colloquially described as a sinking of colder air and a rising of warmer air at the same elevation. There should be two principal methods by which heating can produce available potential energy, first, by heating the warmer regions and cooling the cooler regions at the same elevation, thereby increasing the horizontal temperature variance, and second, by heating the lower levels and cooling the upper levels, thereby decreasing the static stability.

The fact that anticyclones are asymmetric formations and cannot be regarded by far as being homogeneous systems is proved by the presence of temperature inversion. This state, however, is untenable from the view-point of the stability of the system. To discontinue it, the particles follow – with the aid of descending motion – along a route until they

are in equilibrium with their environment according to their density. In this way the thickness of the inversion layer decreases and finally disappears. Thus, by the fact that through an effort of the stability state being regained in the interior of the anticyclone the inversion layer becomes gradually thinner, kinetic energy is produced by the transformation of the released potential energy. This theorem was already known, though in a somewhat different concept. The dissipation of the radiation inversion was then explained by an increase in intensity of the incoming radiation, and the dissipation of subsidence inversions by the wind getting stronger. In case of the latter, however, the process is a reversed one. Statistically, the strengthening of the wind and the dissipation of inversions result in a high correlation, due to the fact that the subsidence inversion is untenable for static stability and the discontinuance of the process is followed by dynamic changes.

In Fig. 4 the entire budget of $(P+I)$, as well as the value of kinetic energy are indicated per unit area of the layer between the ground and 700 mb on the relevant days. As the kinetic energy and the potential

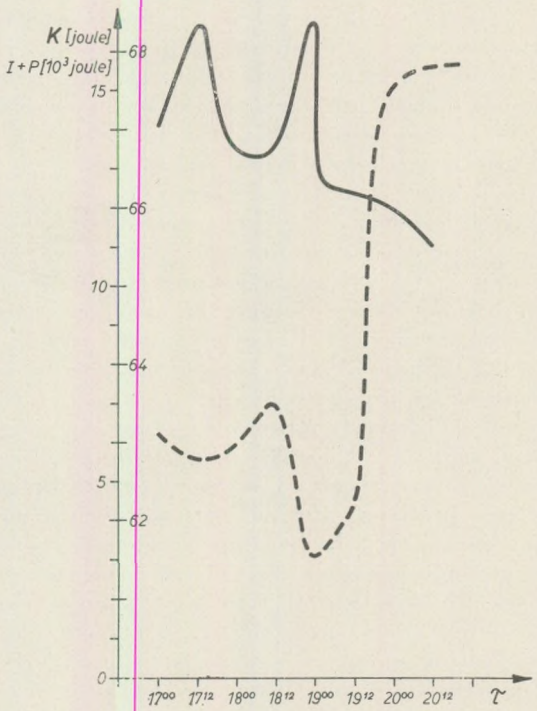

Fig. 4. The summarized value of the total potential energy $(P+I)$ and the kinetic energy (K), between p_0 and 700 mb, in the period of February 20^{12}, 1961

energy cannot be indicated in order of magnitude on the same scale, a special indexing has been applied for both energy-types along axis y. The increase in kinetic energy by a total decrease of potential energy can be followed without difficulty on the diagram. The summarized illustration, however, does not express the vertical profile of kinetic energy, and for this reason Fig. 5 indicates separately the vertical distribution of kinetic energy which has been determined layer by layer on the basis of significant wind points. By a layerwise illustration of the kinetic energy, the volume of horizontal mass transport can be expressed. This serves as a better comparison possibility as if only the scalar values of the horizontal wind had been indicated. Compared with Fig. 2 the increase in kinetic energy can be found at the spots where the inversion layer becomes thinner.

When studying low level jets the authors selected only some characteristic cases on the basis of certain criteria. The dissolution of inversions is followed in every case by an increase in kinetic energy. In our case there were some days when according to the extent of inversions no major potential energy release could be observed. As a typical example perhaps the change from the 19th (12th GMT) to the 20th (00th GMT) can be mentioned when the bottom layer kinetic energy concentraction was observed exactly at the spot where the inversion layer was becoming thinner. It is well-high impossible to guarantee the adiabatic condition in a four-day period. L o r e n z (1955) has already proved that when both forms of energy increase, adiabatic processes are not necessarily involved. This may be an answer concerning the unidirectional changes of both energies in the first half of the period.

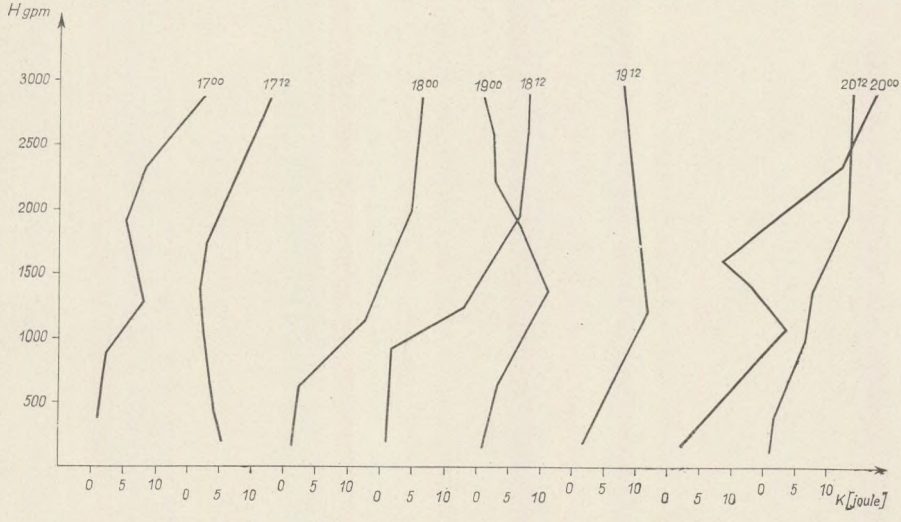

Fig. 5. The vertical profile of kinetic energy between p_0 and 700 mb expressed in joules

Our investigations have been carried out so far concerning local conditions only. In a further phase of the work it seems expedient to extend the calculations also to the dimensions of some particular meteorological systems After having carried out a complex investigation it will become possible to determine the axis of low level jets, similar to high level jets, and to recognize its relation to other elements.

LITERATURE

Ando, T. (1951): Energetics of the Anticyclone. Paper published in "Meteorology and Geophysics". Vol. II, No. 3–4.

Čadez, M. (1960): On Subsidence Inversions. Időjárás 64.

Faust, H. (1953): Die Nullschicht – der Sitz des troposphärischen Windmaximums. (The Zero Zevel – the Seat of Tropospheric Wind Maxima.) Meteorologische Rundschau, 6.

Jakus, E. (1971) Low level Jet Streams in the Carpathían Basin. Időjárás, 75.

Margules, M. (1903): Über die Energie der Stürme (Energy of storms.) Jahrb. Zentralanst. Meteorol.

Lorenz, E. N. (1955): Available Potential Energy and the Maintenance of the General Circulation. Tellus 7, No. 2.

Oort, A. H. (1964): On Estimates of the Atmospheric Energy Cycle. Monthly Weather Review 92, No. 11.

Ozorai, Z. (1952): Energy Transformation in Spreading-out Cold Airmasses. Időjárás, 56.

Smith, P. J. (1969): On the Contribution of a Limited Region to the Global Energy Budget. Tellus, 21. No. 2.

Durst, C. S. (1933): The breakdown of steep wind gradients in inversions. Quarterly Journal of the Royal Met. Society., 59. No. 3.

DESIGN OF SHORT INTERPOLATING FUNCTIONS FOR DIGITAL PROCESSING OF SEISMIC DATA

by

A. MESKÓ

(Geophysical Institute of Loránd Eötvös Universtiy)

(Received: 1st May 1971)

ABSTRACT

Interpolation is necessary in several operations of digital processing of seismic data (static and NMO corrections etc.). The exact interpolating formula has long been known but its application is time consuming and costly. A truncation procedure is reported here which is able to supply interpolating functions for any given accuracy and reasonable length. The Fourier transform of this interpolating function is the convolution of a properly chosen rectangle and a Gaussian function.

Introduction

The problem of reconstitution of a continuous function from its digitalized version has long been solved (Shannon's theorem). The interpolation as a special case of reconstitution and decimation as an inverse operation of the interpolation have also been treated repeatedly in the literature (e.g. B r a c e w e l l, 1965). Interpolation and decimation serve as theoretical basis for any resampling procedure used in digital processing of seismic data.

Theoretically the sinc (t) function should be used for both purposes. Truncated versions of the function, however, may reduce the amount of the necessary computations and thus save computer time and cost. As a consequence of the truncation the interpolated values deviate from the theoretically correct values. The more severe is the truncation the more significant are the deviations. What we have to seek for is a balance between reduced cost and deteriorating accuracy.

Interpolation is necessary at many places in seismic data processing e.g. at the computation of static and NMO corrections. Because of the large amount of data to be processed (the corrections are applied to thousands of seismic records) the application of a slightly shorter interpolating function results in important savings. The inaccuracies of other operations and noises which are always present justify the inaccuracies introduced by the interpolation.

The aim of this contribution is to outline the theory of determination short interpolating functions. Computer programs based on the considerations reported here have been successfully used in interpolation and decimation in connection with seismic data processing.

Summary of previous results

Shannon's fundamental theorem states that if a function $g(t)$ has a band-limited spectrum ranging from zero to an upper limit $f_{\max}$, and the sampling interval τ satisfies the inequality

$$\tau \leqq \frac{1}{f_{\max}}$$

then the continuous $g(t)$ can be completely recovered from its samples $g(k\tau)$ $(k = 0, \pm 1, \pm 2, \ldots)$ by the formula

$$g(t) = \sum_{k=-\infty}^{\infty} g(k\tau) \operatorname{sinc}\left(\frac{t}{\tau} - k\right). \tag{1}$$

In the practical applications the lower and upper limits of summation are chosen to be finite but sufficiently large intergers (k can vary e.g. between -50, $+50$), and the approximate value of the continuous function at any given instance t_0 is computed by

$$g(t_0) = \sum_{k=-50}^{50} g(k\tau) \operatorname{sinc}\left(\frac{t_0}{\tau} - k\right). \tag{2}$$

As it is seen from formula (2) the computation involves the determination of 101 coefficients

$$c_k = \operatorname{sinc}\left(\frac{t_0}{\tau} - k\right); (k = -50, -49, \ldots, +49, +50)$$

and the same number of multiplications and addition of the products. Each new value requires the determination of 101 new coefficients which makes the direct application of (2) tedious and unpractical in the majority of cases. Thus it became a general practice to use a predetermined set of coefficients and carry out the computations for some regularly placed $l\tau_0$ values and use linear interpolation for determining $g(t_0)$ from $g(l\tau_0)$ and $g[(l+1)\tau_0]$ where $l\tau_0 < t_0 < (l+1)\tau_0$. See Fig. 1.

In the followings we deal with the first part of the interpolation problem. The task is to compute some new values corresponding to regularly placed arguments.

Let us denote the sampling interval before and after the interpolation by τ_i and τ_0, respectively. The subscript i is used as an abbreviation for "input" and o refers to "output". Let us suppose, moreover, that $\tau_i = \lambda\tau_0$ (where λ integer), i.e. we want to determine between two "measured sample" $\lambda - 1$ "computed sample". Then $t_0 = l\tau_0$ and we obtain from (2)

$$g(l\tau_0) = \sum_{k=-50}^{50} g(k\tau_i) \operatorname{sinc}\left(\frac{l\tau_0}{\tau_i} - k\right)$$

$$= \sum_{k=-50}^{50} g(k\tau_i) \operatorname{sinc}\left(\frac{l}{\lambda} - k\right).$$

If $\lambda = 4$ two different sets of coefficients have to be applied. (In the case $l = 4n$, interpolation is not necessary and $l = 4n+3$ requires the same coefficients as $l = 4n+1$ but in reverse order.) These two sets can be stored in the memory of the computer and thus the repeated evaluation of the sinc function is avoided. The formulas to be applied are

$$\left.\begin{aligned} c_k &= \operatorname{sinc}\left(\frac{1}{2} - k\right) \qquad \text{if } l = 2n\,, \\ c_k &= \operatorname{sinc}\left(\frac{1}{4} - k\right) \qquad \text{if } l = 4n+1 \end{aligned}\right\} \quad (4)$$

$$(k = 0, \pm 1, \pm 2, \ldots).$$

Up to this point we treated the interpolation problem in the time domain, now let us discuss briefly what is the meaning of the reconstitu-

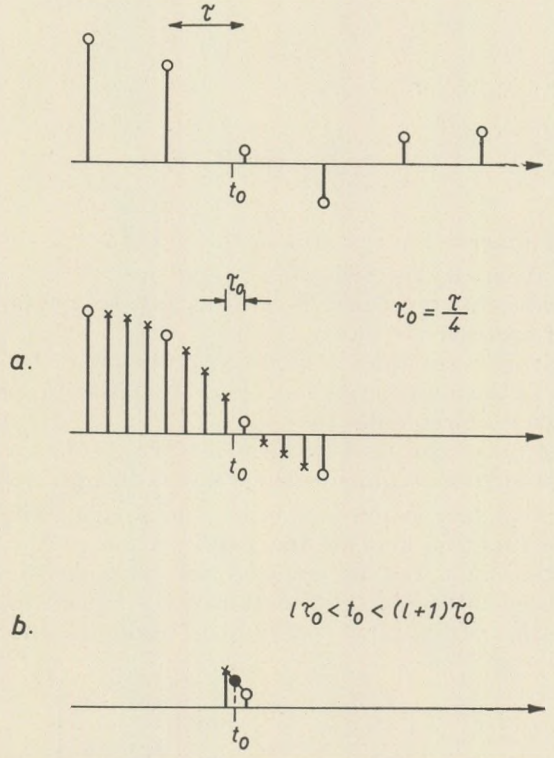

Fig. 1. Interpolation in two steps

a) first step: interpolation for regular grid. New sampling rate: $\tau_0 = \frac{\tau}{4}$

b) second step: linear interpolation

tion formula (1) in the frequency domain. This discussion will help to find effective truncation functions.

Let us denote the spectrum of the continuous function by $G(f)$ and that of its sampled version by $G^*(f)$. The Fourier transform of Equ. (1) gives

$$G(f) = G^*(f)\tau r(f\tau) \tag{5}$$

where $r(f)$ is rectangle function of unit area and unit width. This equation expresses the fact that the spectrum of the continuous function is proportional to the spectrum of the digitalized signal within the Nyquist interval and zero outside, if the sampling has been made in accordance with the Shannon's rule. The proportionality factor is the sampling rate. The rectangle function eliminates the superfluous part of the periodical spectrum and preserves the whole Nyquist interval. Any linear form of truncation results in the application of some other function than the rectangle. Let us denote this function by $V(f)$. Then we have in place of (5)

$$G(f) = G^*(f) \cdot V(f), \tag{6}$$

and in the time domain

$$g(t) = \sum_{k=-\infty}^{+\infty} g(k\tau)\, v(t-k\tau), \tag{7}$$

where $v(t)$ is the inverse Fourier transform of $V(f)$.

We expect from $v(t)$ the following properties:

a) It should converge towards zero as fast as possible in order to make the set of coefficients short.

b) Its application should not modify significantly the essential part of the spectrum of the continuous function. The latter property comprises the following two requirements:

b1) $V(f)$ should be constant over the interval of the signals and

b2) zero outside the Nyquist interval if only to a good approximation.

As a matter of fact requirements *a)* and *b)* contradict each other. If we make the function shorter the modification of the spectrum becomes more significant. Let us consider an example to enlighten this fact. A widely used interpolating function is the square of the sinc function. For the sake of simplicity assuming midpoint interpolation the following formula applies

$$g_{\text{int}}(l\tau_0) = \sum_{k=-\infty}^{+\infty} g(k\tau_i)\, \frac{1}{2}\, \operatorname{sinc}^2\left(\frac{lv_0}{2\tau_i} - \frac{k}{2}\right). \tag{8}$$

In the frequency domain the relation

$$G(f) = G^*(f)V(f)$$

holds, where $V(f)$ is a triangle function

$$V(f) = (f_n - f)\frac{1}{2f_n} \qquad \text{if } |f| \leqq f_n, \tag{9}$$

$$= 0 \qquad \text{if } |f| > f_n,$$

f_n is the Nyquist frequency.

The multiplication by $V(f)$ certainly modifies the spectrum but in many cases the attenuation of the high frequencies might be justified and sometimes even advantegeous. E.g. if interpolation is applied to a seismic record, sampled at 2 ms intervals and $f_N = 250$ Hz, the variation of $V(f)$ is about 20% over the interval which is of interest for the interpretation. This corresponds to a slight smoothing and is certainly admittable. On the other hand the $\text{sinc}^2 t$ function converges toward zero in the order of t^2 while the $\text{sinc}\, t$ function in the order of t. Hence it allows for the application of about ten times fewer coefficients than the exact interpolating function. The saved computer time compensates for the slight smoothing.

As a consequence of the smoothing the "measured samples" should also be modified. Otherwise a systematic deviation between original and interpolated values would set up. Thus when using formula (8) and the aim is to modify the sampling rate by a factor of 1/4 (i.e. $\lambda = 4$) three sets of coefficients should be applied:

$$a. \quad \text{sinc}^2\left(\frac{1}{2} - \frac{k}{2}\right) \qquad \text{if } l = 4n,$$

$$b. \quad \text{sinc}^2\left(\frac{1}{4} - \frac{k}{2}\right) \qquad \text{if } l = 2n,$$

$$c. \quad \text{sinc}^2\left(\frac{1}{8} - \frac{k}{2}\right) \qquad \text{if } l = 4n+1;$$

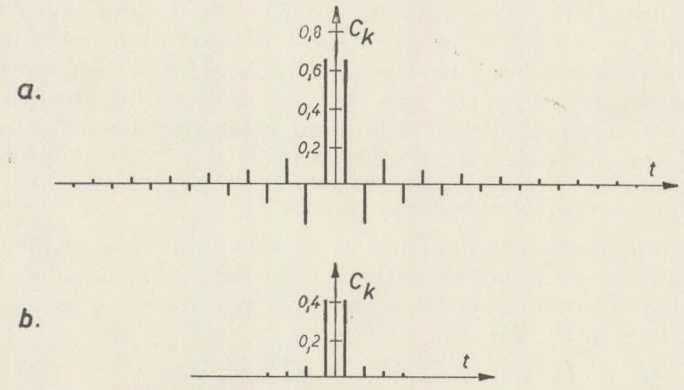

Fig. 2. Coefficients for midpoint interpolation
a) exact formula $\text{sinc}\,(t/\tau)$ for $t = (n+1/2)\tau$
b) $\text{sinc}^2\,(/2\tau)$ for $t = (n+1/2)\tau$

the coefficients corresponding to $l = 4n+3$ are the same as those to be applied in the case $l = 4n+1$, only their order should be reversed.

The coefficients derived from the exact and the $\mathrm{sinc}^2 t$ formula can be compared on Fig. 2. The relations in the frequency domain are shown on Fig. 3.

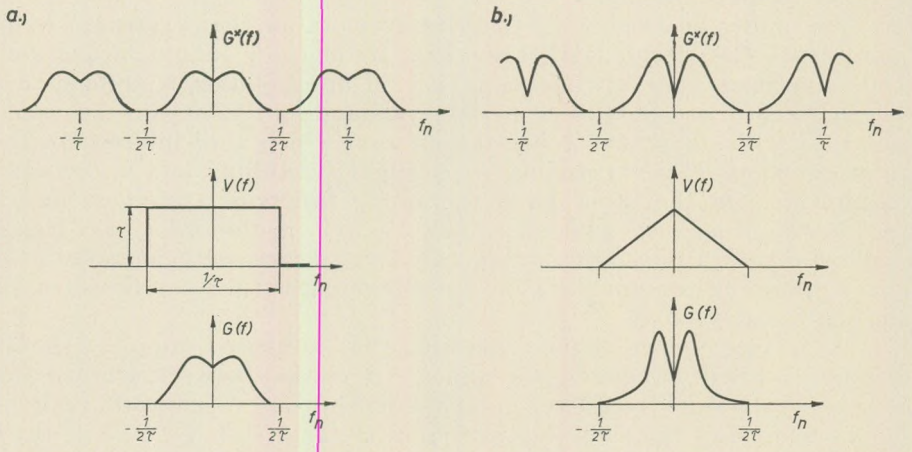

Fig. 3. The effect of reconstitution with the exact formula compared to the application of the approximate reconstitution (*a)* and *b)* respectively)

Some useful interpolating formulas

The example treated in the previous section has shown the underlying thoughts and some essential features of shortening the interpolation function. The next question is which function could supply better results than the $\mathrm{sinc}^2 (t/2\tau)$ does. After having investigated a number of functions we found that a Gaussian function or the product of a Gaussian function and a sinc $(\lambda t/\tau)$ (where λ is a properly chosen constant) in most cases serves best our purposes. The application of Gaussian functions can also be supported by the fact that the duration-bandwidth product for this function equals to the minimum value permitted by the uncertainity relation. (B r a c e w e l l, 1965.)

Gaussian function as interpolating function

The sampling rate, the amount of noises at the high frequency range and some other factors might influence the desirable shape of the Gaussian function. Therefore we allow one free parameter, q and use in the frequency domain the function

$$V(f) = \tau \, \mathrm{e}^{-\pi \left(\frac{fq}{f_n}\right)^2} \tag{10}$$

– f_n is the Nyquist frequency.

Let us remind that we expected two properties from this function: It should be flat over the frequency range essential to characterize the signal and zero outside the Nqyuist interval, if only to a good approximation. If q is too small the flatness in the neighbourhood of the origin satisfies with a very good approximation but $V(f_n)$ is too large to be acceptable. If q is too large the flatness is violated though the second condition is satisfied. The sampling rate plays an important role in establishing the lower and upper limits permittable for the parameter q, because it determines which portion of the Nyquist interval is to be preserved. In seismic data processing the following sampling rates are to be considered: 4 ms, 2 ms and 1 ms. For the sake of simplicity we might suppose that the essential part of the signal streches up to 62.5 cps, i.e. the spectrum of the interpolating function should be approximately constant from zero frequency up to the first half (if $\tau = 4$ ms), up to the first quarter (if $\tau = 2$ ms) and up to the one eighth (if $\tau = 1$ ms) of the Nyquist frequency. This implies the following requirements upon $V(f)$:

$$\left.\begin{aligned} e^{-\pi(q/2)^2} &\geqq \lambda_4 \qquad if = 4 \text{ ms} \\ e^{-\pi(q/4)^2} &\geqq \lambda_2 \qquad if = 2 \text{ ms} \\ e^{-\pi(q/8)^2} &\geqq \lambda_1 \qquad if = 1 \text{ ms} \end{aligned}\right\} \quad (11)$$

where λ_d ($\alpha = 4$, 2 or 1) is the greatest permitted deviation from flatness.

The second condition requires that

$$e^{-\pi q^2} \leqq \mu \quad (12)$$

independently of the sampling rate. (μ is an accepted approximation of zero.)

From equations (11) and (12) follows that

$$\ln \mu \geqq 4 \ln \lambda_4$$

$$\ln \mu \geqq 16 \ln \lambda_2$$

$$\ln \mu \geqq 64 \ln \lambda_1$$

Because the aim is to make λ as great as possible and – at the same time – μ as small as possible we conclude that the optimum is arrived at if the equation sign holds. Consequently, if a μ value is chosen the corresponding λ values are unambiguously determined. Table I. shows some μ and the corresponding λ values. It is seen that for $\tau = 1$ ms both requirements (small μ and sufficiently large λ) can be satisfied, but for $\tau = 4$ ms λ could not be sufficiently large, the smoothing is too severe even if $\mu = 10^{-2}$. In the case $\tau = 2$ ms, $\mu = 0.01$ and $\lambda = 0.75$ could be accepted but some improvement is desirable.

Before embarking upon designing improved interpolating functions, let us review again our aim. In the most difficult case ($\tau = 4$ ms) the spectrum should be flat in the first half of the Nyquist interval and about zero at the Nyquist frequency. Between $f_n/2$ and f_n the exact shape of the

spectrum is nearly indifferent if it smoothly decreases from unity towards zero: see Fig. 4. The flatness has been spoilt by the far too rapid decreas-

Table I

Values of λ parameters for somed fixe μ parameters (attenuation at Nyquist frequency) for the Gaussian interpolating function

μ	10^{-4}	10^{-3}	10^{-2}
λ_4	0.100	0.178	0.316
λ^2	0.563	0.649	0.750
λ_1	0.866	0.898	0.933

ing of the Gaussian function. We might hope that convolution with a flat function e.g. with a rectangle of length f_r might improve the situation.

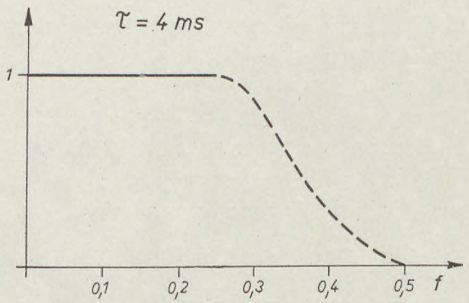

Fig. 4. A schematic representation of the "ideal" spectrum of an interpolating function if $\tau = 4$ ms

Convolution in frequency domain corresponds to multiplication in time domain. Thus the time function, corresponding to the Gaussian can be interpreted as a truncating function applied to the time function, corresponding to the rectangle.

Gaussian truncation

The interpolating function takes then the following shape

$$v(t) = \frac{1}{k} e^{-\pi\left(\frac{t}{k}\right)^2} \tau w \operatorname{sinc}(wt) \tag{13}$$

where w is the width of the rectangle. The Fourier transform of (13) reads as

$$V(f) = \tau\, e^{-\pi(kf)^2} * r\left(\frac{f}{w}\right). \tag{14}$$

Hence the smoothing which modifies the spectrum of the continuous function can be described by

$$S(f) = e^{-\pi(kf)^2} * r\left(\frac{f}{w}\right) = \int_{-w}^{w} e^{-\pi k^2 (f-f')^2}\, df'$$

Substituting φ for $f'-f$ and taking into consideration that the integrand is even function we obtain

$$S(f) = \int_{-w-f}^{w+f} e^{-\pi k^2 \varphi^2}\, d\varphi = \int_{0}^{w-f} e^{-\pi k^2 \varphi^2}\, d\varphi + \int_{0}^{w+f} e^{-\pi k^2 \varphi^2}$$

$$= erf[\sqrt{\pi}\, k(w-f)] + erf[\sqrt{\pi} k(w+f)], \tag{15}$$

where erf denotes the error function:

$$erf\, x = \frac{1}{\sqrt{\pi}} \int_{0}^{x} e^{-t^2}\, dt.$$

The requirements upon the interpolating function and its spectrum are as follows

$$e^{-\pi\left(\frac{t}{k}\right)^2} \leqq \varepsilon_t \tag{16}$$

– where $2n$ is the number of coefficients used in the interpolation;

$$S(0.25) \geqq 1 - \varepsilon_p \tag{17}$$

and

$$S(0.5) \leqq \varepsilon_p. \tag{18}$$

Requirement (16) expresses that the application of $2n$ coefficients is justified because the others are very small and thus might be cut out. Requirements (17) and (18) fomulate that attenuation in the first half of the Nyquist interval does not decrease significantly but approximates zero at the neighbourhood of $f_n = 0.5$.

It is difficult to give some generally applicable range for ε_t, ε_p and ε_r, because sometimes accuracy is the more important factor (and then all parameters should be small, consequently n must be large enough) while in other occasions the processing time is our main concern and we allow ε_t to be larger in order to make n small. Reasonable ranges for the parameters are as follows

$$\varepsilon_t \approx (10^{-3}, 10^{-6})$$

$$\varepsilon_p \approx (10^{-1}, 10^{-3})$$

$$\varepsilon_r \approx (10^{-2}, 10^{-5}).$$

Once the parameters are set the corresponding n, k and w can be determined by a trial and error method. It should be done by the computer for the amount of the computational work is too large. The following example illustrate the main features of the process.

Suppose we require

$$\varepsilon_t = 10^{-4}, \quad \varepsilon_p = 10^{-1} \quad \text{and} \quad \varepsilon_r = 10^{-2}.$$

At first we might try $n = 6$ (i.e. 12 coefficients). From equation (16) we obtain

$$e^{-\pi\left(\frac{6}{k}\right)} \leqq 10^{-4}$$

which gives the following limit for k

$$k < 3.49 \tag{19}$$

(17) and (18), on the other hand, requires that

$$S(0.25) \geqq 0.9$$

$$S(0.5) \leqq 0.001.$$

It is clear from the shape of the error function that k should be as great as possible. But (19) sets up an upper limit, thus we are compelled to use $k = 3.49$ and compute $S(0.25)$ and $S(0.5)$ for some w. The computation yields the following values

w	$S(0.25)$	$S(0.5)$
.15	0.192	0.002
.20	0.433	0.005
.25	0.500	0.015
.30	0.688	0.041

Thus it soon turns out that either $S(0.25)$ is too small or $S(0.5)$ is too great. The required accuracy can not be achieved by 12 coefficients.

After increasing n several times and repeating the computational procedure we find that with the parameters $n=12$ (i.e. 24 coefficients) $k=6.97$ and $w=0.35$ all conditions are satisfied.

The coefficients can be determined from Equ. (13) and interpolation can be carried out.

Acknowledgements

The theoretical considerations outlined here served as the basis of developing two computer programs design interpolation and apply interpolation under project no. GSP−1971/3 for the TIOPS 980 computer. The author is grateful to the Geophysical Prospecting Company of OKGT for making available computing facilities and supporting the development of these programs.

REFERENCES

Bracewell, T. (1965): The Fourier transform and its application New York. McGraw-Hill Book Co.

Meskó, A. (1969): Digital processing of seismic data Lecture notes. Vol. II. (In Hungarian) NIMDOK. Budapest

Robinson, E. A. (1967): Statistical communication theory Griffin. London

FAUNA- UND FAZIESVERBREITUNG DER OBERTRIAS DES TRANSDANUBISCHEN MITTELGEBIRGES

von

DR. E. VÉGH-NEUBRANDT

(Lehrstuhl für Angewandte Geologie Eötvös Loránd Universität)

(Eingegangen: 12 März 1971)

РЕЗЮМЕ

В верхнетриасовых отложениях Задунайского среднегорья можно выделить четыре биостратиграфических подразделения и четыре формации горных пород. Границы между формациями не являются синхронными поверхностями, так как в юго-западном направлении наблюдается постоянно более позднее наступление смены фаций. Биостратиграфические подразделения, обоснованные фауной и считаемые синхронными, более или менее соответствуют стратиграфическим ярусам. При этом границы их, соответствующие границам карнийского, норийского и рэтского ярусов, частично разбивают формации на две части, частично же пересекают их контактовые линии. Последовательность формаций такая: карнийская толща мергелей, карнийско-норийские главные доломиты и норийско-рэтские известняки дахштейн. В юго-западной части рассматриваемой области норийские главные доломиты и рэтские известняки дахштейн разделяются между собой кессенской серией.

Мергелисто-доломитово-известняковые толщи обнаруживают не только определенную последовательность во времени, но также и расположение рядом друг с другом по горизонтали, так как палеогеографические границы их в верхнетриасовое время постепенно перемещались на юго-запад.

Im transdanubischen Teil des Ungarischen Mittelgebirges haben sich von der karnischen Stufe an bis zum Ende der Triasperiode vier aufeinander lagernde, lithostratigraphische Grosseinheiten, Formationen entwickelt: 1. die „obere Mergel"-Gruppe und deren heteropische Fazies, die den Grossteil der Karn-Stufe vertreten; 2. der oberkarnisch-norische Hauptdolomit und 3. der norisch-rhätische Dachsteinkalkkomplex, den im SW-Teil des Mittelgebirges die 4. Kössener Serie in zwei Teile gliedert.

Die Grenzen dieser Formationen sind keine synchronen Flächen: im NO erfolgt der Fazieswechsel früher, gegen SW tritt er immer später auf. Die Mergel, die Dolomite und die Kalksteine lagern jedoch in allen Profilen konsequent aufeinander und liegen räumlich ebenso in der gleichen Reihenfolge nebeneinander.

Diese Anordnung hat sich eigentlich bereits in der Ladin-Zeit entwickelt, aber damals herrschte noch bis zu den NO-Gebieten der diploporenführende Dolomit vor, die sich daran anschliessende Kalksteinausbildung ist an der Tagesoberfläche nicht bekannt. Die nächst vorkommende ladinische Kalksteinausbildung ist nur noch im Raume des

Bükk-Gebirges zu finden. Die paläogeographische Verbindung des Bükk-Gebirges mit der Trias von Transdanubien ist jedoch nicht geklärt, daher können die beiden nicht als sichere angrenzende Gebiete betrachtet werden.

Das Nebeneinander der Fazies zeigen die Abbildungen 1 – 6, bezüglich ihrer vertikalen Aufeinanderfolge sei hier auf das prinzipielle Profil von J. Oravecz (1963, Abb. 3) hingewiesen.

Die karnische Mergelserie ist der mannigfaltigste Komplex. In ihm wechseln sich Kalksteine, Mergelkalke, bituminöse Hornsteinkalke, ja an manchen stellen des oberen Teiles sogar dolomitische Mergel sowohl zeitlich, als auch räumlich ab. Nicht nur die lithologische Zusammensetzung ist veränderlich, sondern auch die Farbe des Gesteins: eine Farbenskala von gelb bis braun, von hellgrau bis schwarz, sowie grünliche

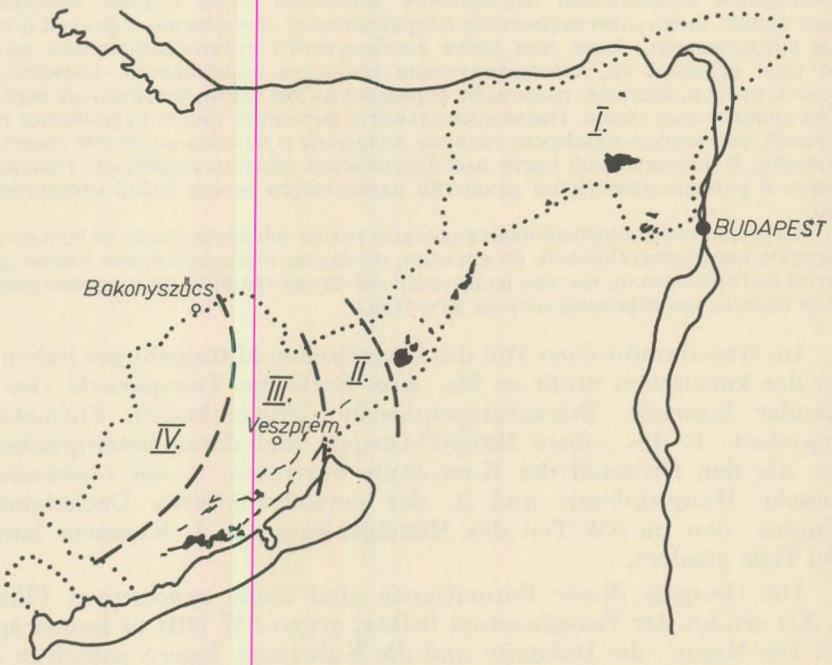

Abb. 1. Paläogeographische Anordnung der Fazieseinheiten während des Ladins im Raume des Transdanubischen Mittelgebirges

und lila Töne sind charakteristisch. Dominante Faunenelemente im Balatonhochland sind die Ammoniten und Brachiopoden, mit Muscheln, Korallen und Hydrozoen in den höheren Schichten. Im Gebiete der Berge Iszkahegy – Vértes – Buda – Pilis sind für die Serie hauptsächlich Muscheln, in den Schollen am Linksufer der Donau wieder Ammoniten, Brachiopoden und Muscheln charakteristisch.

Diese symmetrische Veränderung des Faunenbildes in der Streichrichtung bleibt in den jüngeren Schichten nicht erhalten, denn mit der Veränderung der Mergelfazies verschwinden die für den SW-Teil charakteristischen Ammoniten – Brachiopoden-Faunen.

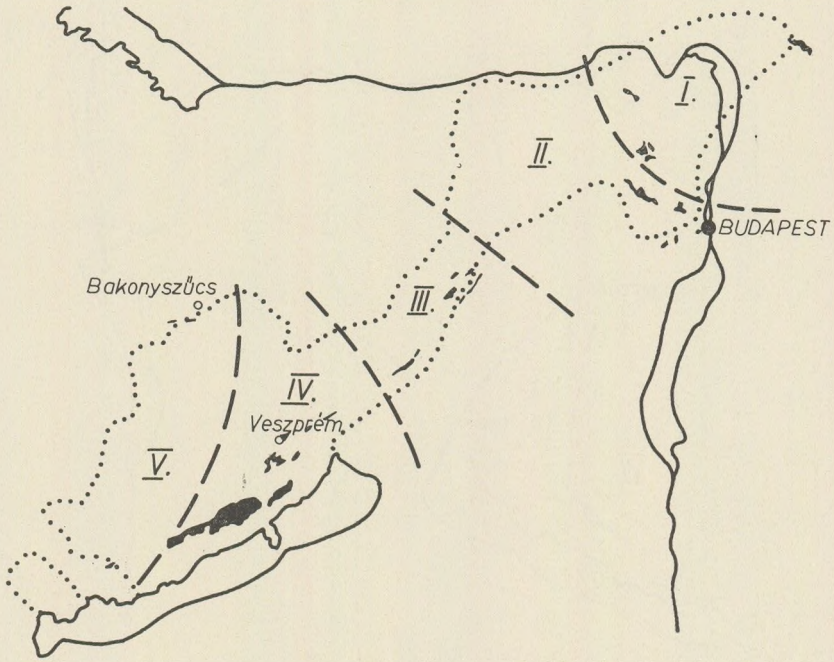

I. Kalk, hornsteinführender Kalkstein
II. Dolomit, mergeliger Dolomit
III. Mergel, hornsteinführender Mergel, dolomitischer Mergel
IV. Mergel mit Kalk- Zwischenlagerungen
V. Mergel

Abb. 2. Paläogeographische Anordnung der Fazieseinheiten während des unteren Karns im Raume des Transdanubischen Mittelgebirges

Die Serien des Hauptdolomites und des Dachsteinkalkes sind wesentlich einheitlicher ausgebildet. Für die beiden Serien ist das Vorherrschen der Lamellibranchiaten und Gastropoden charakteristisch. Ihre Leitfossilien sind die Megalodontiden.

Im Hauptdolomit sind Brachiopoden am NO-Rand des Gebietes (Gruppe von Iszkahegy, Vértes, Budapest: Újlaki-hegy), Ammoniten aber nur im Raume des Budaer Gebirges (Apáthy szikla, Hármashatárhegy) auf einen engen Horizont beschränkt zu finden.

Die Kössener Serie ist von kleinerer geographischer Verbreitung: vom Keszthely-Gebirge bis zum NO-Bakony verbreitet. Sie wird durch eine reiche Muschelfauna mit *Rheatavicula contorta* charakterisiert. In

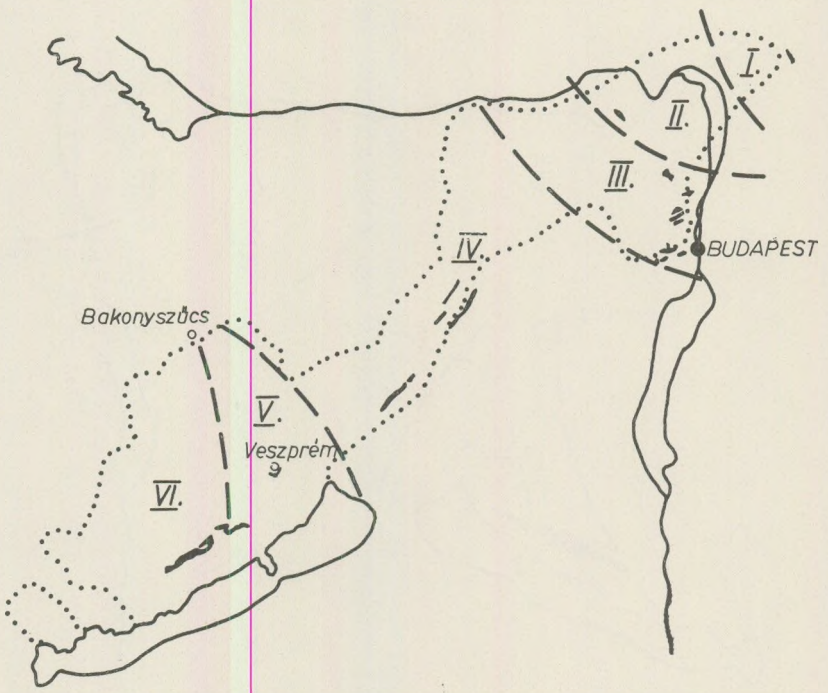

Abb. 3. Paläogeographische Anordnung der Fazieseinheiten während des mittleren Karns im Raume des Transdanubischen Mittelgebirges

ihren basalen Bänken treten im nördlichen Bakony (Borzavár: Templomdomb) Brachiopoden auf, im Raume des Vértes (Máriavölgy) und Gerecse (Herkályos) wird dagegen die ganze Serie durch eine verjüngte, in den Dachsteinkalk eingelagerte, brachiopodenführende Bank ersetzt. Die Kössener Serie kann auf Grund der Megalodontiden-Fauna des liegenden Dolomites und Kalksteines bzw. des hangenden Kalksteines im ganzen Gebiet als eine, mit dem unteren Teil der Rhät-Stufe synchrone Formation aufgefasst werden.

Im Dachsteinkalk sind die Megalodontiden und ein paar Gastropoden-Arten – neben den ebenfalls charakteristischen, stellenweise massenhaft vorkommenden Vertreter der Foraminiferen-Art *Triasina hantkeni* M a j z o n – fast die ausschliesslichen, makrofaunistischen Elemente. Eine Ammoniten-Fauna ist lediglich vom Aufschluss Fazekashegy in Buda-

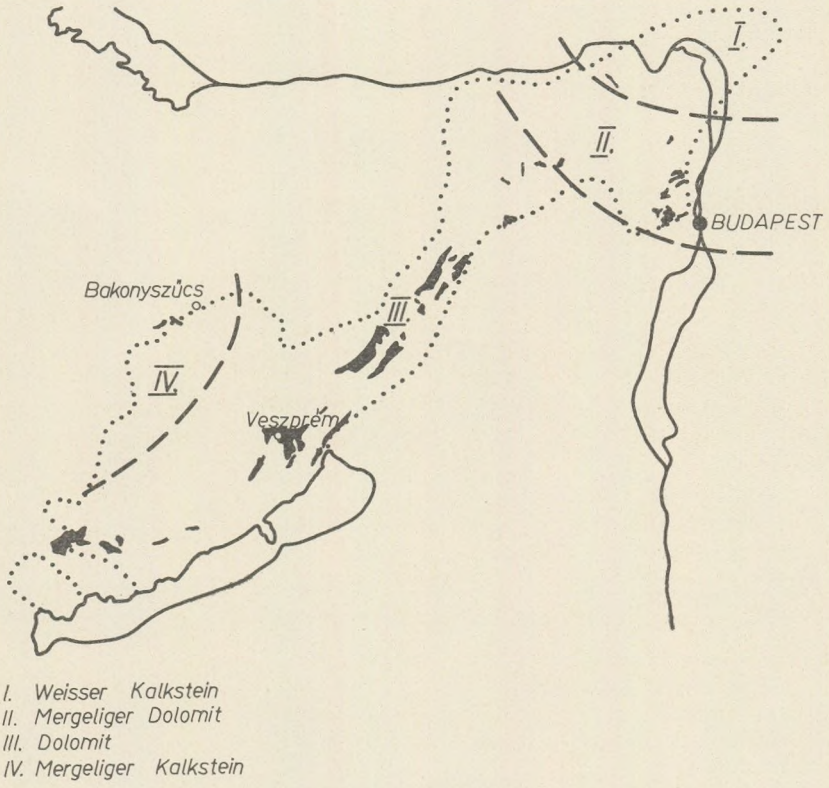

Abb. 4. Paläogeographische Anordnung der Fazieseinheiten während des oberen Karns im Raume des Transdanubischen Mittelgebirges

pest, aus den Grenzschichten Karn/Nor bekannt, ausserdem wurde *Rhabdoceras suessi* von E. Kutassy aus dem norischen Dachsteinkalk des in der Nähe befindlichen Berges Remetehegy beschrieben.

Auf Grund der Megalodontiden und der Mikrofazies lässt sich der Dachsteinkalk in ein hauptsächlich chemogenes norisches Glied und ein hauptsächlich aus biogenen Elementen bestehendes, rhätisches Glied teilen, sogar dort, wo die die Nor/Rhät-Grenze markierende Kössener Serie fehlt.

In den höchsten Bänken des rhätischen Dachsteinkalkes kann die Brachiopoden-Art *Rhaetina gregariaeformis* (Zugm.) in mehreren Punkten des nördlichen Bakony-Gebirges angetroffen werden, allerdings immer nur in solchen Profilen, wo ein almählicher Übergang in die Liasschichten sich verfolgen lässt.

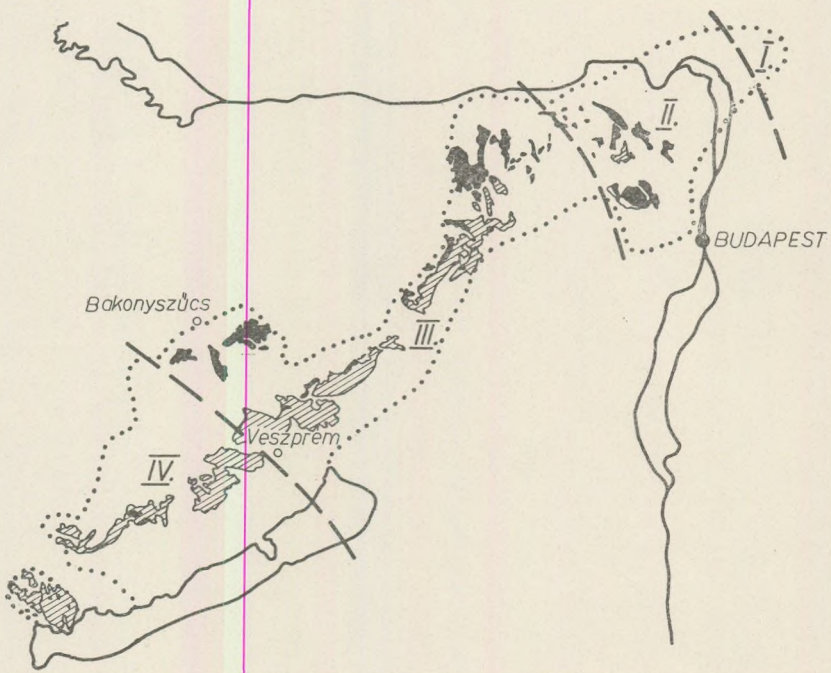

I. Gebiet ohne Sedimentation
II. Dachsteinkalk
III. Hauptdolomit mit überlagerndem Dachsteinkalk
IV. Hauptdolomit

Abb. 5. Paläogeographische Anordnung der Fazieseinheiten während des Nors im Raume des Transdanubischen Mittelgebirges

Aus dem Gesagten folgt eindeutig, dass nach der Karn-Stufe sowohl die brachiopoden- als auch die cephalopodenführenden Fazies auf die nordöstlichen Gebirgsteile beschränkt sind und den südwestlichsten Punkt in der Umgebung von Zirc im Rhät erreichen.

Den Faunenlisten der einzelnen Lokalitäten ist zu entnehmen, dass in der Brachiopoden-Cephalopoden-Fazies die Megalodontiden zurückgedrängt sind bzw. vollkommen fehlen und, umgekehrt, die megalodontidenführenden Schichten gar keine Brachiopoden oder Cephalopoden enthalten. Diese Feststellung ist vom Gesichtspunkt der Vergleichbarkeit von Schichten von gleichem Alter, aber von unterschiedlichem Faunencharakter äusserst wichtig .

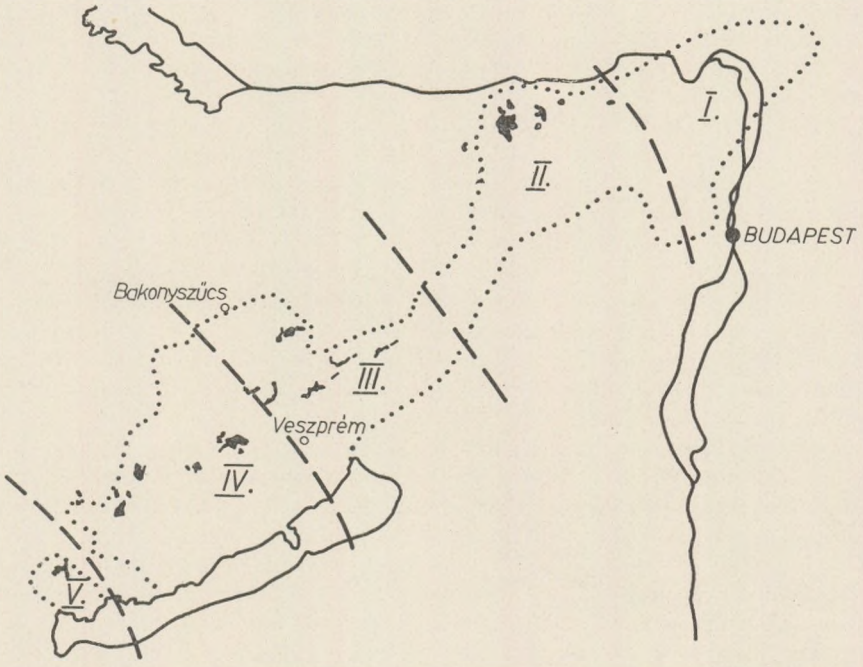

I. Gebiet ohne Sedimentation
II. Oberer Dachsteinkalk
III. Dachsteinkalk über auskeilenden kössener Mergeln
IV. Kössener Mergel mit überlagerndem oberen Dachsteinkalk
V. Kössener Kalk, Mergel und plattiger Dolomit

Abb. 6. Paläogeographische Anordnung der Fazieseinheiten während des Rhäts im Raume des Transdanubischen Mittelgebirges

Die Faunenlisten aller bisher bekannten und bearbeiteten Lokalitäten der vorher besprochenen vier Formationen vergleichend kann man die Zahl der identischen Arten bestimmen. Für die Klarheit hat Verfasserin das Material von ca. 160 Lokalitäten in Form einer Tabelle auf solche Weise aufgearbeitet, dass die Nummer jeder Lokalität von 1 bis 160 sowohl in der horizontalen Kopfleistenreihe der Tabelle, als auch in ihrer vertikalen Säule angegeben wurde. In der Kreuzung der vom Kopfleisten und der vertikalen Säule aus projektierten Geraden wurde die entsprechende Zahl der gemeinsamen Arten eingeschrieben. Die den gleichen Lokalitäten entsprechenden Kreuzungspunkte zeigen die Artenzahlen der betreffenden Lokalitäten. Das wurde speziell zum Ausdruck gebracht. Mit dieser Methode lässt sich jede Lokalität bezüglich der Zahl der gemeinsamen Arten mit den sämtlichen anderen Lokalitäten vergleichen und man kann das ganze Bild gleichzeitig überblicken. Nachdem Verfasserin die Nummern der miteinander gleichwertigen (äquivalenten) und eine grosse Anzahl gemeinsamer Arten führenden Lokalitäten in verschiedenen Farben eingekreist hatte, stellte sich eindeutig heraus, dass die vier Formationen verschiedene Faunentypen enthalten, wenn man von den lokalen cephalopoden- und brachiopodenführenden Fazies absieht.

Die charakteristischsten und zugleich die häufigsten Elemente der ältesten Faunengemeinschaft, die sich zum Karn rechnen lässt, sind *Cornucardia hornigi* (Hauer), *Neomegalodon carinthiacus* Hauer, *Neomegalodon triqueter pannonicus* Frech, *Neomegalodon paronai praenoricus* mihi (= *Megalodus seccoi juvenilis* Hoernes 1898) und *Cuspidaria gladius* Hauer.

Die mittlere Faunengemeinschaft besteht aus Arten, die für das Nor charakteristisch sind mit massenhaftem Auftreten, von: *Neomegalodon gümbeli* Stoppani, *N. complamatus* Gümbel, *N seccoi* Parona sowie von verschiedenen Arten der Gattungen *Dicerocardium*, *Myophoria* und *Worthenia*.

Die Faunengemeinschaft der Kössener Fazies ist ganz eigenständig, sie weist keine Identität oder Ähnlichkeit weder zur liegenden, noch zur hangenden Ausbildung auf. Die charakteristischste Art ist *Rhaetavicula contorta* (Portlock), am häufigsten kommen *Parallelodon azzarolae* (Stoppani), *Modiola faba* (Winkler), *Modiola minuta* (Goldfuss), *Pteria falcata* (Stoppani), *Entolium helli* (Emmrich), *Placunopsis alpina* (Winkler) und *Cardita austriaca* (Hauer) vor.

Die beweislich dem obersten Rhät angehörende Faunengemeinschaft wird durch *Conchodon infraliassicus* Stoppani und die Arten der Gattung *Rhaetomegalodon* charakterisiert, die nicht nur stratigraphische Leitfossilien sind, sondern in diesem sog. oberen Dachsteinkalk-Komplex auch massenhaft vorkommen.

Die vier Faunengemeinschaften mit den vier Formationen vergleichend, beobachtet man, dass die lithologischen und faunistisch-biostratigraphischen Grenzen nicht koinzidieren, da die letzteren die Gesteinsgrenzen überschneiden.

Unter Berücksichtigung der lithologischen und faunistischen Grenzen lässt sich die Obertrias des Transdanubischen Mittelgebirges in sechs Einheiten teilen. Die karnische Fauna verteilt sich zwischen der Mergel- und Hauptdolomit-Kalkstein-Fazies, die norische zwischen dem Hauptdolomit und dem Dachsteinkalk. Nur die Fauna- und die Lithofazies der Kössener Schichten und des oberen Dachsteinkalkes sind es, die eng aneinander gebunden sind.

Der Hauptdolomit verteilt sich also in einen karnischen und einen norischen Teil, der Dachsteinkalk in einen norischen und rhätischen.

Wenn man die auf solche Weise erhaltene Fauna der soeben geschilderten Tabelle angibt, und auch mit den dazu gehörigen Lithofazies ergänzt, ergibt sich das folgende Bild über die Anzahl der gemeinsamen Arten:

	1.	2.	3.	4.	5.	6.
1. Karnischer Mergel	137					
2. Karnischer Dolomit und Kalkstein	18	115				
3. Norischer Dolomit	6	12	126			
4. Norischer Kalkstein	2	4	29	90		
5. Kössener Serie	0	0	2	2	60	
6. Rhätischer Kalkstein	0	0	0	1	1	23

Aus der Tabelle ist ersichtlich, dass in den zeitlich mehr voneinander entfernten Schichtengruppen die Zahl der gemeinsamen Arten kleiner, als in den mehr angenäherten ist. Trotzdem fällt die ausserordentlich geringe Zahl der gemeinsamen Arten sogar in den aufeinanderfolgenden stratigraphischen Einheiten ins Auge. Das ist sehr pregnant im Falle des norischen Hauptdolomites und norischen Dachsteinkalkes, die nicht nur übereinander lagernde Schichten verschiedenen Alters, sondern auch in einem grösseren Raum in einander ersetzende Fazies bilden. Es lässt sich jedoch nicht einmal im Hauptdolomit, der im südlichen Bakony das ganze stratigraphische Intervall des Nors ausfüllt, die Scheidung von zwei norischen Faunen-Horizonten beobachten.

12 von den 18 gemeinsamen Arten der karnischen Mergel- und karnischen Dolomit-Kalkstein-Ausbildung sind charakteristische Leitfossilien der Karn-Stufe, welche die beiden Schichtengruppen enger miteinander verknüpfen, als das Vielfache von indifferenten Formen.

Die 12 gemeinsamen Arten der Mergel- und Dolomit-Kalksteinserie des Karn und der Dolomite des Nor bestehen dagegen aus persistenten Formen von grosser stratigraphischer Reichweite.

Bei den 29 gemeinsamen Arten der norischen Dolomite und Kalksteine ist derselbe der Fall, wie bei den karnischen Mergeln und karnischen Dolomiten-Kalksteinen. Verhältnissmässig wenig sind die gemeinsamen Arten, aber gerade diese gehören zu den charakteristischsten und häufigsten Formen *(Neomagalodon, Dicerocardium, Myophoria, Worthenia)*.

Die geringste Beziehung lässt sich zwischen den Faunen des Nor und Rhät erkennen. Ihr charakteristisches gemeinsames Leitfossil ist nur *Triasina hantkeni* M a j z o n. Dieser scharfe Unterschied ist auf einen, durch die Ablagerung der Kössener Mergelserie bedingten Fazieswechsel zurückzuführen. Diese veränderten Sedimentationsverhältnisse haben nämlich auch auf jene Gebiete ausgewirkt, wo die Kössener Mergelserie sich nicht ausgebildet hat.

Aus den obigen ist also eindeutig wahrzunehmen, dass auf dem Gebiete des Transdanubischen Mittelgebirges die den Stufen Karn, Nor und Rhät entsprechenden Komplexe auf biostratigraphischer Basis gut voneinander abgetrennt werden können, aber die Weitergliederung der einzelnen Stufen, wie sie in manchen Teilen der Alpen auf Grund der reichen Ammoniten-Faunen durchgeführt wurde, nicht realisierbar ist.

LITERATUR

O r a v e c z, J. (1963): A Dunántúli Középhegység felsőtriász képződményeinek rétegtani- és fácieskérdései. (Questions stratigraphiques et faciales des formations triasiques supérieures de la Montagne Centrale de Transdanubie). Földt. Közl., 93/1. 63–73.

V é g h n é N e u b r a n d t E. (1964): Triász Megalodontidák rétegtani jelentősége. (Stratigraphische Bedeutung der triasischen Megalodontiden). Földt. Közl. 94/2. 195–205.

РЕШЕНИЕ ДВУМЕРНОЙ КРАЕВОЙ ЗАДАЧИ ТЕПЛОВЫХ И ЭЛЕКТРОМАГНИТНЫХ ПОЛЕЙ НАД ВЕРТИКАЛЬНЫМ КОНТАКТОМ ГОРИЗОНТАЛЬНО-СЛОИСТЫХ СРЕД

Е. А. ЛЮБИМОВА,* В. Н. НИКИТИНА*
(Институт Физики Земли АНСССР, Москва)

Даётся решение двумерной краевой задачи для уравнений $\Delta u = f$ и $\Delta u + \overline{\overline{k}}^2 u = f$ в случае произвольной горизонтально- слоистой среды с вертикальным контактом. Решение получено в замкнутом виде, в явной аналитической форме, удобной при анализе и проведении расчетов. На основе данного метода решения указаны возможные обобщения и круг геофизических приложений.

Важным классом двумерных краевых задач математической физики являются краевые задачи над вертикальным контактом горизонтально-слоистых структур. Двумерно неоднородный разрез среды указанного вида с произвольным ступенчатым профилем типичен для целого ряда задач прикладной математики. Отметим, например, процессы теплопроводности на поверхности двух структур, разделённых вертикальным контактом – уравнение Пуассона $\Delta u = f$ (1); процессы распространения электромагнитных полей – уравнение Гельм- $\Delta u + \overline{\overline{k}}^2 u = f$ (2); и др. Как известно, явное решение данной краевой задачи в случае ступенчатого разреза среды до сих пор не получено. Существуют лишь способы сведения её к интегральным уравнениям (Дмитриев, Захаров 1970). Излагаемый ниже метод позволяет решить краевую задачу рассматриваемого класса при общей формулировке условий возбуждения и излучения.

Мы рассмотрим здесь соответствующую краевую задачу на примере уравнения (2), поскольку (1) является его предельным случаем при $\kappa^2 \to 0$. Условия возбуждения и излучения в задачах (1) и (2) могут быть различны, краевые же условия на границах раздела сред, как правило, одинаковы. На рис. 1а указаны кусочно-постоянные значения параметров разреза в тепловых обозначениях: $\nu(x, z) = \nu_k^{\mathrm{I,\,II}}$, коэфициент теплопроводности; $H(x, z) = H_k^{\mathrm{I,\,II}}$ -генерация тепла; h_i, d_j – мощности слоёв для n – слойной структуры I $(x \leq x_0)$ $i = 1, \ldots, n$ и для m – слойной структуры II $(x \geq x_0)$ $j = 1, \ldots, m$. Параметры электромагнитной задачи указаны на рис. 1б: $\sigma(x, z) = \sigma_K^{\mathrm{I,\,II}}$-проводимость; $\varepsilon(x, z) = \varepsilon_K^{\mathrm{I,\,II}}$-диэлектрическая проницаемость. Вводим, как показано на рисунке, единую сводную нумерацию границ

$z = z_k$ ($k = 0, 1, \ldots, N$), $N = n+m$. При этом раздел $z = z_k$, существующий реально в одной из структур, продолжен фиктивно в соседнюю.

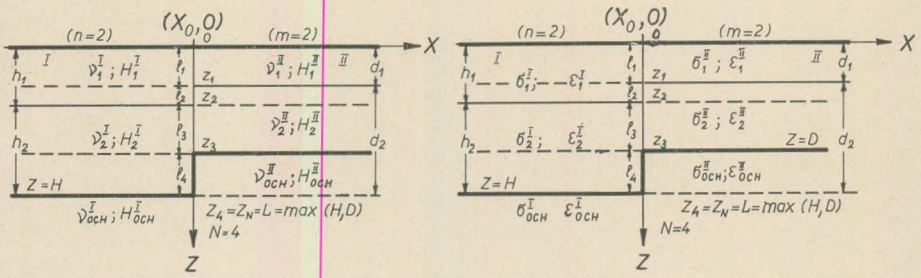

рис. 1.

Иллюстрируем возможности предлагаемого метода решения на конкретном примере теплового контакта между континентом и океаном. Задача сводится к определению температурного поля $T = u(x, z)$ из уравнения (I) в области $z \geq 0$.

Представляем решение двумерной краевой задачи в виде суммы

$$u = \begin{cases} u_0^{\mathrm{I}}(z) + v^{\mathrm{I}}(x, z), & x \leq x_0; \\ u_0^{\mathrm{II}}(z) + v^{\mathrm{II}}(x, z), & x \geq x_0; \end{cases}$$

Здесь функции u_0^{I} и u_0^{II} — известные решения соответствующей одномерной краевой задачи для одномерно неоднородных структур, а именно I-ой и II-ой со строением, изменяющимся только в направлении z. Аддитивная функция $v(x, z)$ означает чисто аномальную часть поля, обусловленную наличием в составной среде вертикального контакта $x = x_0$. Для v приходим к вспомогательной краевой задаче. Функция контакта v удовлетворяет уравнению $\Delta v = 0$ (3), и следующим дополнительным условиям:

а) условиям сопряжения при $x = x_0$

$$v^{\mathrm{I}}|_{x=x_0-0} - v^{\mathrm{II}}|_{x=x_0+0} = \varphi(z); \; v^{\mathrm{I}}(z) \cdot \frac{\partial v^{\mathrm{I}}}{\partial x}\bigg|_{x=x_0-0} - v^{\mathrm{II}}(z) \cdot \frac{\partial v^{\mathrm{II}}}{\partial x}\bigg|_{x=x_0+0} = 0; \tag{4}$$

где

$$\varphi(z) = u_0^{\mathrm{II}}(z) - u_0^{\mathrm{I}}(z);$$

б) граничному условию на поверхности $z = 0$

$$v^{\mathrm{I}}|_{z=0+0} = 0; \qquad v^{\mathrm{II}}|_{z=0+0} = 0; \tag{5^{I, II}}$$

в) однородным краевым условиям на горизонтальных границах

$$[v^{\mathrm{I}}]_{z_k+0}^{z_k-0} = 0; \qquad \left[v^{\mathrm{I}}(z)\cdot\frac{\partial v^{\mathrm{I}}}{\partial z}\right]_{z_k+0}^{z_k-0} = 0; \tag{6$^{\mathrm{I}}$}$$

$$[v^{\mathrm{II}}]_{z_k+0}^{z_k-0} = 0; \qquad \left[v^{\mathrm{II}}(z)\cdot\frac{\partial v^{\mathrm{II}}}{\partial z}\right]_{z_k+0}^{z_k-0} = 0; \tag{6$^{\mathrm{II}}$}$$

г), д) условиям на бесконечности

$$\left.\frac{\partial v^{\mathrm{I,\,II}}}{\partial z}\right|_{z\to\infty} = 0; \qquad (7^{\mathrm{I,\,II}}) \quad \text{и} \quad \begin{cases} \left.\dfrac{\partial v^{\mathrm{I}}}{\partial x}\right|_{x\to-\infty} = 0; \\ \left.\dfrac{\partial v^{\mathrm{II}}}{\partial x}\right|_{x\to+\infty} = 0; \end{cases} \tag{8$^{\mathrm{I,\,II}}$}$$

Подобная же задача возникает для электромагнитного поля. Например, в схеме плоской падающей волны $e^{-i(\omega t-k_0 z)}$, $z<0$ в случае магнитной поляризации поля $\vec{H} = (0, H_y, 0)$ и $\vec{E} = (E_x, 0, E_z)$ задача сводится к определению магнитного поля $H_y = u(x, z)$ из уравнения (2) в области $z \geq 0$. После разбиения решения u на сумму $u_0^{\mathrm{I,\,II}}(z)$ и $v(x, z)$ приходим к вспомогательной краевой задаче для v. Функция контакта v удовлетворяет волновому уравнению $\Delta v + \kappa^2 v = 0$ (3*) где $\mathrm{k}^2 = i\omega\cdot\sigma^*\cdot\mu$: $\sigma^* = \sigma - i\omega\varepsilon$: $Imk > 0$ и следующим дополнительным условиям.

а) при $x = x_0$

$$v^{\mathrm{I}}|_{x_0-0} - v^{\mathrm{II}}|_{x=x_0+0} = \varphi(z); \qquad \left.\frac{1}{\sigma^{*\mathrm{I}}}\cdot\frac{\partial v^{\mathrm{I}}}{\partial x}\right|_{x=x_0-0} - \left.\frac{1}{\sigma^{*\mathrm{II}}}\cdot\frac{\partial v^{\mathrm{II}}}{\partial x}\right|_{x=x_0+0} = 0; \tag{4}$$

где $\varphi(z) = u_0^{\mathrm{II}}(z) - u_0^{\mathrm{I}}(z)$;

б) на поверхности $z = 0$

$$v^{\mathrm{I}}|_{z=0+0} = 0; \qquad v^{\mathrm{II}}|_{z=0+0} = 0; \tag{5$^{\mathrm{I,\,II}}$}$$

в) однородным красвым условиям на горизонтальных границах раздела ($\kappa = 1, \ldots, N$)

$$[v^{\mathrm{I}}]_{z_k+0}^{z_k-0} = 0; \qquad \left[\frac{1}{\sigma^{*\mathrm{I}}}\cdot\frac{\partial v^{\mathrm{I}}}{\partial z}\right]_{z_k+0}^{z_k-0} = 0; \tag{6$^{\mathrm{I}}$}$$

$$[v^{\mathrm{II}})_{z_k+0}^{z_k-0} = 0; \qquad \left[\frac{1}{\sigma^{*\mathrm{II}}}\cdot\frac{\partial v^{\mathrm{II}}}{\partial z}\right]_{z_k+0}^{z_k-0} = 0: \tag{6$^{\mathrm{II}}$}$$

г); д) условиям на бесконечности

$$v^{I,\,II}|_{z\to\infty} = 0; \qquad (7^{I,\,II}) \quad \text{и} \quad \begin{cases} v^{I}|_{x\to-\infty} = 0; \\ v^{II}|_{x\to+\infty} = 0; \end{cases} \qquad (8^{I,\,II})$$

Теорема единственности в параллельных задачах (3–8) и (3*–8) для $v(x, z)$ всегда выполняется, т.к. разность двух решений задачи (3–8) [или (3*–8)] удовлетворяет основному уравнению (3) [или (3*)] с повсюду однородными и нулевыми дополнительными условиями и поэтому тождественно равна нулю.

Дальнейшие построения мы проведем для задачи (3*–8) с волновым уравнением, поскольку уравнение Лапласа является его предельным случаем, а краевые условия в задачах (3* и (3*–8) при замене коэфициентов $\frac{1}{\sigma^{*I}}$ и $\frac{1}{\sigma^{*II}}$ на v^{I} и v^{II} одинаковы в частном случае $\sigma \gg \omega\varepsilon$ и условия на бесконечности за вычетом постоянных слагаемых определяемых из условия на поверхности $z=0$ также одинаковы.

Решение задачи (3–8) строим методом разделения переменных x и z

$$v = X(x)\cdot Z(z) : \begin{cases} z'' + \mu^2 \cdot z = 0; \\ x'' - \beta^2 \cdot x = 0; \end{cases} \quad (\beta^2 = \mu^2 - k^2),$$

$$\text{либо} \begin{cases} x'' + \lambda^2 \cdot x = 0; \\ z'' - \alpha^2 \cdot z = 0; \end{cases} \quad (\alpha^2 = \lambda^2 - k^2);$$

в классической форме интегралов Фурье по μ, либо λ. Воспользуемся способом интегральных преобразований Фурье в комплексной форме для функций, определённых на полубесконечной оси [Титчмарш(1948)]. Применение преобразований на полубесконечной оси даёт удобный математический аппарат для построения решений в смежных угловых областях $z \leqq z_0$, $x \leqq x_0$. При этом, преобразование одинаково возможно как по z, так и по x.

При преобразовании по z функция-оригинал рассматривается раздельно при $x \leqq x_0$ и при $x \geqq x_0$ и обозначается v^{I} и v^{II}: соответственно получаем образы V^{I} и V^{II}. Вначале предположим, что $\sigma^*|_{x\leq x_0} = \sigma_I$ и $\sigma^*|_{x\geq x_0} = \sigma_{II}$, а $v(x, z)$ непрерывна и непрерывно дифференцируема по z в области $z \geqq z_0$, где z_0 – фиксированная постоянная, равная нулю или принимающая произвольное положительное значение. Полагаем

$$V(\mu, x; z_0) = \int_{z_0}^{\infty} v \cdot e^{-i\mu z} \cdot dz; \qquad Im\,\mu < 0 \qquad (9)$$

и

$$\frac{1}{2\pi} \cdot \int_{-\infty}^{+\infty} V \cdot e^{i\mu z} \cdot d\mu = \begin{cases} 0, & z \leqq z_0 \\ v(x, z), & z \geqq z_0 \end{cases} \qquad (10)$$

Дифференцируя (9) по x под знаком интеграла и пользуясь (3*), получим

$$\left.\frac{\partial^2 V(\mu, x; z_0}{\partial x^2}\right|_{z=z_0} = -\int_{\mathcal{L}}^{\infty} \frac{\partial^2 v}{\partial z^2} \cdot e^{-i\mu z} \cdot dz - k^2 \cdot \int_{z_0}^{\infty} v \cdot e^{-i\mu z} \cdot dz =$$

$$= -\left[\frac{\partial v}{\partial z} e^{-i\mu z}\right]_{z_0}^{\infty} - i\mu \left[v \cdot e^{-i\mu z}\right]_{z_0}^{\infty} + (\mu^2 - k^2) \cdot \int_{z_0}^{\infty} v \cdot e^{-i\mu z} \cdot dv =$$

$$= e^{-i\mu z_0} \cdot (\psi(x) + i\mu \cdot \chi(x) + (\mu^2 - k^2) \cdot V(\mu, x; z_0);$$

Здесь $\psi(x) = \left.\frac{\partial v}{\partial z}\right|_{z_0+0}$; $\chi(x) = v|_{z_0=0}$; (11)

Обозначаем $F(\mu, x; z_0) = e^{-i\mu z_0} \cdot (\psi(x) + i\mu \cdot \chi(x))$; (12)

Приходим к обыкновенному дифференциальному уравнению

$$\frac{d^2 V}{d x^2} - \beta^2 \cdot V = F(\mu, x; z_0); \qquad \beta^2 = \begin{cases} \beta_{\mathrm{I}}^2 = \mu^2 - k_{\mathrm{I}}^2; & x \leq x_0 \\ \beta_{\mathrm{II}}^2 = \mu^2 - k_{\mathrm{II}}^2; & x \geq x_0 \end{cases} \qquad (13)$$

где κ_{I} и κ_{II} постоянны для всех $z \geq z_0$. Условия сопряжения при $x \to x_0$ следуют из (4) и (3*). На бесконечности при $x \to \mp\infty$, $V^{\mathrm{I,\,II}}$ стремится к нулю.

Решением уравнения (13) является сумма общего решения V_0 однородного уравнения с $F = 0$ и неоднородными краевыми условиями и частного решения $\overline{V}$ неоднородного уравнения с $F \neq 0$ и однородными краевыми условиями: $V = V_0 + \overline{V}$.

Решение V_0 равно

$$V_0^{\mathrm{I,\,II}} = \begin{cases} D^{\mathrm{I}}(\mu) \cdot \underline{\underline{\Phi}}(\mu; z_0) \cdot e^{\beta_{\mathrm{I}} x}; & x \leq x_0 \\ D^{\mathrm{II}}(\mu) \cdot \underline{\underline{\Phi}}(\mu; z_0) \cdot e^{\beta_{\mathrm{II}} x}; & x \geq x_0 \end{cases} \quad Re\beta_{\mathrm{I,\,II}} > 0.$$

$$D^{\mathrm{I}} = \frac{\sigma_{\mathrm{I}} \cdot \beta_{\mathrm{II}}}{\sigma_{\mathrm{I}} \cdot \beta_{\mathrm{II}} + \sigma_{\mathrm{II}} \cdot \beta_{\mathrm{I}}} \cdot e^{-\beta_{\mathrm{I}} x_0}$$

$$D^{\mathrm{II}} = \frac{-\sigma_{\mathrm{II}} \cdot \beta_{\mathrm{I}}}{\sigma_{\mathrm{I}} \cdot \beta_{\mathrm{II}} + \sigma_{\mathrm{II}} \cdot \beta_{\mathrm{I}}} \cdot e^{\beta_{\mathrm{II}} x_0} \qquad (14)$$

– здесь $\underline{\underline{\Phi}}(\mu; z_0)$ – преобразование Фурье (9) от функции $\overline{\overline{\varphi}}(z)$, заданной при $z_0 \leq z < \infty$.

Решение $\overline{V}$ найдём, например, методом вариации постоянных. Подчиним его однородным условиям сопряжения при $x \to x_0$:

$$\overline{V}^{\mathrm{I}}\big|_{x=x_0-0}-\overline{V}^{\mathrm{II}}\big|_{x=x_0+0}=0;\qquad \frac{1}{\sigma_{\mathrm{I}}}\cdot\frac{\partial V^{\mathrm{I}}}{\partial x}\bigg|_{x=x_0-0}-\frac{1}{\sigma^{\mathrm{II}}}\cdot\frac{\partial V^{\mathrm{II}}}{\partial x}\bigg|_{x=x_0+0}=0; \tag{15}$$

и нулевым условиям при $x\to\mp\infty$. Получим

$$\overline{V}^{\mathrm{I,\ II}}=\begin{cases}-\dfrac{e^{-i\mu z_0}}{2\beta_{\mathrm{I}}}\cdot\displaystyle\int_{-\infty}^{x_0}f^{\mathrm{I}}(\xi)\cdot e^{-\beta_{\mathrm{I}}|x-\xi|}\cdot d\xi+A\cdot e^{\beta_{\mathrm{I}}x}\ ; & (x\le x_0)\\ -\dfrac{e^{-i\mu z}}{2\beta_{\mathrm{II}}}\cdot\displaystyle\int_{x_0}^{\infty}f^{\mathrm{II}}(\xi)\cdot e^{-\beta_{\mathrm{II}}|x-\xi|}\cdot d\xi+B\cdot e^{-\beta_{\mathrm{II}}x}; & (x\ge x_0)\end{cases} \tag{16}$$

где

$$A(\mu)=\frac{e^{-i\mu z_0}}{2\cdot\beta_{\mathrm{I}}}\cdot\left[(D^{\mathrm{I}}+D^{\mathrm{II}})\cdot S^{\mathrm{I}}-2\cdot D^{\mathrm{I}}\cdot\frac{\beta_{\mathrm{I}}}{\beta_{\mathrm{II}}}\cdot S^{\mathrm{II}}\right];$$

$$B(\mu)=\frac{e^{-i\mu z_0}}{2\cdot\beta_{\mathrm{II}}}\cdot\left[2\cdot D^{\mathrm{II}}\frac{\beta_{\mathrm{II}}}{\beta_{\mathrm{I}}}\cdot S^{\mathrm{I}}-(D^{\mathrm{I}}+D^{\mathrm{II}})\cdot S^{\mathrm{II}}\right]; \tag{17}$$

$$S^{\mathrm{I}}(\mu)=\int_{-\infty}^{x_0}f^{\mathrm{I}}(\xi)\cdot e^{\beta_{\mathrm{I}}\cdot\xi}\cdot d\xi\ ;\qquad S^{\mathrm{II}}(\mu)=\int_{x_0}^{\infty}f^{\mathrm{II}}(\xi)\cdot e^{-\beta_{\mathrm{II}}\xi}\cdot d\xi\ ;$$

причем функции $f(x)=\psi^{\mathrm{I}}+i\mu\cdot\chi^{\mathrm{I}}$ и $f^{\mathrm{II}}(x)=\psi^{\mathrm{II}}+\mu\chi^{\mathrm{II}}$ заданы только на полубесконечной оси x, т.е. при $-\infty<x\le x_0$ и $x_0\le x<\infty$ соответственно. Вторые слагаемые вида $A\cdot e^{\beta_{\mathrm{I}}\cdot x}$ и $B\cdot{}^{-\beta_{\mathrm{II}}\cdot x}$ (16) — добавочные. Коэфициенты $A(\mu)$ и $B(\mu)$ — это постоянные интегрирования. Они однозначно определяются из условий сопряжения (15).

В решении (16) и (10) краевую задачу (11) для полуплоскости $z\ge z_0$ на линии $z=z_0$ решают только первые слагаемые, а вторые слагаемые при $z=z_0+0$ обращаются в нуль вместе с их нормальной производной. Однако на линии сопряжения $x=x_0$ именно эти добавочные члены решают задачу сопряжения (15). Они ликвидируют разрыв между значениями первых слагаемых и их производных по x при $x\to x_0$ и обеспечивают выполнение условий (15) для двух смежных угловых областей с различными комплексными параметрами σ_{I} и σ_{II}.

При желании построить решение для $z\le z_0$ следует пользоваться преобразованием Фурье в другую сторону $V(\mu,x;z_0)=\int_{-\infty}^{z_0}v\cdot e^{-i\mu z}\cdot dz$ и правую часть в (13) брать с противоположным знаком.

Обе переменные x и z в данном методе решения математически равноправны. Например: для смежных угловых областей $x \geq x_0$ $z \leq z_0$, $\sigma^* = \sigma_1$ и $x \geq x_0$, $z \geq z_0$, $\sigma^* = \sigma_2$ полагаем

$$W(\lambda, z; x_0) = \int_{x_0}^{\infty} v \cdot e^{-i\lambda x} \cdot dx, \quad Im\,\mu < 0 \qquad \text{и} \qquad \frac{1}{2\pi} \int_{-\infty}^{+\infty} W \cdot e^{i\lambda x} \cdot d\lambda =$$

$$= \begin{cases} 0, & x \leq x_0 ; \\ v(x, z), & x \geq x_0 ; \end{cases} \tag{18}$$

и точно так же получим: $W = W_0(\lambda, z; x_0) + \overline{W}(\lambda, z; x_0)$ (19)

Таким образом, решение двумерной краевой задачи для полуплоскости $z \leqslant z_0$ (либо $x \leqslant x_0$), составленной из смежных угловых областей, построено. Возвращаясь к исходной задаче (3*–8), заключаем, что решение (14) и совокупность граничных условий (5–7) в сочетании с данным методом построения решений типа (16) позволяют однозначно определить искомое решение, так чтобы выполнялись одновременно все условия поставленной задачи. В самом деле, полное решение задачи (3–8) может быть представлено в виде суммы:

$$v(x, z) = v_0(x, z) + \bar{v}(x, z) ; \tag{20}$$

где первичная функция v_0 в слое $z_{k-1} \leq z \leq z_k$ $(k = 1, \ldots, N+1)$ равна

$$\overline{\overline{v}}_{0k}^{\,\mathrm{I,\ II}}(x, z) = \begin{cases} \dfrac{1}{2\pi} \cdot \displaystyle\int_{-\infty}^{+\infty} D_k^{\mathrm{I}} \cdot \overline{\overline{\Phi}}_k(\mu) \cdot e^{\beta_{\mathrm{I}} x} \cdot e^{i\mu z} \cdot d\mu, & (x \leq x_0) \\ \dfrac{1}{2\pi} \cdot \displaystyle\int_{-\infty}^{+\infty} D_k^{\mathrm{II}} \cdot \overline{\overline{\Phi}}_k(\mu) \cdot e^{-\beta_{\mathrm{II}} x} \cdot e^{i\mu z} \cdot d\mu, & (x \geq x_0) \end{cases} \tag{21}$$

$$D_k^{\mathrm{I}}(\mu) = \frac{\sigma_k^{\mathrm{I}} \cdot \beta_k^{\mathrm{II}}}{\sigma_k^{\mathrm{I}} \cdot \beta_k^{\mathrm{II}} + \sigma_k^{\mathrm{II}} \cdot \beta_k^{\mathrm{I}}} \cdot e^{-\beta_k^{\mathrm{I}} x_0} ; \qquad D_k^{\mathrm{II}}(\mu) = -\frac{\sigma_k^{\mathrm{II}} \cdot \beta_k^{\mathrm{I}}}{\sigma_k^{\mathrm{I}} \cdot \beta_k^{\mathrm{II}} + \sigma_k^{\mathrm{II}} \cdot \beta_k^{\mathrm{I}}} \cdot e^{\beta_k^{\mathrm{I}} x_0} ;$$

$$\overline{\overline{\Phi}}_k(\mu) = \int_{z_{k-1}}^{z_k} \varphi(z) \cdot e^{-i\mu z} \cdot dz; \tag{22}$$

Функция (21–22) удовлетворяет условиям сопряжения (4), но в отличие от (14), она разрывна на линиях $z = z_k$ $(-\infty < x < +\infty)$ вслед за D_k^I и D_k^{II}. Добавление к v_0 вторичной функции $\bar{v}$ должно, не нарушая (4), обеспечивать удовлетворение (5–7). Исследование показывает, что $\bar{v}$ выражается в виде: $\bar{v} = \sum_{i=1}^{\infty} \bar{v}^{(i)}(x, z)$.

Используем преобразование Фурье по x (17–18) в обе стороны: $-\infty < x \le x_0$ и $x_0 \le x < \infty$. Решение для $x \le x_0$ и $x \ge x_0$ строится раздельно. В слое $z_{k-1} \le z \le z_k$ ($k = 1, \ldots, N+1$) имеем:

$$\frac{d^2 W_k}{dz^2} - \alpha_k^2 W_k = P_k(\lambda, z; x_0); \qquad \alpha_k = \begin{cases} \alpha_k^{\mathrm{I}} = \sqrt{\lambda^2 - k_k^{\mathrm{I}2}}; \\ \alpha_k^{\mathrm{II}} = \sqrt{\lambda^2 - k_k^{\mathrm{II}2}}; \end{cases}$$

$$\begin{matrix} (x \le x_0) \\ (x \ge x_0) \end{matrix} \quad Re\, \alpha_k^{\mathrm{I,\,II}} > 0 \qquad (23^{\mathrm{I,II}})$$

Для левой структуры $x \le x_0$: $P_k^{\mathrm{I}} = -e^{-i\lambda x_0}(h_k^{\mathrm{I}}(z) + i\lambda \cdot g_k^{\mathrm{I}}(z))$; $\qquad (24^{\mathrm{I}})$

Для правой структуры $x \ge x_0$: $P_k^{\mathrm{II}} = +e^{-i\lambda x_0} \cdot (h_k^{\mathrm{II}}(z) + i\lambda \cdot g_k^{\mathrm{II}}(z))$ $\qquad (24^{\mathrm{II}})$

Здесь $g^{\mathrm{I,\,II}}(z)$ и $h^{\mathrm{I,\,II}}(z)$ – суть известные левые и правые предельные значения функции (21–22) и её производной по x при $x = x_0 \mp 0$:

$$g_k^{\mathrm{I,\,II}}(z) = v_{0k}^{\mathrm{I,\,II}}(x, z)|_{x \to x_0 \mp 0}; \qquad h_k^{\mathrm{I,\,II}}(z) = \left.\frac{\partial v_{0k}^{\mathrm{I,\,II}}(x, z)}{\partial x}\right|_{x \to x_0 \mp 0};$$

Образы Фурье $W_k(\lambda, z; x_0)$ имеют вид

$$W_k^{\mathrm{I,\,II}}(\lambda, z; x_0) = -\int_{z_{k-1}}^{z_k} P_k^{\mathrm{I,\,II}}(\xi) \cdot \frac{e^{-\alpha_k^{\mathrm{I,\,II}} \cdot |z-\xi|}}{2 \cdot \alpha_k^{\mathrm{I,\,II}}} \cdot d\xi +$$

$$+ A_k^{\mathrm{I,\,II}} \cdot e^{\alpha_k^{\mathrm{I,\,II}} \cdot z} + B_k^{\mathrm{I,\,II}} e^{-\alpha_k^{\mathrm{I,\,II}} \cdot z}; \qquad (25^{\mathrm{I,\,II}})$$

Здесь A_k^{I}, B_k^{I} – константы интегрирования уравнения (23^{I}); A_k^{II}, B_k^{II} – постоянные интегрирования для (23^{II}). Они определяются из условий $(5^{\mathrm{I}}-7^{\mathrm{I}})$ и $(5^{\mathrm{II}}-7^{\mathrm{II}})$ для W_k^{I} и W_k^{II} соответственно. Получаются две системы уравнений относительно A_k, B_k, разрешаемые алгебраически.

Таким образом, требуемое решение (20) задачи (3*–8) найдено в замкнутом виде, в явной аналитической форме:

$$v_{0k}^{\mathrm{I,\,II}}(x, z) = \pm\frac{1}{2\pi}\int_{-\infty}^{+\infty} \frac{1}{2\alpha_k^{\mathrm{I,\,II}}} \cdot \int_{z_{k-1}}^{z_k} (h_k^{\mathrm{I,\,II}}(\xi) +$$

$$+ i\lambda \cdot g_k^{\mathrm{I,\,II}}(\xi)) \cdot e^{-\alpha_k^{\mathrm{I,\,II}}|z-\xi|} \cdot d\xi \cdot e^{i\lambda x} \cdot d\lambda; \qquad (26^{\mathrm{I,\,II}})$$

$$\overline{v}_k^{\mathrm{I,\,II}}(x, z)^{(1)} = \frac{1}{2\pi} \cdot \int_{-\infty}^{+\infty} (A_k^{\mathrm{I,\,II}}(\lambda) \cdot e^{\alpha_k^{\mathrm{I,\,II}} \cdot z} + B_k^{\mathrm{I,\,II}}(\lambda) \cdot e^{-\alpha_k^{\mathrm{I,\,II}} \cdot z}) \cdot e^{i\lambda x} \cdot d\lambda;$$

$$(27^{\mathrm{I,\,II}})$$

Выражения (26–27 отличаются от точного решения поправочным слагаемым: $\delta v = v - v^{(1)}$. Для δv возникает та же самая задача (3*–8), что и для v, не имеющая нигде источников ноля, кроме скачка на контакте $x = x_0$:

$$\left[\delta v\right]_{x_0+0}^{x_0-0} = \delta\varphi \;; \qquad \left[\frac{1}{\sigma^*}\cdot\frac{\partial(\delta v)}{\partial x}\right]_{x_0+0}^{x_0-0} = \delta\tau \;;$$

причем

$$\delta\varphi(z) = -\left[\bar{v}^{(1)}\right]_{x_0+0}^{x_0-0} \quad \text{и} \quad \delta\tau(z) = -\left[\frac{1}{\partial^*}\cdot\frac{\partial\bar{v}^{(1)}}{\partial x}\right]_{x_0+0}^{x_0-0}.$$

Отсюда найдем первое приближение δv в форме (26 – 27), являющееся вторым приближением для $v(x, z)$. В данном способе приближения к точному решению (20) сходимость имеет место в силу ограниченности коэфициентов отражения и преломления: $D_k(\mu)$; $A_k(\lambda)$ и $B_k(\lambda)$. Произведения $D\cdot A$ и $D\cdot B$ по модулю всегда строго меньше единиды.

Преимущества этого решения в его простоте и общности. Явная форма решения (26 – 27) достаточно удобна для прямого анализа (можно показать, что выражения ($26^{\text{I, II}}$) и (21 – 22) совпадают между собой. Это – две разные формы записи одной и той же функции $v_0(x, z)$.) и проведения расчетов, а круг приложений и обобщений настоящего метода решения широк и разнообразен. Укажем лишь некоторые из них.

1. Полученное решение органически распространяется на случай двух (и более) вертикальных контактов.

2. Метод решения легко допускает введение в постановку задачи общего граничного условия 3-го рода на поверхности $z=0$:

$$\left.\frac{\partial u}{\partial z}\right|_{z=0+0} - \gamma\cdot[u|_{z=0+0} - \vartheta(x, y)] = 0; \qquad (28^{\text{I, II}})$$

где $\vartheta(x, y)$ – произвольная функция, имеющая интегрируемые образы Фурье по x:

$$\Theta^{(+)}(\lambda, y; x_0) = \int_{x_0}^{\infty} \vartheta^{\text{II}}(x, y)\cdot e^{-i\lambda x}\cdot dx \text{ и } \Theta^{(-)}(\lambda. y; x_0) = \int_{-\infty}^{x_0} o^{\text{I}}(x,y)\cdot e^{-i\lambda x}\cdot dx$$

При этом производная $\left.\frac{\partial u}{\partial z}\right|_{z=0}$ т.е. поверхностный тепловой поток для зоны контакта океанической и континентальной коры определяется выражением

$$q(x) = \gamma_{\text{I, II}}\cdot\left(u|_{z=0} + \vartheta(x, y)\right) =$$

$$= \gamma_{\text{I, II}}\cdot\left[U_0^{\text{I, II}}(z) - \vartheta(x) + \frac{D_1^{\text{I, II}}}{2\pi}\cdot\int_{-\infty}^{+\infty}\underline{\underline{\Phi}}_1(\mu)\cdot e^{\pm|\mu|\cdot x}\cdot d\mu + \right.$$

$$\left. + \frac{1}{\pi}\int_0^{\infty}(A_1^{\text{I, II}} + B_1^{\text{I, II}})\cdot\cos\lambda x\cdot d\lambda\right] \qquad (29)$$

3. В случае точечного источника (горизонтальный или вертикальный диполь) решение для вертикального контакта горизонтально-

слоистых сред (рис. 1б) также строится по методу, изложенному в данной работе. Оно имеет явное представление в замкнутой аналитической форме интегралов Фурье.

4. Данный метод позволяет решать двумерные краевые задачи математической физики для кусочно-составных сред с взаимно пересекающимися границами раздела. Кроме рассмотренного примера в декартовых координатах (рис. 1), метод может быть применён также и в других координатных системах к краевым задачам со смежными угловыми областями. Например, в сферических координатах — исследование геофизических полей в зоне перехода от континента к океану с учетом сферичности Земли; в цилиндрических координатах — задача каротажа с одновременным учетом плоских горизонтальных и цилиндрических вертикальных границ раздела; и т.п.

ЛИТЕРАТУРА

Дмитриев В. И., Захаров Е. В. (1970): Метод решения задач электродинамики неоднородных сред.
Журнал Выч. математики и математич. физики, т. X, вып. 6.
Титчмарш Е. (1948): Введение в теорию интегралов Фурье. ОГИЗ, М. Л.

INDEX

Szádeczky-Kardoss E.: Professor Elemér Vadász (1885–1970) 3

Abdel Dayem, M. M., Márton, P., Szalay-Márton, E.: Thermomagnetic analysis and optical examinations of post-orogenic basalts from Hungary 7

Czelnai, R., Rákóczi, F.: Expansions of certain meteorological fields in Chebyshev polynomials 17

Dank, V.: Hydrocarbon prospecting and geochemistry 29

Galácz, A.: Trilobiticeras (Ammonoidea, Otoitidae) from the Bajocian (Middle Jurassic) of the Bakony Mountains 39

Géczy, B.: Ammonite Faunae on the Lower Jurassic Standard Profile at Lókút Bakony Mountains, Hungary 47

Kis, K.: A comparison between the normal and regional magnetic fields of Hungary 79

Császár, M. M.: The relationship of contraction inversion and low-level jets 89

Meskó, A.: Design of short interpolating functions for digital processing of seismic data 99

Végh-Neubrandt, E.: Fauna- und Faziesverbreitung der Obertrias des Transdanubischen Mittelgebirges 111

Е. А. Любимова, В. Н. Никитина.: Решение двумерной краевой задачи тепловых и электромагнитных полей над вертикальным контактом горизонтально-слоистих сред 121

A kiadásért felelős: az Eötvös Loránd Tudományegyetem rektora
A kézirat nyomdába érkezett: 1971. augusztus — Megjelent: 1972. május
Terjedelem: 11,5 (A/5) ív — Példányszám: 800
Készült monó szedéssel, íves magasnyomással, az MSZ 5601—59 és az 5602—55 szabvány szerint
71.1349. Állami Nyomda, Budapest